UNIVERSITY OF CALIFORNIA
RIVERSIDE

Nonsense-Mediated RNA Decay in Neuronal Cell Stress and Survival

A Dissertation submitted in partial satisfaction
of the requirements for the degree of

Doctor of Philosophy

in

Genetics, Genomics, and Bioinformatics

by

Zhelin Li

March 2020

Dissertation Committee:

Dr. Sika Zheng, Chairperson
Dr. Fedor V. Karginov
Dr. Xuan Liu
Dr. Yinsheng Wang

The Dissertation of Zhelin Li is approved:

_____

_____

_____

_____
Committee Chairperson

University of California, Riverside

Acknowledgements

I would like to thank Dr. Sika Zheng for his guidance and mentorship. I admire and respect your integrity, discipline, and your relentless pursuit for the scientific truth. I would like to thank my fellow lab mates, Cheryl Stork and John Vuong, for their support over the years. Thank you, John, for optimizing various protocols used in this dissertation. Thanks to Dr. Min Zhang, Dr. Lin Lin, Dr. Volkan Ergin, and Dr. JR Zhao for their help with experiments such as progenitor cell culturing, CRISPR, and more. They were always available and engaging. I also would like to thank my undergraduate students, Ruchira Puri, Kelvin Liu, and Isreal Nunez for their assistance with my experiments and lab chores. I hope you each find your path forward in your studies and careers. To current committee members, Dr. Ted Karginov, Dr. Yinsheng Wang, Dr. Xuan Liu, and past committee members Dr. Weifeng Gu, Dr. Meera Nair, and Dr. Sean O'Leary, I appreciate your time and I sincerely thank you for your mentorship.

Lastly, parts of Chapter 2 and 3 from this dissertation are rewritten or reprinted based on my first authorship publication in the journal of RNA, 2018. Co-author Sika Zheng supervised and funded the research. The other authors John Voung who helped with dosage treatments of thapsigargin used in figure 8, Dr. Min for preparing animal samples, and Cheryl Stork for initiating the study. The citation is as followed:

Li, Zhelin, John K. Vuong, Min Zhang, Cheryl Stork, and Sika Zheng. 2017. "Inhibition of Nonsense-Mediated RNA Decay by ER Stress." *RNA* 23 (3): 378–94.

Dedications

I dedicate this dissertation work to my grandfather who inspired me to become a scientist. Also, to my father who passed away during my graduate tenure, I hope I have made you proud. To my mother, Angie, who has supported me my entire life, thank you for all your sacrifice.

ABSTRACT OF THE DISSERTATION

Nonsense-Mediated RNA Decay in Neuronal Cell Stress and Survival

by

Zhelin Li

Doctor of Philosophy, Graduate Program in Genetics, Genomics, and Bioinformatics
University of California, Riverside, March 2020
Dr. Sika Zheng, Chairperson

Nonsense-mediated RNA decay (NMD) is a cell surveillance system that degrades aberrantly processed RNA transcripts containing premature termination codons (PTCs). PTCs can arise from various genetic mutations. In addition to serving as a passive fail-safe mechanism, recent studies suggest NMD is also actively involved in alternative splicing (AS), stress responses, neurogenesis, and other biological processes. This dissertation is aimed to further investigate the relationship between NMD and other stress mechanisms.

To overcome some inherent problems of assaying endogenous NMD targets, Chapter 2 presents an easily and broadly applicable AS-NMD reporter assay to quantify cellular NMD activity, in real time. This new strategy reliably distinguishes NMD regulation from transcriptional control, AS regulation, and discloses a different sensitivity of NMD targets to NMD inhibition. It is then used to screen molecules for NMD inhibitors including thapsigargin in neuro-2A cells.

Chapter 3 shows stresses affect NMD differently and the mechanistic discovery of NMD inhibition upon thapsigargin treatment. The endoplasmic

reticulum (ER) stress and polysome disassembly caused by thapsigargin suggest that an activated unfolded protein response (UPR) pathway by protein kinase RNA-like endoplasmic reticulum kinase (PERK) is required for NMD inhibition, instead of calcium signaling pathways. Such stress induced NMD inhibition can compound TDP-43 depletion proteinopathy via upregulating NMD isoforms that had been implicated in the pathogenic mechanisms of amyotrophic lateral sclerosis (ALS) and frontotemporal dementia (FTD) which could be completely blocked by PERK deactivation.

In Chapter 4, a pioneer *in vitro* conditional NMD deficient neural progenitor cell (NPC) system is created using adeno-associated virus serotype 9 (AAV9). Significant loss in NPC viability is observed during UPF2 knockout. Candidate genes, *Gadd45b* and *Gadd45g*, knockout using CRISPR-Cas9 failed to rescue NPC survival. This finding suggests NMD activity is essential for cell viability, likely maintaining the homeostasis of NPC transcriptome during renewal processes.

In summary, AS-NMD strategy screens and reveals the pathway of NMD inhibition by ER stress and the implicated ALS proteinopathy. More importantly, the research highlights NMD interaction with stress and cell survival, especially in NPCs, that could provide future therapeutic approaches toward related genetic diseases.

Table of Contents

List of Figures

Chapter 1

Chapter 2

Chapter 3

Chapter 4

Chapter 5

List of Tables

Chapter 1

Chapter 2

Chapter 4

Chapter 1: Introduction

Introduction to nonsense-mediated RNA decay in eukaryotes and mammals

Nonsense-mediated RNA decay (NMD) is a cellular surveillance mechanism that selectively degrades mutated and aberrantly processed transcripts that contain premature termination codons (PTC) (Kurosaki, Popp, and Maquat 2019; S. Lykke-Andersen and Jensen 2015; Hug, Longman, and Cáceres 2016; Y.-F. Chang, Imam, and Wilkinson 2007). PTC arises when a position on an RNA transcript that normally encodes an amino acid is changed to a UAG, UAA, or UGA stop codon prior to its original translation termination site. The presence of such PTCs destabilizes RNA transcripts and initiates NMD. Genome wide studies estimate that these premature termination mutations account for at least 11% of all DNA mutations and can be caused by alternative splicing (AS), genome rearrangements, or random mutations (Kuzmiak and Maquat 2006; J. T. Mendell and Dietz 2001; Shi et al. 2015; Mort et al. 2008). The wide range of downstream targets indicate that the functions of NMD goes well beyond just a failsafe system, but it is also actively involved in molecular and cellular processes, and genetic diseases which will be discussed later in this chapter.

NMD was first described by Dr. Maquat while studying patients with β0-thalassemias caused by a shortage of β-globin due to the reduced stability in the β-globin mRNA during the early 1980s (L. E. Maquat et al. 1981; Losson and Lacroute 1979). Over the past decades, researchers have identified many key factors and details revolving the NMD mechanism (Table 1) (Han et al. 2018).

Early screening of yeast and *c. elegant* identified important NMD factor Up-frameshift protein 1 (UPF1) and Suppressors with Morphological defects on Genitalia (SMG) 1 to be involved in the stability of NMD transcripts (Pulak and Anderson 1993; Leeds et al. 1991; A. Yamashita et al. 2001). Soon, UPF1's interaction with UPF2 was deemed to be essential to initiate NMD mechanism while UPF3B and analog UPF3A stabilize such interaction by anchoring NMD factors on the RNA transcript (Kadlec, Izaurralde, and Cusack 2004; Gehring et al. 2003; Shum et al. 2016). Along with additional SMG family proteins (SMG5, SMG6, SMG7, SMG8 and SMG9), providing dephosphorylation and nuclease activities, the conventional NMD model in eukaryotes can be established (Akio Yamashita et al. 2009; Cali et al. 1999; Chiu et al. 2003; Anders, Grimson, and Anderson 2003).

Table 1. Key eukaryotic NMD factors

Key eukaryotic NMD factors	Major NMD functions
UPF1	RNA-dependent helicase and ATPase that is required for nonsense mediated RNA decay
UPF2	Part of the multiprotein complex at the exon junction that directly interacts with UPF1 to initiate NMD
UPF3B	Anchoring UPF2 and the EJC factors to promote NMD activity
UPF3A	Paralog of UPF3B that is reported to have redundent functions as UPF3B, but a weaker NMD promoter
SMG1	Serine/threonine protein kinase 1 that phosphorylates UPF1
SMG5	Heterodimerize with SMG7 to promote NMD degradation
SMG6	NMD endonuclease that cleaves NMD targets in parallel with SMG5-SMG7 complex
SMG7	Mediate NMD transcript degradation through 5′-to-3′ decapping and exonuclease XRN1
SMG8	Repressor subunit of SMG1
SMG9	Repressor subunit of SMG1

Figure 1 presents a holistic view of the exon junction complexes (EJC) dependent NMD model in eukaryotes and mammals. In a normal mRNA transcript, EJCs consist of core tetramers of eIF4A3 (eukaryotic initiation factor 4A3), MAGOH, Y14, and MLN51 are assembled 20 - 24 nucleotides upstream of exon-exon junctions (EJ) (Figure 1A) (Hervé Le Hir, Saulière, and Wang 2016; H. Le Hir et al. 2000). The pioneer round of translation choreographed by the cap binding protein complex (CBC) including CBP80 - CBP20 heterodimer and eukaryotic initiation factor 4G (eIF4G) initiate ribosome translation at the start codon position, replacing resident EJC and UPF1 along the translated transcript and is terminated at the normal termination position (NTC), positioned after the last EJ (Figure 1B) (Y. K. Kim and Maquat 2019; Kurosaki and Maquat 2013; Hogg and Goff 2010; Schuller et al. 2018; Ishigaki et al. 2001; Lynne E. Maquat, Tarn, and Isken 2010).

However, in an mRNA transcript harboring PTC > 50 to 54 nucleotides upstream of an EJ (Figure 1C), ribosome is prematurely stalled at the PTC position (Figure 1D). If the poly(A)-binding protein 1 (PABPC1) at the 3' untranslated region (3' UTR) is too distant to interfere with the resident UPF1 from joining the eukaryotic release factor 1 and 3 (eRFs) to allow the dissociation of ribosomes, then UPF1 and the eRFs is stabilized at the PTC. A transient translational termination complex is formed to assist ribosome disassembly (Czaplinski et al. 1998; Ivanov et al. 2008; Kashima et al. 2006; Peixeiro et al. 2012; Singh, Rebbapragada, and Lykke-Andersen 2008). Next, the SMG1 lead

SMG1-SMG8-SMG9 serine/threonine kinases directly interact with the resident NMD factor UPF1 and the eRFs to form the “SURF” complex at the PTC location (Figure 1D) (Franks, Singh, and Lykke-Andersen 2010; Serdar, Whiteside, and Baker 2016; Czaplinski et al. 1998; Ivanov et al. 2008). Nearby UPF2 anchored to the EJC-bound UPF3B is recruited to promote UPF1 and SURF complex, restructuring it into the decay inducing DECID complex (Figure 1E) (Kashima et al. 2006; Chamieh et al. 2008). At the same time, UPF2 assists dissociation of SMG8 and SMG9 from SMG1 which allows the conformational activated SMG1 to phosphorylate UPF1 (Melero et al. 2014; Chamieh et al. 2008; Usuki et al. 2013). The phosphorylated UPF1 then recruits either SMG6 for endonuclease degradation and / or XRN1 and SMG5-SMG7 mediated exonuclease degradation (Figure 1E) (Colombo et al. 2017; Franks, Singh, and Lykke-Andersen 2010; Eberle et al. 2009; Huntzinger et al. 2008; Okada-Katsuhata et al. 2012).

NMD encompasses a large variety of functions and mechanisms, this introductory chapter will first focus on the *cis* characteristics of NMD targets and its intimate interactions with alternative splicing. Then, focusing on a specific physiological role of NMD in brain development and the newfound potential in gene therapy in conjunction with gene editing. The information in this chapter will hopefully provide sufficient backgrounds and logic for the dissertation works presented in the upcoming chapters.

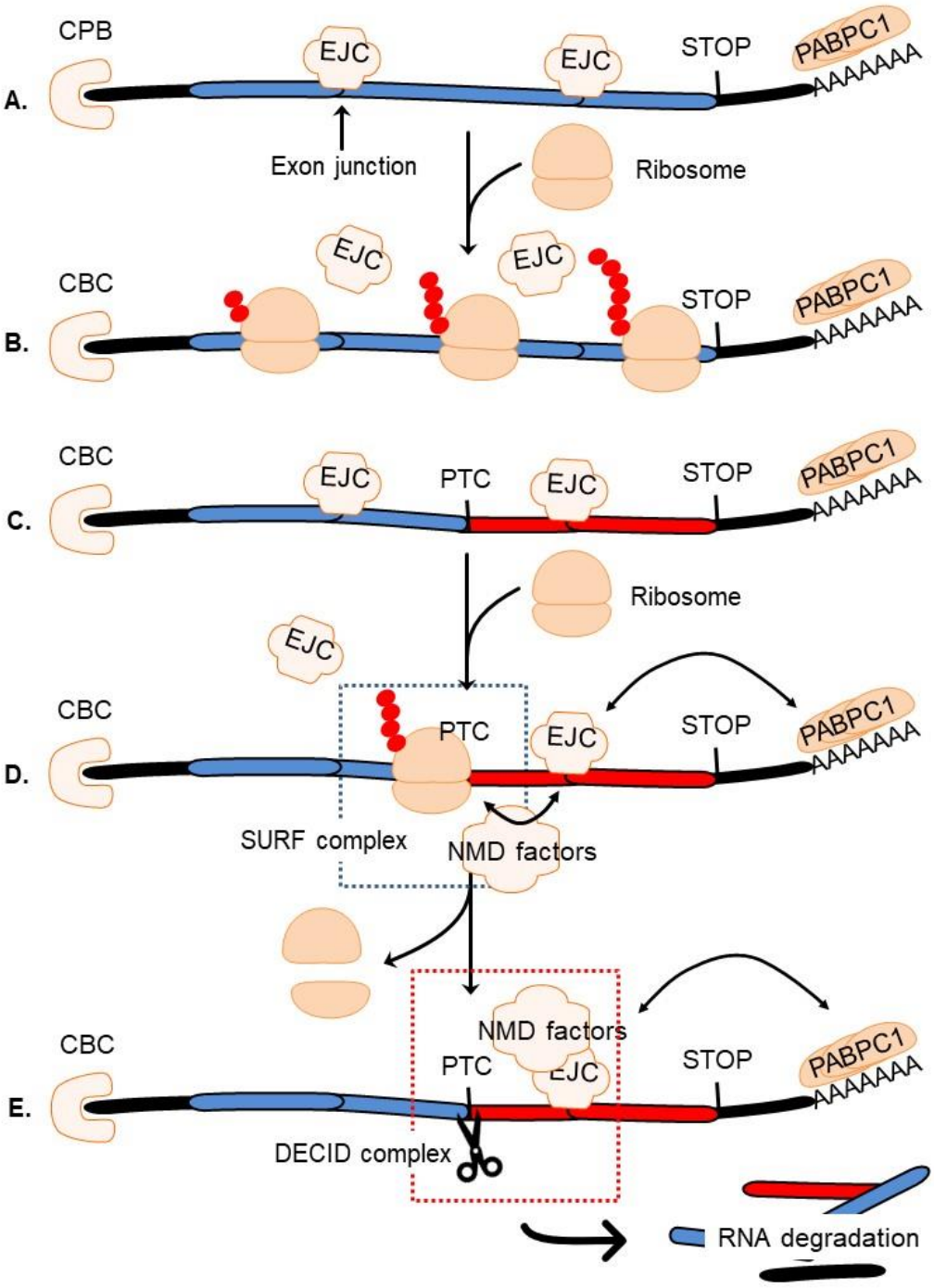
A.
CPB
EJC
EJC
STOP
PABPC1
AAAAAAA
Exon junction
Ribosome
B.
CBC
EJC
EJC
STOP
PABPC1
AAAAAAA
C.
CBC
EJC
PTC
EJC
STOP
PABPC1
AAAAAAA
Ribosome
D.
CBC
EJC
PTC
EJC
STOP
PABPC1
AAAAAAA
SURF complex
NMD factors
E.
CBC
NMD factors
PTC
EJC
STOP
PABPC1
AAAAAAA
DECID complex
RNA degradation

Figure 1. The EJC mediated nonsense-mediated mRNA decay pathway. (A) In a normal mRNA transcript. Exon junction complexes (EJCs) assemble 20-24 nucleotides upstream of exon-exon junctions (EJ). (B) The pioneer ribosome reads and translates along the mRNA transcript while displacing the EJCs. The stop codons are located after the last EJ where full length proteins are translated. (C) In case a PTC arise more than 50-54 nucleotides upstream from the last EJ, (D) the first round of translation is stalled at the PTC instead of the normal termination codons. Leading to the interaction of SMG1 kinase with resident NMD factors UPF1 and eukaryotic release factors (eRFs) to form SURF complex at the PTC location. Note PABP1 competes with UPF1 as a stabilizing factor for the transcript, however, it is distal and insufficient to interfere with SURF formation. (E) At the same time, the nearby EJC resident UPF2 anchored by UPF3B is recruited to interact directly with UPF1, forming the decay inducing complex DECID. DECID enables SMG1 to phosphorylate UPF1 and dissociate eRFs. The phosphorylated UPF1 then recruits either SMG6 for endonuclease degradation and / or SMG5 - SMG7 mediated exonuclease degradation.

NMD targets - what does it mean to be "nonsense"

An RNA physiology marked for NMD may be resulted from any of the following circumstances: an upstream open reading frame in the 5' untranslated region (5' UTR); a spliced intron in the 3'UTR; alternative mRNA splicing shifting the reading frame and resulting in a PTC upstream of an EJC; and the inclusion of a middle alternative "toxic" exon containing an in-frame PTC (Hug, Longman, and Cáceres 2016; Kurosaki, Popp, and Maquat 2019). The most well studied feature of NMD targets in eukaryotes has to be the distance of a PTC from a downstream exon junction. This so called "50 to 55 nts" rule indicates a transcript with a stop codon 50 to 55 nts upstream of an exon-exon junction is consistently selected by NMD for degradation (Lynne E. Maquat, Tarn, and Isken 2010; J. Lykke-Andersen, Shu, and Steitz 2000; H. Le Hir et al. 2000, 2001). Reasoning for this rule is straightforward as a ribosome fails to remove the EJC during translation because it is terminated at the PTC distant enough from the junction. This in turn leads to failure of preventing UPF1 interaction with EJC, initiating the NMD machinery (Nagy and Maquat 1998).

Such NMD sensitivity towards spatial and distal factors could also explain why "pioneer" rounds of translation often trigger NMD. The CBC bound mRNAs are linear during the first round of translation whereas eIF4E replaces CBC after initial translation to circularize the mRNA in coordination with poly(A)-binding proteins (PABP) at the 3' UTR (Lynne E. Maquat, Tarn, and Isken 2010; Matsuda et al. 2007; Fatscher et al. 2014). This brings PABPs to a closer proximity to

compete with UPF1 interaction with the eRFs. Insufficient interaction between UPF1 and the other factors can escape NMD and stabilize the transcripts (Toma et al. 2015; Fatscher et al. 2014; Hogg and Goff 2010; Ivanov et al. 2008; Singh, Rebbapragada, and Lykke-Andersen 2008).

In addition to PABPs, the large heterogeneity of a 3' UTR sequence can also influence NMD efficiency. The residential UPF1 binding level is a good example of innate features of 3' UTR affecting NMD activity (Toma et al. 2015; Hogg and Goff 2010; Bühler et al. 2006). This feature could explain the foundation of an alternative EJC independent model, the 3' faux model. The 3' faux model indicates that longer 3' UTRs are able to host more UPF1 factors which lead to more NMD activities in the yeast *Saccharomyces cerevisiae* (Amrani et al. 2004; Meaux, van Hoof, and Baker 2008; Kurosaki and Maquat 2013; Shigeoka et al. 2012). All these structural organizations can be employed as guides in identifying NMD substrates and their downstream applications of NMD in biology.

NMD and alternative splicing (AS-NMD)

Due to the dependency of NMD activation in relation to EJC position and PTC introduction, NMD is intimately coupled with alternative splicing (AS-NMD). Alternative splicing (AS) is the process that joins exons of an RNA transcripts in order to produce different variants that translate into structurally and functionally different proteins from a certain number of gene templates (Scotti and Swanson

2016; Lee and Rio 2015). AS plays an important role in differential expression of genes that are important for cellular metabolism, growth, differentiation, and apoptosis (Manning and Cooper 2017; Baralle and Giudice 2017).

Up to 80% of human genes are subjected to alternative splicing regulation, and 30 to 35% of alternative splicing events in human and mouse will produce a PTC containing isoform through reading frameshifts (Lewis, Green, and Brenner 2003; Weischenfeldt et al. 2012; Pan et al. 2006; Hervé Le Hir, Saulière, and Wang 2016). For example, AS-NMD is also widely used by splicing regulators and some RNA binding proteins (RBP) to maintain their own homeostatic expression (Lareau et al., n.d.; Ni et al. 2007; Saltzman et al. 2008; Boutz et al. 2007; Spellman, Llorian, and Smith 2007). It can also be harnessed to control the expression of non-RBP genes during development (Zheng et al. 2012; Vuong, Black, and Zheng 2016). Some endogenous snoRNA and alternatively spliced NMD-sensitive gene isoforms are cell types and organs specific, suggesting the NMD can diversify the fate of an alternatively spliced RNA transcript when coupled together (S. Lykke-Andersen et al. 2014; Thoren et al. 2010; Weischenfeldt et al. 2008; S. Lykke-Andersen and Jensen 2015). Evidence of AS-NMD supports the role of NMD as an essential gene regulation mechanism. The potential application of AS-NMD coupling will be discussed in chapter 2 and 3 to develop an assay that can quantitatively determine endogenous NMD activity, using the abundance of AS-NMD physiologic transcripts (Peccarelli and Kebaara 2014; Chan et al. 2007; Isken and Maquat 2008; Rehwinkel et al. 2005;

Nott, Meislin, and Moore 2003). This assay could be useful in future diagnostics and easily applied in all fields of NMD studies.

The intertwining network of NMD and brain development

NMD plays an extremely important role in fine tuning gene expressions and maintaining cellular homeostasis in all cell types (Lulu Huang et al. 2011; Weischenfeldt et al. 2008). Recently, NMD has received the attention of neuroscientists for its important roles in axonogenesis, synaptic growth, neuronal differentiation, and apoptosis (Jaffrey and Wilkinson 2018; Han et al. 2018; Lou et al. 2014; Zheng 2016; Peccarelli and Kebaara 2014). These physiological changes are likely because of the direct or indirect NMD regulations of downstream neural specific transcripts (Joshua T. Mendell et al. 2004; Wittmann, Hol, and Jäck 2006; Schmidt et al. 2015; Weischenfeldt et al. 2012). For instance, a synaptic protein PSD-95, encoded by the *Psd-95* gene undergoes an AS-NMD process during brain development to modulate normal synaptic formation. During late neuron development, exon 18 of *Psd-95* is included, prompting the gene to escape from NMD fate. Therefore, expressing PSD-95 for neuron maturation (Zheng et al. 2012; Zheng 2016). Another example, *Robo3.2*, an alternative variance of *Robo3* axon guidance gene is also a target of NMD due to intron retention, demonstrating the role of NMD in axon guidance (Colak et al. 2013). In the case of neural stem cell differentiation, the *Smad7* mRNA

transcripts are also actively regulated by NMD to enhance TGFβ signalling and promotes neuronal differentiation from proliferation (Lou et al. 2014).

On a brain physiology level, observations of humans and mice lacking *Upf2* in the forebrain show memory, intellectual, and communication deficits from brain inflammation which could be attributed to a slew of inflammatory genes being upregulated from NMD inhibition (Johnson et al. 2019). Another NMD factor causing neuronal impairment is UPF3B. RNA sequencing data obtained from UPF3B deficient mice frontal cortex shows transcripts directly responsible for neural differentiation are significantly affected (L. Huang et al. 2018). Moreover, NMD factors have been closely linked with neural development defects and disorders which will be introduced in the following section. Together, recent studies shed lights on the importance of NMD in neuronal development. This dissertation will explore a novel UPF2 null neuronal progenitor cell (NPC) model in chapter 4, especially in regards to NPC growth and viability.

NMD related human diseases and its applications in gene engineering and therapy

Since first establishing connection of NMD with β0-thalassemias in the 1980s, a plethora of NMD targets and related genetic diseases have been reported (Kurosaki, Popp, and Maquat 2019; Mort et al. 2008; Kurosaki and Maquat 2016; Khajavi, Inoue, and Lupski 2006; L. E. Maquat et al. 1981; J. C. Chang and Kan 1979). Many NMD related diseases are caused by the

introduction of a toxic PTC to normal functional genes. For example, a PTC mutation on the cystic fibrosis transmembrane regulator (CFTR) gene leads to dysfunction in the airway cells that cause cystic fibrosis (CF) (Linde and Kerem, n.d.). Two forms of muscular dystrophy, Duchenne muscular dystrophy (DMD) and Becker muscular dystrophy (BMD), are also results from premature termination on the dystrophin gene (Kerr et al. 2001; Koenig et al. 1987).

Last section discussed NMD's important role in neuronal development, naturally, it also contributes to many neurodegenerative diseases and disorders such as ADHD, autism spectrum disorder, amyotrophic lateral sclerosis (ALS), and many others (Jolly et al. 2013; Jaffrey and Wilkinson 2018; L. Huang et al. 2018). ALS and its associated frontotemporal dementia (FTD) are reported to potentially be caused by the accumulation of aberrant NMD transcripts when the faulty TAR DNA-binding protein (TARDBP) encoding gene *Tdp-43* and FUS RNA-binding protein gene *Fus* are introduced (Arai et al. 2006; Barmada et al. 2015; Ling et al. 2015). These "cryptic" or hidden gene variations overwhelm the endogenous NMD surveillance system that lead ALS - FTD.

Moreover, disruption in NMD are also observed in pancreatic adenosquamous carcinomas, hepatocellular carcinoma, and tumor microenvironments through either faulty NMD factors or NMD targeting genes (Kurosaki, Popp, and Maquat 2019; Bokhari et al. 2018; Gardner 2010; Popp and Maquat 2018). In total, it is estimated that nearly 30% of all genetic disorders are consequences of a nonsense or frameshift mutation that introduces a PTC,

making the modulation of NMD an important approach in curing these diseases (J. N. Miller and Pearce 2014).

One therapeutic approach is called readthrough therapy. Instead of translational termination at the PTC which could activate NMD machinery, the termination signals are suppressed and allowed to proceed toward the normal termination codon position (NTC) (Bidou et al. 2012; Keeling and Bedwell 2011). The nature of termination efficiencies between the three stop codons, UGA, UAG, and UAA, along with additional elements allow some PTC positions to be translated through, but terminated at the NTC position as full length proteins using small molecules and other exogenous agents (Manuvakhova, Keeling, and Bedwell 2000). It is estimated that 3 million individuals in the US could benefit from such PTC readthrough / suppression therapy alone (Keeling and Bedwell 2011).

The most common and well studied method of readthrough therapy is treating with aminoglycosides (AAGs). Discovered in the 1960s as antibiotics, AAGs interferes with condon matching of tRNAs to misread transcripts through of PTC (Burke and Mogg 1985; Anderson, Gorini, and Breckenridge 1965; Davies, Gilbert, and Gorini 1964). Treatments with AAGs have been tried in DMD disease models using gentamicin to restore 10 to 20% of normal dystrophin expression in skeletal muscle cells (Barton-Davis et al. 1999). Another AAG molecule called PTC124 is shown to be one of the most potent readthrough compounds (Welch et al. 2007). Extensive studies and clinical trials have been

done using PTC124 in both CF and DMD patients. However, both clinical trials failed in phase 3 without significant improvement to reach milestone results (Bushby et al. 2014; Kerem et al. 2014; McDonald et al. 2017). This is likely because of the low levels of mRNA substrates available for translational read-through when NMD is normal and active (Kerem 2004; Nagel-Wolfrum et al. 2016). In addition, while many AAGs show low toxicity, they still can lead to kidney damage and hearing loss which limits the dosages that can be used in humans to maximize readthrough. Additional compounds must be co-administered to alleviate side effects which can also inhibit readthrough efficiency (Keeling and Bedwell 2011). To mediate such problems, recent antisense oligos targeting NMD factors and small molecule NMD inhibitors have been used in conjunction with AAGs that show improved readthrough efficiency (Lulu Huang et al. 2018; Martin et al. 2014; Linde et al. 2007).

In recent years, new methods of suppression therapy have been in development. Take engineered tRNA. Instead of using a small molecule to indiscriminately readthrough, the engineered tRNA can substitute the specific disease-causing mutation site with the canonical amino acid using the PTC code. One study showed potent suppression of PTC sites where the engineered tRNAs, Gln-UAA and Arg-UGA, were used to substitute termination signals both *in vivo* and *in vitro* (Lueck et al. 2019). The new generation of readthrough or PTC suppression therapy is promising and advancing rapidly, but still no

approved therapy is available suggests the intricate balance and complexity of NMD that is puzzling over these genetic diseases.

As more and more targets and multitude of biological processes are linked to NMD, the traditional small molecule readthrough may no longer satisfy the standard for today's gene therapy. For the past eight years, a promising gene editing technology called clustered regularly interspaced short palindromic repeat (CRISPR) is extending the potential of NMD in gene therapy (Popp and Maquat 2016). The CRISPR system was originally discovered as a bacterial defense mechanism to defend against foreign viral genomes (Smith and Wilcox 1970; Kelly and Smith 1970; Ishino et al. 1987). It had been pushed into the spotlight with landmark publications and applications in editing eukaryotic cells (Doudna and Charpentier 2014; Cong et al. 2013; Jinek et al. 2012). It's minimalistic plasmid design of Cas9 nuclease fused with a small guidance RNA (sgRNA) can target any region of interest around the genome. It is much more convenient than the earlier protein engineering based gene editing technologies such as zinc fingers or the TAL effectors site directed editing (Cong and Zhang 2015; Cong et al. 2013; J. Miller, McLachlan, and Klug 1985; Boch et al. 2009; H. Kim and Kim 2014).

Now, CRISPR technology is providing the possibility to hijack the normal function of endogenous NMD to silence mutated genes as a method of gene therapy. For instance, CRISPR gene editing can introduce DNA double strand breaks via Cas9 nickase activity at a designated position on a gene guided by

the sgRNA. Nonhomologous end joining (NHEJ) ensues and repairs the breaking site which often results in DNA insertions or deletions (indels). When designed correctly, NHEJ repairs introduce PTCs to create loss of function genes that will be completely destroyed by NMD before producing any proteins (Popp and Maquat 2016; Tuladhar et al. 2019; Shalem, Sanjana, and Zhang 2015). One obvious limitation of the first generation CRISPR-Cas9 20 nts guidance RNA design is the position of the protospacer-adjacent motif (PAM) sequence. The three-nucleotide NGG PAM site must be adjacent to the target sequence for Cas9 binding (Jinek et al. 2012), thus limiting the freedom of optimal targeting. However, with tremendous amounts of motivation behind this technology, CRISPR is evolving to developing Cas enzymes with flexible PAM recognition, improved fidelity and specificity, inactivated dead enzymatic activity (dCas), and even a repertoire of single stranded DNA or RNA nickase derived from ortholog bacterial species engineering (Zhang 2019).

At the same time, individual genomes are sequenced more often and could be used to pinpoint the exact disease causing polymorphisms. Identification of the precise PTC location could be the key in solving the challenge of NMD therapy regarding specificity. CRISPR gene editing now enables scientists to fully utilize NMD properties that could be extremely beneficial in the future of gene therapy and diagnostics. Designing a CRISPR system to precisely target in accordance with the rules of NMD could be extremely useful for diagnosis and treatments in the future of personalized

medicine (Shalem, Sanjana, and Zhang 2015; Zhang 2019). The hope of using gene editing in conjunction with NMD to exponentially improve existing treatment for NMD based genetic disorders such as CF, DMD, and ALS - FTD are finally within reach.

Summary

NMD is an important molecular mechanism that is involved in safeguarding normal cell functions as well as fine tuning the transcriptome. Despite decades of research, NMD's implication in neuronal development and genetic diseases have only recently been realized. Further, the potential of harnessing NMD to treat related diseases have been limited due to the lack of tools, broad range of NMD targets, and the related generic cascade effects. This dissertation will first focus on the development of a robust AS-NMD reporter assay that can be used to accurately quantify endogenous NMD activity without introducing foreign agents. As a proof of principle, the assay will be used to screen existing chemical molecules for novel NMD regulators. Followed by the detection of NMD inhibition via ER stress and the consequences of such alternated NMD activities in the neurodegenerative disorder ALS - FTD. Finally, to further understand the role of NMD in neuronal development, chapter 4 focuses on one aspect of NMD in brain development by generating an *in vitro* NMD deficient neural progenitor cell (NPC) model. NPCs directly derived from existing *Upf2*$^{loxP/loxP}$ conditional knockout mouse cortical neurons. Establishing an

NMD deficient model is one crucial step forward in understanding the role of NMD in progenitor cells which have never been studied before. The goal is to highlight NMD as an important regulator in early stage neurogenesis.

References

Amrani, Nadia, Robin Ganesan, Stephanie Kervestin, David A. Mangus, Shubhendu Ghosh, and Allan Jacobson. 2004. “A Faux 3’-UTR Promotes Aberrant Termination and Triggers Nonsense-Mediated mRNA Decay.” *Nature* 432 (7013): 112–18.

Anders, Kirk R., Andrew Grimson, and Philip Anderson. 2003. “SMG-5, Required for C.elegans Nonsense-Mediated mRNA Decay, Associates with SMG-2 and Protein Phosphatase 2A.” *The EMBO Journal* 22 (3): 641–50.

Anderson, W. F., L. Gorini, and L. Breckenridge. 1965. “Role of Ribosomes in Streptomycin-Activated Suppression.” *Proceedings of the National Academy of Sciences of the United States of America* 54 (4): 1076–83.

Arai, Tetsuaki, Masato Hasegawa, Haruhiko Akiyama, Kenji Ikeda, Takashi Nonaka, Hiroshi Mori, David Mann, et al. 2006. “TDP-43 Is a Component of Ubiquitin-Positive Tau-Negative Inclusions in Frontotemporal Lobar Degeneration and Amyotrophic Lateral Sclerosis.” *Biochemical and Biophysical Research Communications* 351 (3): 602–11.

Baralle, Francisco E., and Jimena Giudice. 2017. “Alternative Splicing as a Regulator of Development and Tissue Identity.” *Nature Reviews. Molecular Cell Biology* 18 (7): 437–51.

Barmada, Sami J., Shulin Ju, Arpana Arjun, Anthony Batarse, Hilary C. Archbold, Daniel Peisach, Xingli Li, et al. 2015. “Amelioration of Toxicity in Neuronal Models of Amyotrophic Lateral Sclerosis by hUPF1.” *Proceedings of the National Academy of Sciences of the United States of America* 112 (25): 7821–26.

Barton-Davis, E. R., L. Cordier, D. I. Shoturma, S. E. Leland, and H. L. Sweeney. 1999. “Aminoglycoside Antibiotics Restore Dystrophin Function to Skeletal Muscles of Mdx Mice.” *The Journal of Clinical Investigation* 104 (4): 375–81.

Bidou, Laure, Valérie Allamand, Jean-Pierre Rousset, and Olivier Namy. 2012. “Sense from Nonsense: Therapies for Premature Stop Codon Diseases.” *Trends in Molecular Medicine* 18 (11): 679–88.

Boch, Jens, Heidi Scholze, Sebastian Schornack, Angelika Landgraf, Simone Hahn, Sabine Kay, Thomas Lahaye, Anja Nickstadt, and Ulla Bonas. 2009. “Breaking the Code of DNA Binding Specificity of TAL-Type III Effectors.” *Science* 326 (5959): 1509–12.

Bokhari, A ’dem, Vincent Jonchere, Anaïs Lagrange, Romane Bertrand, Magali

Svrcek, Laetitia Marisa, Olivier Buhard, et al. 2018. “Targeting Nonsense-Mediated mRNA Decay in Colorectal Cancers with Microsatellite Instability.” *Oncogenesis* 7 (9): 70.

Boutz, Paul L., Peter Stoilov, Qin Li, Chia-Ho Lin, Geetanjali Chawla, Kristin Ostrow, Lily Shiue, Manuel Ares Jr, and Douglas L. Black. 2007. “A Post-Transcriptional Regulatory Switch in Polypyrimidine Tract-Binding Proteins Reprograms Alternative Splicing in Developing Neurons.” *Genes & Development* 21 (13): 1636–52.

Bühler, Marc, Silvia Steiner, Fabio Mohn, Alexandra Paillusson, and Oliver Mühlemann. 2006. “EJC-Independent Degradation of Nonsense Immunoglobulin-μ mRNA Depends on 3′ UTR Length.” *Nature Structural & Molecular Biology* 13 (5): 462–64.

Burke, J. F., and A. E. Mogg. 1985. “Suppression of a Nonsense Mutation in Mammalian Cells in Vivo by the Aminoglycoside Antibiotics G-418 and Paromomycin.” *Nucleic Acids Research* 13 (17): 6265–72.

Bushby, Katharine, Richard Finkel, Brenda Wong, Richard Barohn, Craig Campbell, Giacomo P. Comi, Anne M. Connolly, et al. 2014. “Ataluren Treatment of Patients with Nonsense Mutation Dystrophinopathy.” *Muscle & Nerve* 50 (4): 477–87.

Cali, B. M., S. L. Kuchma, J. Latham, and P. Anderson. 1999. “Smg-7 Is Required for mRNA Surveillance in Caenorhabditis Elegans.” *Genetics* 151 (2): 605–16.

Chamieh, Hala, Lionel Ballut, Fabien Bonneau, and Hervé Le Hir. 2008. “NMD Factors UPF2 and UPF3 Bridge UPF1 to the Exon Junction Complex and Stimulate Its RNA Helicase Activity.” *Nature Structural & Molecular Biology* 15 (1): 85–93.

Chang, J. C., and Y. W. Kan. 1979. “Beta 0 Thalassemia, a Nonsense Mutation in Man.” *Proceedings of the National Academy of Sciences of the United States of America* 76 (6): 2886–89.

Chang, Yao-Fu, J. Saadi Imam, and Miles F. Wilkinson. 2007. “The Nonsense-Mediated Decay RNA Surveillance Pathway.” *Annual Review of Biochemistry* 76: 51–74.

Chan, Wai-Kin, Lulu Huang, Jayanthi P. Gudikote, Yao-Fu Chang, J. Saadi Imam, James A. MacLean 2nd, and Miles F. Wilkinson. 2007. “An Alternative Branch of the Nonsense-Mediated Decay Pathway.” *The EMBO Journal* 26 (7): 1820–30.

Chiu, Shang-Yi, Guillaume Serin, Osamu Ohara, and Lynne E. Maquat. 2003. "Characterization of Human Smg5/7a: A Protein with Similarities to Caenorhabditis Elegans SMG5 and SMG7 That Functions in the Dephosphorylation of Upf1." *RNA* 9 (1): 77–87.

Colak, Dilek, Sheng-Jian Ji, Bo T. Porse, and Samie R. Jaffrey. 2013. "Regulation of Axon Guidance by Compartmentalized Nonsense-Mediated mRNA Decay." *Cell* 153 (6): 1252–65.

Colombo, Martino, Evangelos D. Karousis, Joël Bourquin, Rémy Bruggmann, and Oliver Mühlemann. 2017. "Transcriptome-Wide Identification of NMD-Targeted Human mRNAs Reveals Extensive Redundancy between SMG6- and SMG7-Mediated Degradation Pathways." *RNA* 23 (2): 189–201.

Cong, Le, F. Ann Ran, David Cox, Shuailiang Lin, Robert Barretto, Naomi Habib, Patrick D. Hsu, et al. 2013. "Multiplex Genome Engineering Using CRISPR/Cas Systems." *Science* 339 (6121): 819–23.

Cong, Le, and Feng Zhang. 2015. "Genome Engineering Using CRISPR-Cas9 System." *Methods in Molecular Biology* 1239: 197–217.

Czaplinski, K., M. J. Ruiz-Echevarria, S. V. Paushkin, X. Han, Y. Weng, H. A. Perlick, H. C. Dietz, M. D. Ter-Avanesyan, and S. W. Peltz. 1998. "The Surveillance Complex Interacts with the Translation Release Factors to Enhance Termination and Degrade Aberrant mRNAs." *Genes & Development* 12 (11): 1665–77.

Davies, J., W. Gilbert, and L. Gorini. 1964. "STREPTOMYCIN, SUPPRESSION, AND THE CODE." *Proceedings of the National Academy of Sciences of the United States of America* 51 (May): 883–90.

Doudna, Jennifer A., and Emmanuelle Charpentier. 2014. "Genome Editing. The New Frontier of Genome Engineering with CRISPR-Cas9." *Science* 346 (6213): 1258096.

Eberle, Andrea B., Søren Lykke-Andersen, Oliver Mühlemann, and Torben Heick Jensen. 2009. "SMG6 Promotes Endonucleolytic Cleavage of Nonsense mRNA in Human Cells." *Nature Structural & Molecular Biology* 16 (1): 49–55.

Fatscher, Tobias, Volker Boehm, Benjamin Weiche, and Niels H. Gehring. 2014. "The Interaction of Cytoplasmic poly(A)-Binding Protein with Eukaryotic Initiation Factor 4G Suppresses Nonsense-Mediated mRNA Decay." *RNA* 20 (10): 1579–92.

Franks, Tobias M., Guramrit Singh, and Jens Lykke-Andersen. 2010. “Upf1 ATPase-Dependent mRNP Disassembly Is Required for Completion of Nonsense- Mediated mRNA Decay.” *Cell* 143 (6): 938–50.

Gardner, Lawrence B. 2010. “Nonsense-Mediated RNA Decay Regulation by Cellular Stress: Implications for Tumorigenesis.” *Molecular Cancer Research: MCR* 8 (3): 295–308.

Gehring, Niels H., Gabriele Neu-Yilik, Thomas Schell, Matthias W. Hentze, and Andreas E. Kulozik. 2003. “Y14 and hUpf3b Form an NMD-Activating Complex.” *Molecular Cell* 11 (4): 939–49.

Han, Xin, Yanling Wei, Hua Wang, Feilong Wang, Zhenyu Ju, and Tangliang Li. 2018. “Nonsense-Mediated mRNA Decay: A ‘Nonsense’ Pathway Makes Sense in Stem Cell Biology.” *Nucleic Acids Research* 46 (3): 1038–51.

Hogg, J. Robert, and Stephen P. Goff. 2010. “Upf1 Senses 3’UTR Length to Potentiate mRNA Decay.” *Cell* 143 (3): 379–89.

Huang, L., E. Y. Shum, S. H. Jones, C-H Lou, J. Dumdie, H. Kim, A. J. Roberts, et al. 2018. “A Upf3b-Mutant Mouse Model with Behavioral and Neurogenesis Defects.” *Molecular Psychiatry* 23 (8): 1773–86.

Huang, Lulu, Chih-Hong Lou, Waikin Chan, Eleen Y. Shum, Ada Shao, Erica Stone, Rachid Karam, Hye-Won Song, and Miles F. Wilkinson. 2011. “RNA Homeostasis Governed by Cell Type-Specific and Branched Feedback Loops Acting on NMD.” *Molecular Cell* 43 (6): 950–61.

Huang, Lulu, Audrey Low, Sagar S. Damle, Melissa M. Keenan, Steven Kuntz, Susan F. Murray, Brett P. Monia, and Shuling Guo. 2018. “Antisense Suppression of the Nonsense Mediated Decay Factor Upf3b as a Potential Treatment for Diseases Caused by Nonsense Mutations.” *Genome Biology* 19 (1): 4.

Hug, Nele, Dasa Longman, and Javier F. Cáceres. 2016. “Mechanism and Regulation of the Nonsense-Mediated Decay Pathway.” *Nucleic Acids Research* 44 (4): 1483–95.

Huntzinger, Eric, Isao Kashima, Maria Fauser, Jérôme Saulière, and Elisa Izaurralde. 2008. “SMG6 Is the Catalytic Endonuclease That Cleaves mRNAs Containing Nonsense Codons in Metazoan.” *RNA* 14 (12): 2609–17.

Ishigaki, Y., X. Li, G. Serin, and L. E. Maquat. 2001. “Evidence for a Pioneer Round of mRNA Translation: mRNAs Subject to Nonsense-Mediated Decay

in Mammalian Cells Are Bound by CBP80 and CBP20." *Cell* 106 (5): 607–17.

Ishino, Y., H. Shinagawa, K. Makino, M. Amemura, and A. Nakata. 1987. "Nucleotide Sequence of the Iap Gene, Responsible for Alkaline Phosphatase Isozyme Conversion in Escherichia Coli, and Identification of the Gene Product." *Journal of Bacteriology* 169 (12): 5429–33.

Isken, Olaf, and Lynne E. Maquat. 2008. "The Multiple Lives of NMD Factors: Balancing Roles in Gene and Genome Regulation." *Nature Reviews. Genetics* 9 (9): 699–712.

Ivanov, Pavel V., Niels H. Gehring, Joachim B. Kunz, Matthias W. Hentze, and Andreas E. Kulozik. 2008. "Interactions between UPF1, eRFs, PABP and the Exon Junction Complex Suggest an Integrated Model for Mammalian NMD Pathways." *The EMBO Journal* 27 (5): 736–47.

Jaffrey, Samie R., and Miles F. Wilkinson. 2018. "Nonsense-Mediated RNA Decay in the Brain: Emerging Modulator of Neural Development and Disease." *Nature Reviews. Neuroscience* 19 (12): 715–28.

Jinek, Martin, Krzysztof Chylinski, Ines Fonfara, Michael Hauer, Jennifer A. Doudna, and Emmanuelle Charpentier. 2012. "A Programmable Dual-RNA-Guided DNA Endonuclease in Adaptive Bacterial Immunity." *Science* 337 (6096): 816–21.

Johnson, Jennifer L., Loredana Stoica, Yuwei Liu, Ping Jun Zhu, Abhisek Bhattacharya, Shelly A. Buffington, Redwan Huq, et al. 2019. "Inhibition of Upf2-Dependent Nonsense-Mediated Decay Leads to Behavioral and Neurophysiological Abnormalities by Activating the Immune Response." *Neuron* 104 (4): 665–79.e8.

Jolly, Lachlan A., Claire C. Homan, Reuben Jacob, Simon Barry, and Jozef Gecz. 2013. "The UPF3B Gene, Implicated in Intellectual Disability, Autism, ADHD and Childhood Onset Schizophrenia Regulates Neural Progenitor Cell Behaviour and Neuronal Outgrowth." *Human Molecular Genetics* 22 (23): 4673–87.

Kadlec, Jan, Elisa Izaurralde, and Stephen Cusack. 2004. "The Structural Basis for the Interaction between Nonsense-Mediated mRNA Decay Factors UPF2 and UPF3." *Nature Structural & Molecular Biology* 11 (4): 330–37.

Kashima, Isao, Akio Yamashita, Natsuko Izumi, Naoyuki Kataoka, Ryo Morishita, Shinichi Hoshino, Mutsuhito Ohno, Gideon Dreyfuss, and Shigeo Ohno. 2006. "Binding of a Novel SMG-1–Upf1–eRF1–eRF3 Complex (SURF) to

the Exon Junction Complex Triggers Upf1 Phosphorylation and Nonsense-Mediated mRNA Decay." *Genes & Development* 20 (3): 355–67.

Keeling, Kim M., and David M. Bedwell. 2011. "Suppression of Nonsense Mutations as a Therapeutic Approach to Treat Genetic Diseases." *Wiley Interdisciplinary Reviews. RNA* 2 (6): 837–52.

Kelly, T. J., Jr, and H. O. Smith. 1970. "A Restriction Enzyme from Hemophilus Influenzae. II." *Journal of Molecular Biology* 51 (2): 393–409.

Kerem, Eitan. 2004. "Pharmacologic Therapy for Stop Mutations: How Much CFTR Activity Is Enough?" *Current Opinion in Pulmonary Medicine* 10 (6): 547–52.

Kerem, Eitan, Michael W. Konstan, Kris De Boeck, Frank J. Accurso, Isabelle Sermet-Gaudelus, Michael Wilschanski, J. Stuart Elborn, et al. 2014. "Ataluren for the Treatment of Nonsense-Mutation Cystic Fibrosis: A Randomised, Double-Blind, Placebo-Controlled Phase 3 Trial." *The Lancet. Respiratory Medicine* 2 (7): 539–47.

Kerr, T. P., C. A. Sewry, S. A. Robb, and R. G. Roberts. 2001. "Long Mutant Dystrophins and Variable Phenotypes: Evasion of Nonsense-Mediated Decay?" *Human Genetics* 109 (4): 402–7.

Khajavi, Mehrdad, Ken Inoue, and James R. Lupski. 2006. "Nonsense-Mediated mRNA Decay Modulates Clinical Outcome of Genetic Disease." *European Journal of Human Genetics: EJHG* 14 (10): 1074–81.

Kim, Hyongbum, and Jin-Soo Kim. 2014. "A Guide to Genome Engineering with Programmable Nucleases." *Nature Reviews. Genetics* 15 (5): 321–34.

Kim, Yoon Ki, and Lynne E. Maquat. 2019. "UPFront and Center in RNA Decay: UPF1 in Nonsense-Mediated mRNA Decay and beyond." *RNA* 25 (4): 407–22.

Koenig, M., E. P. Hoffman, C. J. Bertelson, A. P. Monaco, C. Feener, and L. M. Kunkel. 1987. "Complete Cloning of the Duchenne Muscular Dystrophy (DMD) cDNA and Preliminary Genomic Organization of the DMD Gene in Normal and Affected Individuals." *Cell* 50 (3): 509–17.

Kurosaki, Tatsuaki, and Lynne E. Maquat. 2013. "Rules That Govern UPF1 Binding to mRNA 3′ UTRs." *Proceedings of the National Academy of Sciences* 110 (9): 3357–62.

———. 2016. "Nonsense-Mediated mRNA Decay in Humans at a Glance."

Journal of Cell Science 129 (3): 461–67.

Kurosaki, Tatsuaki, Maximilian W. Popp, and Lynne E. Maquat. 2019. “Quality and Quantity Control of Gene Expression by Nonsense-Mediated mRNA Decay.” *Nature Reviews. Molecular Cell Biology* 20 (7): 406–20.

Kuzmiak, Holly A., and Lynne E. Maquat. 2006. “Applying Nonsense-Mediated mRNA Decay Research to the Clinic: Progress and Challenges.” *Trends in Molecular Medicine* 12 (7): 306–16.

Lareau, Liana F., Angela N. Brooks, David A. W. Soergel, Qi Meng, and Steven E. Brenner. n.d. “The Coupling of Alternative Splicing and Nonsense-Mediated mRNA Decay.” http://compbio.berkeley.edu/people/brenner/pubs/lareau-2007-landes-nmd.pdf.

Leeds, P., S. W. Peltz, A. Jacobson, and M. R. Culbertson. 1991. “The Product of the Yeast UPF1 Gene Is Required for Rapid Turnover of mRNAs Containing a Premature Translational Termination Codon.” *Genes & Development* 5 (12A): 2303–14.

Lee, Yeon, and Donald C. Rio. 2015. “Mechanisms and Regulation of Alternative Pre-mRNA Splicing.” *Annual Review of Biochemistry* 84 (March): 291–323.

Le Hir, Hervé, Jérôme Saulière, and Zhen Wang. 2016. “The Exon Junction Complex as a Node of Post-Transcriptional Networks.” *Nature Reviews. Molecular Cell Biology* 17 (1): 41–54.

Le Hir, H., D. Gatfield, E. Izaurralde, and M. J. Moore. 2001. “The Exon-Exon Junction Complex Provides a Binding Platform for Factors Involved in mRNA Export and Nonsense-Mediated mRNA Decay.” *The EMBO Journal* 20 (17): 4987–97.

Le Hir, H., E. Izaurralde, L. E. Maquat, and M. J. Moore. 2000. “The Spliceosome Deposits Multiple Proteins 20-24 Nucleotides Upstream of mRNA Exon-Exon Junctions.” *The EMBO Journal* 19 (24): 6860–69.

Lewis, Benjamin P., Richard E. Green, and Steven E. Brenner. 2003. “Evidence for the Widespread Coupling of Alternative Splicing and Nonsense-Mediated mRNA Decay in Humans.” *Proceedings of the National Academy of Sciences of the United States of America* 100 (1): 189–92.

Linde, Liat, Stephanie Boelz, Malka Nissim-Rafinia, Yifat S. Oren, Michael Wilschanski, Yasmin Yaacov, Dov Virgilis, et al. 2007. “Nonsense-Mediated mRNA Decay Affects Nonsense Transcript Levels and Governs Response of

Cystic Fibrosis Patients to Gentamicin." *The Journal of Clinical Investigation* 117 (3): 683–92.

Linde, Liat, and Batsheva Kerem. n.d. "Nonsense-Mediated mRNA Decay and Cystic Fibrosis." In *Cystic Fibrosis*, edited by Margarida D. Amaral and Karl Kunzelmann, 137–54. Methods in Molecular Biology . Humana Press.

Ling, Jonathan P., Olga Pletnikova, Juan C. Troncoso, and Philip C. Wong. 2015. "TDP-43 Repression of Nonconserved Cryptic Exons Is Compromised in ALS-FTD." *Science* 349 (6248): 650–55.

Losson, R., and F. Lacroute. 1979. "Interference of Nonsense Mutations with Eukaryotic Messenger RNA Stability." *Proceedings of the National Academy of Sciences of the United States of America* 76 (10): 5134–37.

Lou, Chih H., Ada Shao, Eleen Y. Shum, Josh L. Espinoza, Lulu Huang, Rachid Karam, and Miles F. Wilkinson. 2014. "Posttranscriptional Control of the Stem Cell and Neurogenic Programs by the Nonsense-Mediated RNA Decay Pathway." *Cell Reports* 6 (4): 748–64.

Lueck, John D., Jae Seok Yoon, Alfredo Perales-Puchalt, Adam L. Mackey, Daniel T. Infield, Mark A. Behlke, Marshall R. Pope, et al. 2019. "Engineered Transfer RNAs for Suppression of Premature Termination Codons." *Nature Communications* 10 (1): 822.

Lykke-Andersen, J., M. D. Shu, and J. A. Steitz. 2000. "Human Upf Proteins Target an mRNA for Nonsense-Mediated Decay When Bound Downstream of a Termination Codon." *Cell* 103 (7): 1121–31.

Lykke-Andersen, Søren, Yun Chen, Britt R. Ardal, Berit Lilje, Johannes Waage, Albin Sandelin, and Torben Heick Jensen. 2014. "Human Nonsense-Mediated RNA Decay Initiates Widely by Endonucleolysis and Targets snoRNA Host Genes." *Genes & Development* 28 (22): 2498–2517.

Lykke-Andersen, Søren, and Torben Heick Jensen. 2015. "Nonsense-Mediated mRNA Decay: An Intricate Machinery That Shapes Transcriptomes." *Nature Reviews. Molecular Cell Biology* 16 (11): 665–77.

Manning, Kassie S., and Thomas A. Cooper. 2017. "The Roles of RNA Processing in Translating Genotype to Phenotype." *Nature Reviews. Molecular Cell Biology* 18 (2): 102–14.

Manuvakhova, M., K. Keeling, and D. M. Bedwell. 2000. "Aminoglycoside Antibiotics Mediate Context-Dependent Suppression of Termination Codons in a Mammalian Translation System." *RNA* 6 (7): 1044–55.

Maquat, L. E., A. J. Kinniburgh, E. A. Rachmilewitz, and J. Ross. 1981. “Unstable Beta-Globin mRNA in mRNA-Deficient Beta O Thalassemia.” *Cell* 27 (3 Pt 2): 543–53.

Maquat, Lynne E., Woan-Yuh Tarn, and Olaf Isken. 2010. “The Pioneer Round of Translation: Features and Functions.” *Cell* 142 (3): 368–74.

Martin, Leenus, Arsen Grigoryan, Ding Wang, Jinhua Wang, Laura Breda, Stefano Rivella, Timothy Cardozo, and Lawrence B. Gardner. 2014. “Identification and Characterization of Small Molecules That Inhibit Nonsense-Mediated RNA Decay and Suppress Nonsense p53 Mutations.” *Cancer Research* 74 (11): 3104–13.

Matsuda, Daiki, Nao Hosoda, Yoon Ki Kim, and Lynne E. Maquat. 2007. “Failsafe Nonsense-Mediated mRNA Decay Does Not Detectably Target eIF4E-Bound mRNA.” *Nature Structural & Molecular Biology* 14 (10): 974–79.

McDonald, Craig M., Craig Campbell, Ricardo Erazo Torricelli, Richard S. Finkel, Kevin M. Flanigan, Nathalie Goemans, Peter Heydemann, et al. 2017. “Ataluren in Patients with Nonsense Mutation Duchenne Muscular Dystrophy (ACT DMD): A Multicentre, Randomised, Double-Blind, Placebo-Controlled, Phase 3 Trial.” *The Lancet* 390 (10101): 1489–98.

Meaux, Stacie, Ambro van Hoof, and Kristian E. Baker. 2008. “Nonsense-Mediated mRNA Decay in Yeast Does Not Require PAB1 or a poly(A) Tail.” *Molecular Cell* 29 (1): 134–40.

Melero, Roberto, Akiko Uchiyama, Raquel Castaño, Naoyuki Kataoka, Hitomi Kurosawa, Shigeo Ohno, Akio Yamashita, and Oscar Llorca. 2014. “Structures of SMG1-UPFs Complexes: SMG1 Contributes to Regulate UPF2-Dependent Activation of UPF1 in NMD.” *Structure* 22 (8): 1105–19.

Mendell, Joshua T., Neda A. Sharifi, Jennifer L. Meyers, Francisco Martinez-Murillo, and Harry C. Dietz. 2004. “Nonsense Surveillance Regulates Expression of Diverse Classes of Mammalian Transcripts and Mutes Genomic Noise.” *Nature Genetics* 36 (10): 1073–78.

Mendell, J. T., and H. C. Dietz. 2001. “When the Message Goes Awry: Disease-Producing Mutations That Influence mRNA Content and Performance.” *Cell* 107 (4): 411–14.

Miller, Jake N., and David A. Pearce. 2014. “Nonsense-Mediated Decay in Genetic Disease: Friend or Foe?” *Mutation Research-Reviews in Mutation Research* 762 (October): 52–64.

Miller, J., A. D. McLachlan, and A. Klug. 1985. “Repetitive Zinc-Binding Domains in the Protein Transcription Factor IIIA from Xenopus Oocytes.” *The EMBO Journal* 4 (6): 1609–14.

Mort, Matthew, Dobril Ivanov, David N. Cooper, and Nadia A. Chuzhanova. 2008. “A Meta-Analysis of Nonsense Mutations Causing Human Genetic Disease.” *Human Mutation* 29 (8): 1037–47.

Nagel-Wolfrum, Kerstin, Fabian Möller, Inessa Penner, Timor Baasov, and Uwe Wolfrum. 2016. “Targeting Nonsense Mutations in Diseases with Translational Read-Through-Inducing Drugs (TRIDs).” *BioDrugs: Clinical Immunotherapeutics, Biopharmaceuticals and Gene Therapy* 30 (2): 49–74.

Nagy, E., and L. E. Maquat. 1998. “A Rule for Termination-Codon Position within Intron-Containing Genes: When Nonsense Affects RNA Abundance.” *Trends in Biochemical Sciences* 23 (6): 198–99.

Ni, Julie Z., Leslie Grate, John Paul Donohue, Christine Preston, Naomi Nobida, Georgeann O’Brien, Lily Shiue, Tyson A. Clark, John E. Blume, and Manuel Ares Jr. 2007. “Ultraconserved Elements Are Associated with Homeostatic Control of Splicing Regulators by Alternative Splicing and Nonsense-Mediated Decay.” *Genes & Development* 21 (6): 708–18.

Nott, Ajit, Shlomo H. Meislin, and Melissa J. Moore. 2003. “A Quantitative Analysis of Intron Effects on Mammalian Gene Expression.” *RNA* 9 (5): 607–17.

Okada-Katsuhata, Yukiko, Akio Yamashita, Kei Kutsuzawa, Natsuko Izumi, Fumiki Hirahara, and Shigeo Ohno. 2012. “N- and C-Terminal Upf1 Phosphorylations Create Binding Platforms for SMG-6 and SMG-5:SMG-7 during NMD.” *Nucleic Acids Research* 40 (3): 1251–66.

Pan, Qun, Arneet L. Saltzman, Yoon Ki Kim, Christine Misquitta, Ofer Shai, Lynne E. Maquat, Brendan J. Frey, and Benjamin J. Blencowe. 2006. “Quantitative Microarray Profiling Provides Evidence against Widespread Coupling of Alternative Splicing with Nonsense-Mediated mRNA Decay to Control Gene Expression.” *Genes & Development* 20 (2): 153–58.

Peccarelli, Megan, and Bessie W. Kebaara. 2014. “Regulation of Natural mRNAs by the Nonsense-Mediated mRNA Decay Pathway.” *Eukaryotic Cell* 13 (9): 1126–35.

Peixeiro, Isabel, Ângela Inácio, Cristina Barbosa, Ana Luísa Silva, Stephen A. Liebhaber, and Luísa Romão. 2012. “Interaction of PABPC1 with the Translation Initiation Complex Is Critical to the NMD Resistance of AUG-

Proximal Nonsense Mutations.” *Nucleic Acids Research* 40 (3): 1160–73.

Popp, Maximilian W., and Lynne E. Maquat. 2016. “Leveraging Rules of Nonsense-Mediated mRNA Decay for Genome Engineering and Personalized Medicine.” *Cell* 165 (6): 1319–22.

———. 2018. “Nonsense-Mediated mRNA Decay and Cancer.” *Current Opinion in Genetics & Development* 48 (February): 44–50.

Pulak, R., and P. Anderson. 1993. “mRNA Surveillance by the Caenorhabditis Elegans Smg Genes.” *Genes & Development* 7 (10): 1885–97.

Rehwinkel, Jan, Ivica Letunic, Jeroen Raes, Peer Bork, and Elisa Izaurralde. 2005. “Nonsense-Mediated mRNA Decay Factors Act in Concert to Regulate Common mRNA Targets.” *RNA* 11 (10): 1530–44.

Saltzman, Arneet L., Yoon Ki Kim, Qun Pan, Matthew M. Fagnani, Lynne E. Maquat, and Benjamin J. Blencowe. 2008. “Regulation of Multiple Core Spliceosomal Proteins by Alternative Splicing-Coupled Nonsense-Mediated mRNA Decay.” *Molecular and Cellular Biology* 28 (13): 4320–30.

Schmidt, Skye A., Patricia L. Foley, Dong-Hoon Jeong, Linda A. Rymarquis, Francis Doyle, Scott A. Tenenbaum, Joel G. Belasco, and Pamela J. Green. 2015. “Identification of SMG6 Cleavage Sites and a Preferred RNA Cleavage Motif by Global Analysis of Endogenous NMD Targets in Human Cells.” *Nucleic Acids Research* 43 (1): 309–23.

Schuller, Anthony P., Boris Zinshteyn, Syed Usman Enam, and Rachel Green. 2018. “Directed Hydroxyl Radical Probing Reveals Upf1 Binding to the 80S Ribosomal E Site rRNA at the L1 Stalk.” *Nucleic Acids Research* 46 (4): 2060–73.

Scotti, Marina M., and Maurice S. Swanson. 2016. “RNA Mis-Splicing in Disease.” *Nature Reviews. Genetics* 17 (1): 19–32.

Serdar, Lucas D., Dajuan L. Whiteside, and Kristian E. Baker. 2016. “ATP Hydrolysis by UPF1 Is Required for Efficient Translation Termination at Premature Stop Codons.” *Nature Communications* 7 (December): 14021.

Shalem, Ophir, Neville E. Sanjana, and Feng Zhang. 2015. “High-Throughput Functional Genomics Using CRISPR-Cas9.” *Nature Reviews. Genetics* 16 (5): 299–311.

Shigeoka, Toshiaki, Sayaka Kato, Masashi Kawaichi, and Yasumasa Ishida. 2012. “Evidence That the Upf1-Related Molecular Motor Scans the 3′-UTR

to Ensure mRNA Integrity." *Nucleic Acids Research* 40 (14): 6887–97.

Shi, Min, Heng Zhang, Lantian Wang, Changlan Zhu, Ke Sheng, Yanhua Du, Ke Wang, et al. 2015. "Premature Termination Codons Are Recognized in the Nucleus in A Reading-Frame Dependent Manner." *Cell Discovery* 1 (May). https://doi.org/10.1038/celldisc.2015.1.

Shum, Eleen Y., Samantha H. Jones, Ada Shao, Jennifer Dumdie, Matthew D. Krause, Wai-Kin Chan, Chih-Hong Lou, et al. 2016. "The Antagonistic Gene Paralogs Upf3a and Upf3b Govern Nonsense-Mediated RNA Decay." *Cell* 165 (2): 382–95.

Singh, Guramrit, Indrani Rebbapragada, and Jens Lykke-Andersen. 2008. "A Competition between Stimulators and Antagonists of Upf Complex Recruitment Governs Human Nonsense-Mediated mRNA Decay." *PLoS Biology* 6 (4): e111.

Smith, H. O., and K. W. Wilcox. 1970. "A Restriction Enzyme from Hemophilus Influenzae. I. Purification and General Properties." *Journal of Molecular Biology* 51 (2): 379–91.

Spellman, Rachel, Miriam Llorian, and Christopher W. J. Smith. 2007. "Crossregulation and Functional Redundancy between the Splicing Regulator PTB and Its Paralogs nPTB and ROD1." *Molecular Cell* 27 (3): 420–34.

Thoren, Lina A., Gitte A. Nørgaard, Joachim Weischenfeldt, Johannes Waage, Janus S. Jakobsen, Inge Damgaard, Frida C. Bergström, et al. 2010. "UPF2 Is a Critical Regulator of Liver Development, Function and Regeneration." *PloS One* 5 (7): e11650.

Toma, Kalodiah G., Indrani Rebbapragada, Sébastien Durand, and Jens Lykke-Andersen. 2015. "Identification of Elements in Human Long 3' UTRs That Inhibit Nonsense-Mediated Decay." *RNA* 21 (5): 887–97.

Tuladhar, Rubina, Yunku Yeu, John Tyler Piazza, Zhen Tan, Jean Rene Clemenceau, Xiaofeng Wu, Quinn Barrett, et al. 2019. "CRISPR-Cas9-Based Mutagenesis Frequently Provokes on-Target mRNA Misregulation." *Nature Communications* 10 (1): 4056.

Usuki, Fusako, Akio Yamashita, Tadafumi Shiraishi, Atsushi Shiga, Osamu Onodera, Itsuro Higuchi, and Shigeo Ohno. 2013. "Inhibition of SMG-8, a Subunit of SMG-1 Kinase, Ameliorates Nonsense-Mediated mRNA Decay-Exacerbated Mutant Phenotypes without Cytotoxicity." *Proceedings of the National Academy of Sciences of the United States of America* 110 (37):

15037–42.

Vuong, Celine K., Douglas L. Black, and Sika Zheng. 2016. “The Neurogenetics of Alternative Splicing.” *Nature Reviews. Neuroscience* 17 (5): 265–81.

Weischenfeldt, Joachim, Inge Damgaard, David Bryder, Kim Theilgaard-Mönch, Lina A. Thoren, Finn Cilius Nielsen, Sten Eirik W. Jacobsen, Claus Nerlov, and Bo Torben Porse. 2008. “NMD Is Essential for Hematopoietic Stem and Progenitor Cells and for Eliminating by-Products of Programmed DNA Rearrangements.” *Genes & Development* 22 (10): 1381–96.

Weischenfeldt, Joachim, Johannes Waage, Geng Tian, Jing Zhao, Inge Damgaard, Janus Schou Jakobsen, Karsten Kristiansen, Anders Krogh, Jun Wang, and Bo T. Porse. 2012. “Mammalian Tissues Defective in Nonsense-Mediated mRNA Decay Display Highly Aberrant Splicing Patterns.” *Genome Biology* 13 (5): R35.

Welch, Ellen M., Elisabeth R. Barton, Jin Zhuo, Yuki Tomizawa, Westley J. Friesen, Panayiota Trifillis, Sergey Paushkin, et al. 2007. “PTC124 Targets Genetic Disorders Caused by Nonsense Mutations.” *Nature* 447 (7140): 87–91.

Wittmann, Jürgen, Elly M. Hol, and Hans-Martin Jäck. 2006. “hUPF2 Silencing Identifies Physiologic Substrates of Mammalian Nonsense-Mediated mRNA Decay.” *Molecular and Cellular Biology* 26 (4): 1272–87.

Yamashita, Akio, Natsuko Izumi, Isao Kashima, Tetsuo Ohnishi, Bonnie Saari, Yukiko Katsuhata, Reiko Muramatsu, et al. 2009. “SMG-8 and SMG-9, Two Novel Subunits of the SMG-1 Complex, Regulate Remodeling of the mRNA Surveillance Complex during Nonsense-Mediated mRNA Decay.” *Genes & Development* 23 (9): 1091–1105.

Yamashita, A., T. Ohnishi, I. Kashima, Y. Taya, and S. Ohno. 2001. “Human SMG-1, a Novel Phosphatidylinositol 3-Kinase-Related Protein Kinase, Associates with Components of the mRNA Surveillance Complex and Is Involved in the Regulation of Nonsense-Mediated mRNA Decay.” *Genes & Development* 15 (17): 2215–28.

Zhang, F. 2019. “Development of CRISPR-Cas Systems for Genome Editing and beyond.” *Quarterly Reviews of Biophysics* 52. https://doi.org/10.1017/S0033583519000052.

Zheng, Sika. 2016. “Alternative Splicing and Nonsense-Mediated mRNA Decay Enforce Neural Specific Gene Expression.” *International Journal of Developmental Neuroscience: The Official Journal of the International*

Society for Developmental Neuroscience, March. https://doi.org/10.1016/j.ijdevneu.2016.03.003.

Zheng, Sika, Erin E. Gray, Geetanjali Chawla, Bo Torben Porse, Thomas J. O'Dell, and Douglas L. Black. 2012. "PSD-95 Is Post-Transcriptionally Repressed during Early Neural Development by PTBP1 and PTBP2." *Nature Neuroscience* 15 (3): 381–88, S1.

Chapter 2: A new quantitative approach for monitoring nonsense-mediated RNA decay

Abstract

Conventional approaches to monitoring cellular nonsense-mediated RNA decay (NMD), an important post transcriptional regulation mechanism, are either using exogenous PTC-containing reporters or traditional endogenous RT-qPCR splicing assays. Assessing NMD activity using foreign reporter genes often introduces unpredictable factors that can be misleading. On the other hand, traditional RT-qPCR has difficulties distinguishing NMD from other transcriptional events such as increased or decreased transcription and alternative splicing (AS). To overcome these inherently problematic aspects of NMD assays, a broadly applicable AS-NMD assay was developed using exon junction primers to reliably and easily monitor cellular NMD activity. The new AS-NMD assay is genetically validated for distinguishing NMD regulation from transcriptional control and AS regulation. This method is also sensitive enough to quantify the different magnitudes of NMD targets to NMD inhibition. Further, the AS-NMD method is applied toward screening for NMD modulators such as ouabain, ionomycin, and other chemical inhibitors.

Introduction

Nonsense-mediated RNA decay (NMD) is a surveillance mechanism that selectively degrades mutated and aberrantly processed transcripts harboring premature termination codons (S. Lykke-Andersen and Jensen 2015; Kurosaki, Popp, and Maquat 2019; Chang, Imam, and Wilkinson 2007). A transcript with a stop codon >50 nts upstream of an exon-exon junction (EJ) is consistently targeted by NMD for degradation. Such an RNA structure may result from the following circumstances: an upstream open reading frame in the 5' untranslated region; a spliced intron in the 3'UTR; alternative mRNA splicing shifting the reading frame and resulting in a PTC upstream of an exon junction complex (EJC); and the inclusion of a middle alternative "toxic" exon containing an in-frame PTC (S. Lykke-Andersen and Jensen 2015; Pan et al. 2006; Lareau et al., n.d.; Popp and Maquat 2013).

In addition to serving as a surveillance mechanism, NMD is also an essential gene regulation mechanism that quantitatively finetunes the abundance of physiologic transcripts with NMD features (Nott, Meislin, and Moore 2003; Rehwinkel et al. 2005; Chang, Imam, and Wilkinson 2007; Isken and Maquat 2007; Wang et al. 2011; Yepiskoposyan et al. 2011; Tani et al. 2012; S. Lykke-Andersen and Jensen 2015). It directly or indirectly controls the expression levels of many natural transcripts that are responsible for cell fates, functions, and developments (Jaffrey and Wilkinson 2018; Han et al. 2018; Sika Zheng 2016; Sika Zheng et al. 2013).

Nonsense mutations often lead to the loss of protein products due to NMD activity, which accounts for the molecular pathogenesis of over 20% monogenic diseases (Lindeboom, Supek, and Lehner 2016; Kurosaki, Popp, and Maquat 2019). Given NMD's essential role in disease pathogenesis and gene expression regulation, methods that precisely detect changes in cellular NMD activity are of great interest and can facilitate the analysis of NMD controls in response to extracellular stimuli or during development. Traditional methods rely on a pair of plasmid reporters, with one containing a PTC and the other lacking a PTC (Pereverzev et al. 2015; Nickless and You 2018; Bonifacino et al. 2001; Paillusson et al. 2005). The two contrasting reporters are separately delivered into the cultured cells, usually along with a third plasmid to control cell-to-cell variation, and the reporter transcripts are assayed individually. The reporter pair is engineered to normalize the impact of transcription and other regulatory mechanisms affecting transcript abundance in order to isolate NMD regulation (Pereverzev et al. 2015; Nickless and You 2018; Bonifacino et al. 2001; Paillusson et al. 2005). Variables inherent to a general reporter gene approach, including the degree of overexpression, transfection methods, the choice of the reporters and cell density, affect the robustness of the assay and have to be painstakingly controlled to enhance the signal-to-noise ratio. Cell lines stably expressing a reporter gene can mitigate variation induced by transient transfection, but they introduce new variables, such as integration loci and copy numbers, which unpredictably affect reporter readout (Gerbracht, Boehm, and

Gehring 2017; Sika Zheng 2016; S. Zheng 2016).

Even though exogenous reporter assays have been invaluable in characterizing molecular mechanisms of NMD, their application has unfortunately been restricted to transfectable cells and are handicapped in certain aforementioned aspects. There is an urgent need for a broadly applicable method to track cellular NMD activity where transfection of reporters is difficult, e.g., in primary cells, tissue organs and animals. Ideally this new method would also be simpler, faster, and less expensive than the conventional exogenous reporter assays. To address these needs, this chapter aims to detail a novel assay based on endogenous NMD targets. Assaying endogenous targets does not have the limitations associated with exogenous reporters and does not require secondary validations. Hard-to-transfect samples and postmortem tissues also become assessable. Furthermore, multiple endogenous targets can be examined in parallel to improve the robustness of the assay, whereas the reporter approach usually deals with one exogenous target at a time. The advantages of directly assaying endogenous targets are summarized in Table 2.

Monitoring NMD activity through endogenous NMD targets is, however, inherently challenging. It is hard to discern direct NMD targets. Although many genes have altered expression levels in NMD-deficient cells, some of the changes observed upon NMD deficiency may instead result from transcriptional regulation as an indirect consequence of NMD inhibition (Rehwinkel et al. 2005; Colombo et al. 2017). It is also unclear whether their responses to NMD

regulation depend on the cell type or cellular context (Huang et al. 2011). All endogenous NMD targets, direct or indirect, are under constant transcriptional regulation and subject to myriad possibilities of multifactorial regulation; hence, changes in their expression levels alone are not robust predictors of cellular NMD efficiency. These endogenous NMD targets are not suitable for unbiased screening of NMD modulators expecting high specificity and low false discovery, because transcriptional modulators would constitute a great proportion of the false positives (Andreassi, Crerar, and Riccio 2018; Chapin et al. 2014). When a change in cellular NMD activity is unknown and a change in the abundance of an NMD target is detected, researchers need a robust method to distinguish the pertinent regulatory processes and either confidently claim a change or avoid falsely reporting a change in NMD activity.

Table 2. New AS-NMD method vs conventional exogeneous NMD reporter method

Comparison between the AS-AMD method and conventional NMD reporter method		
	AS-NMD method	Exogenous NMD reporters
Endogenous targets	Yes	No
Exogenous targets	No	Yes
Target delivery	None	Plasmid or Virus
Generalized applications	Broad	Transfectable samples with specified promoters
Application in primary cells	Possible	Difficult
Application in tissue organs	Possible	Difficult
Application in animals	Possible	Difficult
Application in samples of low quantity	Possible	Difficult
Application in postmortem samples	Possible	Difficult
Assay throughput	Parallel assessments of multiple endogenous reporter genes	One reporter gene sets per sample
Secondary validation with endogenous targets	Optional	Necessary
Possible sources of variability in addition to sample variation	NA	The degree of reporter overexpression, the transfection method, transfection efficiency
Signal-to-noise ratio	++	+
Overall cost	$	$$$

Results

Development of a quantitative assay for monitoring changes in cellular NMD activity

A transcript with a stop codon >50 nt upstream of an exon–exon junction is prefered for NMD for degradation (J. Lykke-Andersen, Shu, and Steitz 2000; Maquat, Tarn, and Isken 2010). Such RNA structure can be resulted from alternative RNA splicing shifting the reading frame and creating a PTC (Soergel, Lareau, and Brenner 2013; Kurosaki and Maquat 2016; Pan et al. 2006). One gene can have an NMD isoform and a regular translational isoform. To more effectively distinguish NMD regulation from transcriptional control and knowing transcriptional regulations should equally affect the NMD and non-NMD isoforms of a given gene, this AS-NMD assay takes advantage of this isoform-centric quantitation instead of gene-centric quantitation. It incorporates and compares the non-NMD isoform and the NMD isoform of the same gene; thus distinguishes transcriptional regulations from those of NMD regulation. Alternative isoforms that include or skip a small cassette exon are of interest to minimize the sequence difference between the two isoforms while deliberately excluding alternative 5′ UTR, alternative 3′ UTR, and intron retention to avoid complications reflecting differential translation efficiency or miRNA targeting.

AS-NMD method measures the individual abundance of NMD-sensitive isoforms and that of their non-NMD counterparts via quantitative real-time PCR (RT-qPCR). The NMD isoforms are quantified for differential expression between

a treatment and a control condition. An increase in an NMD isoform may be due to NMD inhibition, transcriptional activation or a change in alternative splicing favoring the NMD isoform. To distinguish from these three events, the expression of the non-NMD counterparts are then quantified as references. Genuine NMD regulation, transcriptional activation and alternative splicing regulation would lead to no change, up-regulation, and down-regulation of the NMD-insensitive isoforms, respectively (Figure 2A). Similarly, a decrease in an NMD isoform can be interpreted as a result of enhanced cellular NMD activity if the non-NMD isoform exhibits no change (Figure 2B).

For specifically detection of an inclusion isoform, a primer entirely annealing to the cassette exon (exon B in Figure 2C) are preferred. However, one technical difficulty of the AS-NMD method is designing RT-qPCR primers specific to the cassette exon-skipping isoform. To overcome this, primers annealing to the exon-skipping junction appear to be the only possible choices. This can be either a reverse primer (exclusion isoform in Figure 2C) with its 5′ portion reverse complementary to the downstream constitutive exon (exon C) and its 3′ portion to the upstream constitutive exon (exon A) or a forward primer (not shown) with its 5′ and 3′ portions matching the upstream and downstream exons, respectively. This challenge is visualized with reverse primers but also applies to forward primers that many exon-skipping junction primers are able to amplify the inclusion isoforms (Figure 2D). The longer the 3′ portion of the junction primer annealing to exon A, the easier the primer amplifies the exon-

inclusion transcripts (inclusion isoform 1 in Figure 2D). Some exon-skipping junction primers with 3′ portions as short as 6 nts can still anneal to the inclusion isoform at 55°C–60°C, albeit at a lower efficiency than the exclusion isoform. On the other hand, a long 5′ portion and a short 3′ portion of the reverse junction primer increase the possibility of annealing to the exon B–exon C junction (inclusion isoform 2 and 3 in Figure 2D). This is due to the general sequence similarity around 5′ splice sites.

To summarize, AS-NMD assay reporters must satisfy several premises. First, the NMD associated cassette exons containing a 3′ end different from their upstream exons are preferred. Secondly, exon-skipping junction primers must amplify only the exclusion isoform and not the inclusion isoform. All selected primer pairs were then tested and confirmed for their specificity, RT-qPCR efficiency, and linear dynamic ranges using RT-qPCR (Table 3). Finally, two stably expressed housekeeping genes, the geometric average of *Gapdh* and *Sdha*, were used as internal controls for calculating expression changes to complete the AS-NMD assay setup.

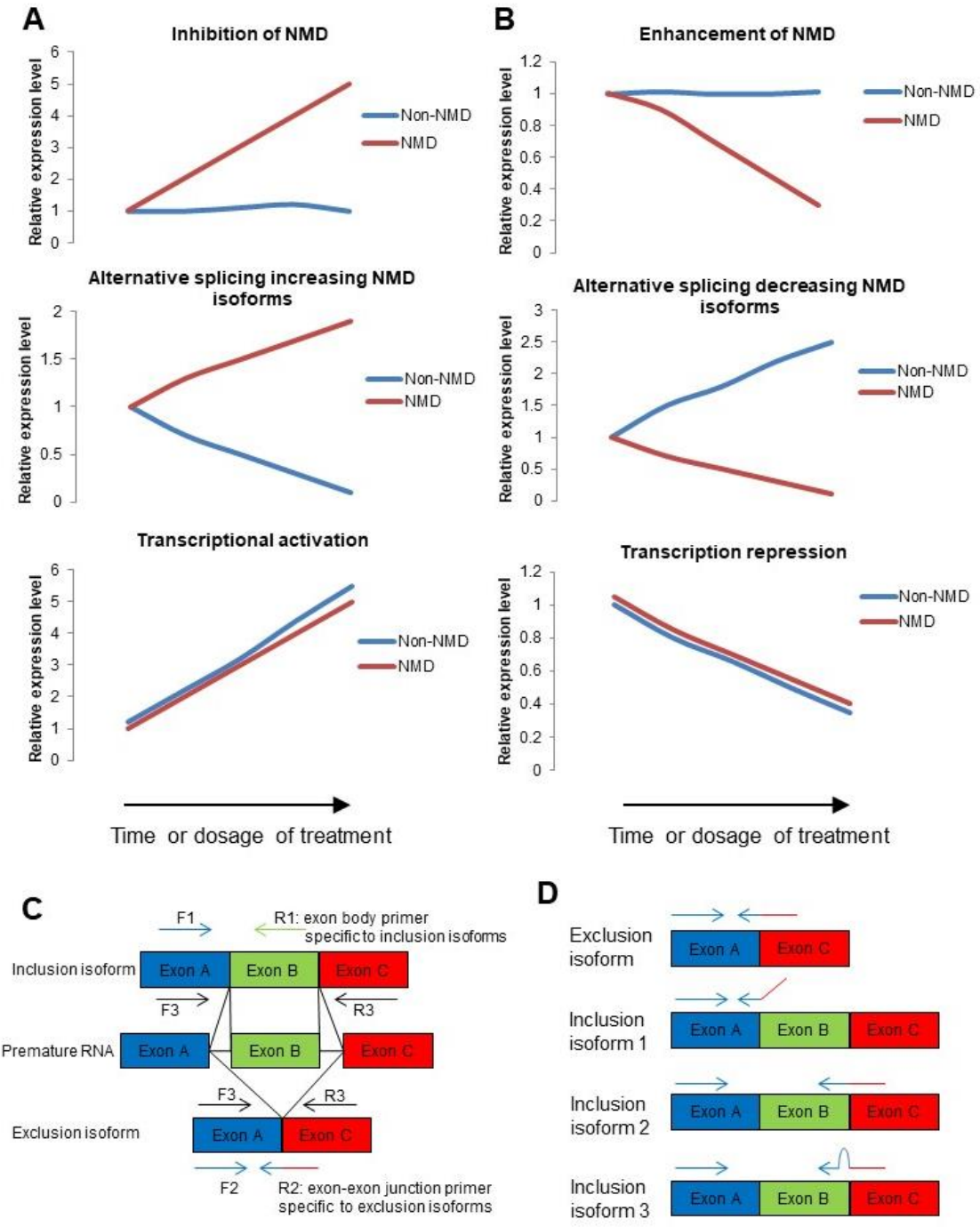
A
Inhibition of NMD
Relative expression level
Non-NMD
NMD
Alternative splicing increasing NMD isoforms
Transcriptional activation
B
Enhancement of NMD
Alternative splicing decreasing NMD isoforms
Transcription repression
Time or dosage of treatment
C
F1
R1: exon body primer specific to inclusion isoforms
Inclusion isoform
Exon A
Exon B
Exon C
F3
R3
Premature RNA
Exclusion isoform
F2
R2: exon-exon junction primer specific to exclusion isoforms
D
Exclusion isoform
Inclusion isoform 1
Inclusion isoform 2
Inclusion isoform 3

Figure 2. Illustrative RT-qPCR readouts to demonstrate AS-NMD method using junction primers to distinguish NMD from transcriptional and splicing events. (A) In scenarios where NMD isoform levels increase, assaying the non-NMD isoforms distinguishes NMD regulation from transcriptional activation and alternative splicing regulation. (B) In scenarios where NMD isoform levels decrease, assaying the non-NMD isoforms distinguishes NMD regulation from transcriptional repression and alternative splicing regulation. (C) Schematics of the AS-NMD junction primer design method using RT-qPCR to specifically detect alternative isoform. The NMD isoform can be either the inclusion or exclusion isoform, while the other isoform is designated as the non-NMD by primer F1 and isoform-specific primer R1. The exclusion isoform is detected by F2 and isoform-specific junction primer R2. Primers F3 and R3 are commonly used in alternative splicing assays to detect both inclusion and exclusion isoforms. (D) Potential complementary binding of the skipping isoform specific junction primers to the exclusion isoform or the three inclusion isoforms.

Validation of the new AS-NMD quantitative assay in vitro

A traditional alternative splicing assay simultaneously amplifies both isoforms in one PCR with primers flanking constitutive exons, then resolves the two isoforms by electrophoresis and derives an expression ratio between the inclusion and exclusion isoforms (F3 and R3, Figure 2C). Such assay has been used to confirm AS-NMD targets but has not been used on its own to monitor NMD activity, because it cannot definitively distinguish NMD regulation from alternative splicing regulation. For example, the splicing assay could not discriminate between NMD regulation and alternative splicing regulation of postsynaptic density protein 95 (*Psd-95*, *Dlg4*). *Psd-95* is transcribed in many cells including embryonic stem cells (Sika Zheng 2016). Both polypyrimidine tract binding proteins, PTBP1 and PTBP2, inhibit exon 18 of *Psd-95* (*NPsd-95*), leading to a frameshift of the transcripts, which are then targeted by NMD (Sika Zheng et al. 2012). The inclusion of exon 18 yields the non-NMD isoform of *Psd-95*. Thus, RNAi-mediated knockdown of the NMD factor *Upf1* increased the exon 18-skipping NMD isoform, and PTBP1 overexpression promoted exon 18 skipping through alternative splicing (Figure 3A). Yet, both the exclusion to inclusion isoform ratios derived from the alternative splicing assay and NMD inhibition were similar and unable to differentiate NMD regulation from alternative splicing regulation (Figure 3A).

In contrast, the AS-NMD method utilizes junction primers to effectively distinguish NMD regulation from alternative splicing regulation. When differential

expression of the NMD isoform is detected, the expression of the non-NMD isoform is also measured simultaneously to determine how the two isoforms are contrasted. In cells deprived of *Upf1*, the NMD isoform but not the non-NMD isoform exhibited significant upregulation (Figure 3B). In cells overexpressing PTBP1, the non-NMD isoform significantly decreased while the NMD isoform increased in accordance with previous prediction (Figure 3C). Further, AS-NMD assay also accurately reported the response of *Psd-95* to the loss of PTBPs. Both PTBP1 and PTBP2 promote the splicing of translational non-NMD *Psd-95* isoform. As expected, RNAi-mediated knockdown of both PTBP1 and PTBP2 significantly decreased the level of *NPsd-95* while increased *Psd-95* isoform (Figure 3D).

To test whether the new assay could discern transcriptional regulation as proposed, actinomycin D was applied to N2a cells to inhibit global transcription while using U6 snRNA as the internal control for these RT-qPCR assays. As expected, AS-NMD method was able to correctly assign transcriptional inhibition to the suppression of both NMD and non-NMD isoforms of *Psd-95*, rather than NMD regulation (Figure 3E). In summary, the AS-NMD assay precisely disclosed the distinct expression profiles of the NMD and non-NMD isoforms of *Psd-95* to transcriptional regulation, alternative splicing regulation, and NMD regulation.

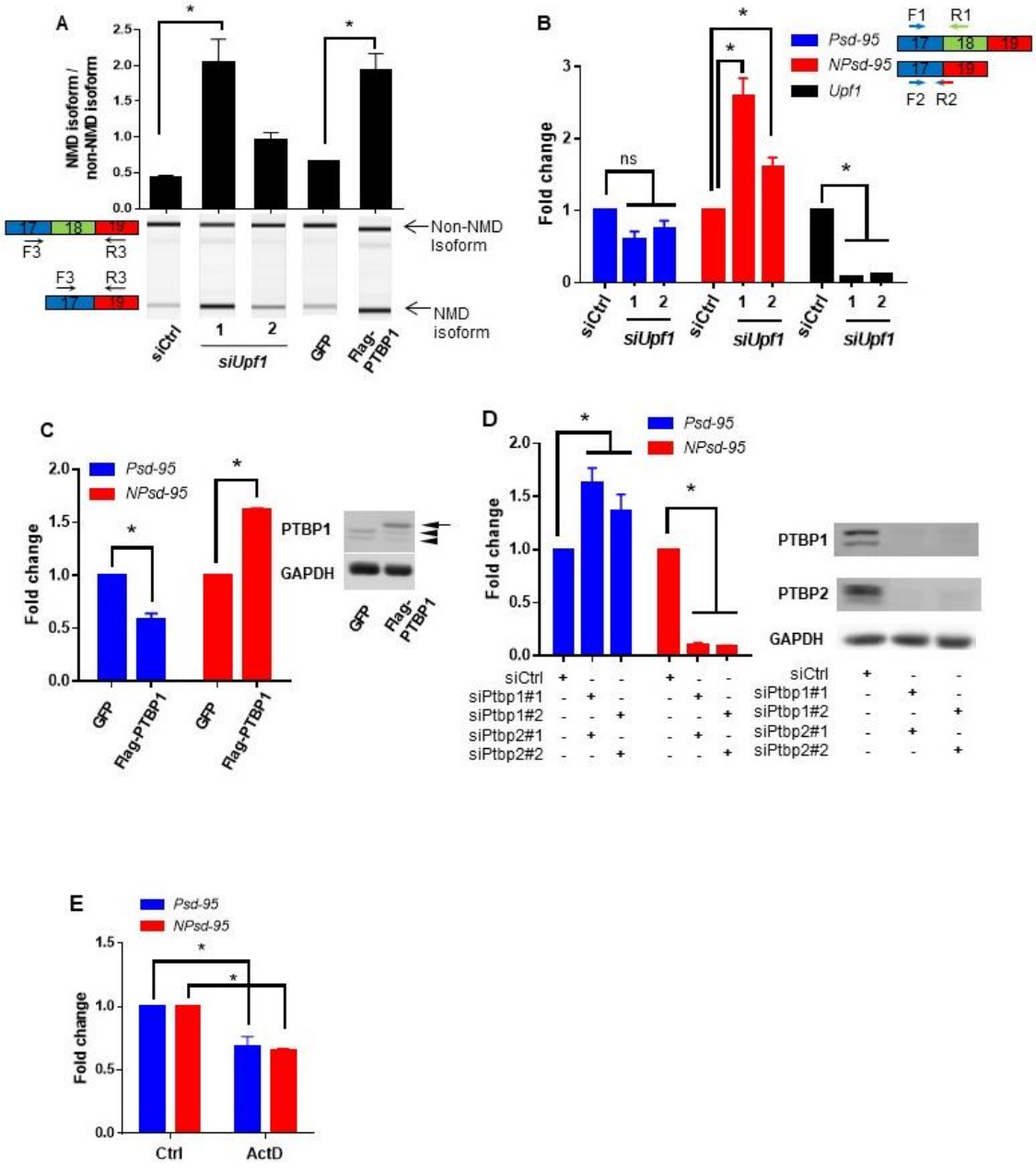
A
NMD isoform / non-NMD isoform
Non-NMD Isoform
NMD isoform
siCtrl
siUpf1
GFP
Flag-PTBP1
B
Psd-95
NPsd-95
Upf1
Fold change
ns
C
PTBP1
GAPDH
D
PTBP1
PTBP2
GAPDH
siCtrl
siPtbp1#1
siPtbp1#2
siPtbp2#1
siPtbp2#2
E
Ctrl
ActD

Figure 3. Validation of the new AS-NMD quantitative assay, differentiate from alternative splicing assays, distinguishes NMD activity from alternative splicing and transcriptional regulation. (A) Conventional splicing assay to derive expression ratios of the *Psd-95* NMD isoform relative to the non-NMD isoform in N2a cells depleted of UPF1 using two independent siRNAs or N2a cells overexpressing PTBP1. The ratios alone do not distinguish NMD regulation from alternative splicing regulation. Representative digital gel images are shown in the lower panel. A one-way ANOVA test was used to determine significant ratio changes between different samples, followed by a Tukey's multiple comparison test. N = 3. (B) RT-qPCR analysis of the *Upf1* deficient cells as in B but using different primers specific to the *Psd-95* non-NMD isoform and *Psd-95* NMD (*NPsd-95*) isoform along with validation of the *siUpf1* knockdown efficiency. (C) RT-qPCR analysis of the PTBP1-overexpressing cells as in B but using different primers specific to the *Psd-95* isoforms described in C. Western blots (right panel) of the samples transfected with GFP and Flag-PTBP1 plasmids. Arrow: Flag-PTBP1; arrowheads: endogenous PTBP1 proteins that are down-regulated by PTBP1 overexpression. (D) Responses of the two *Psd-95* isoforms to double knockdown of PTBP1 and PTBP2 in N2a cells assayed by RT-qPCR. Right panel shows the Western blots verifying the knockdown efficiencies. (E) RT-qPCR analysis of the two *Psd-95* isoforms 4 h after 4 μg/μL actinomycin D treatment. (B–E) A two-way ANOVA test followed by Dunnett's multiple comparison tests was used to determine significant expression changes between samples. N = 3. (*) $P < 0.05$. Error bars represent mean ± SEM.

Validation of the new AS-NMD assay in animal samples

Since using exogenous PTC reporters is unviable in hard-to-transfect cells, tissue organs, postmortem samples, and samples of low quantity, endogenous NMD targets are often used to examine NMD regulations, especially *in vivo* (Table 2). However, conventional alternative splicing assays alone could not distinguish NMD regulation from alternative splicing regulation in these kinds of samples. In Figure 4A, the molar ratio between the *Psd-95* exclusion and inclusion isoforms increased from 0.21 in control wild-type cortices to 1.7 in the conditional knockout cortices of Upf2 (*Upf2*$^{loxP/loxP}$*; Emx1-cre*), a NMD core factor, at embryonic day 17 (Figure 4A, left panel). This ratio decreased to 0.11 and 0.02 in *Ptbp2*$^{+/-}$ and *Ptbp2*$^{-/-}$ cortices of the same age, respectively (Figure 4A, right panel). Without prior knowledge of the sample identities, it would be impossible to attribute the observed ratio changes to either NMD regulation or alternative splicing regulation.

In contrast, without relying on prior knowledge or ratio analysis, the new junction AS-NMD method effectively distinguished NMD regulation from alternative splicing regulation *in vivo*. No change in the exon 18-inclusion isoform but an eightfold increase in the skipping (NMD) isoform was detected in the *Upf2*$^{loxP/loxP}$*; Emx1-cre* cortices (Figure 4B), matching the gene expression profile of NMD inhibition. Consistent with PTBP2 inhibiting exon 18 splicing, the levels of the inclusion isoform in the *Ptbp2*$^{-/-}$ cortices increased twofold relative to wild-type, while the exclusion isoform decreased significantly (Figure 4C). These

changes were attributed to alternative splicing regulation. Altogether, the new AS-NMD method can be used on its own to effectively monitor cellular NMD activity in hard-to-transfect cells and organs as well as postmortem tissues.

To further improve the robustness and specificity of the assay, additional known endogenous AS-NMD targets were included such as heterogeneous nuclear ribonucleoprotein L (Hnrnpl), serine/arginine-rich splicing factor 11 (Srsf11 or Sfrs11), transformer 2 beta (Tra2b), and polypyrimidine tract binding protein 2 (Ptbp2, nPTB, or brPTB). The NMD transcript isoforms of these genes are as follows: Hnrnpl including exon 6, Srsf11 including exon 4, Tra2b including exon 2, and Ptbp2 excluding exon 10 (Stoilov et al. 2004; Boutz et al. 2007; Spellman, Llorian, and Smith 2007; Saltzman et al. 2008). These are all small cassette exons that moderately distinguish the two isoforms at the sequence level. Monitoring additional genes that are targeted by NMD upon either exon inclusion or exon skipping was intended to exclude false positives affecting splicing and to confirm consistent NMD regulatory patterns. These genes were used in the final assay also because RT-qPCR primers specific to their exclusion isoforms were successfully screened.

To allow future improvement and standardization of the method by the community, the guidelines of the international Real-time PCR Data Markup Language (RDML) consortium were strictly followed and detailed information were provided about the AS-NMD junction primers and RT-qPCR assays (Table 3 and Materials and Methods). When tested using AS-NMD method in the

conditional *Upf2*$^{loxP/loxP}$*; Emx1-cre* cortices, the non-NMD isoform levels of these genes barely changed. In contrast, the NMD isoforms were up-regulated significantly by seven- to 50-fold (Figure 4D-G). These data were consistent with *Psd-95* AS-NMD expression profile and confirmed Upf2 knockout induced NMD inhibition. Together, these five genes encode very different proteins and have been studied in various cell lines and tissues. They are also widely transcribed and are not known to be transcriptionally coupled, making them suitable targets for broadly monitoring NMD activity.

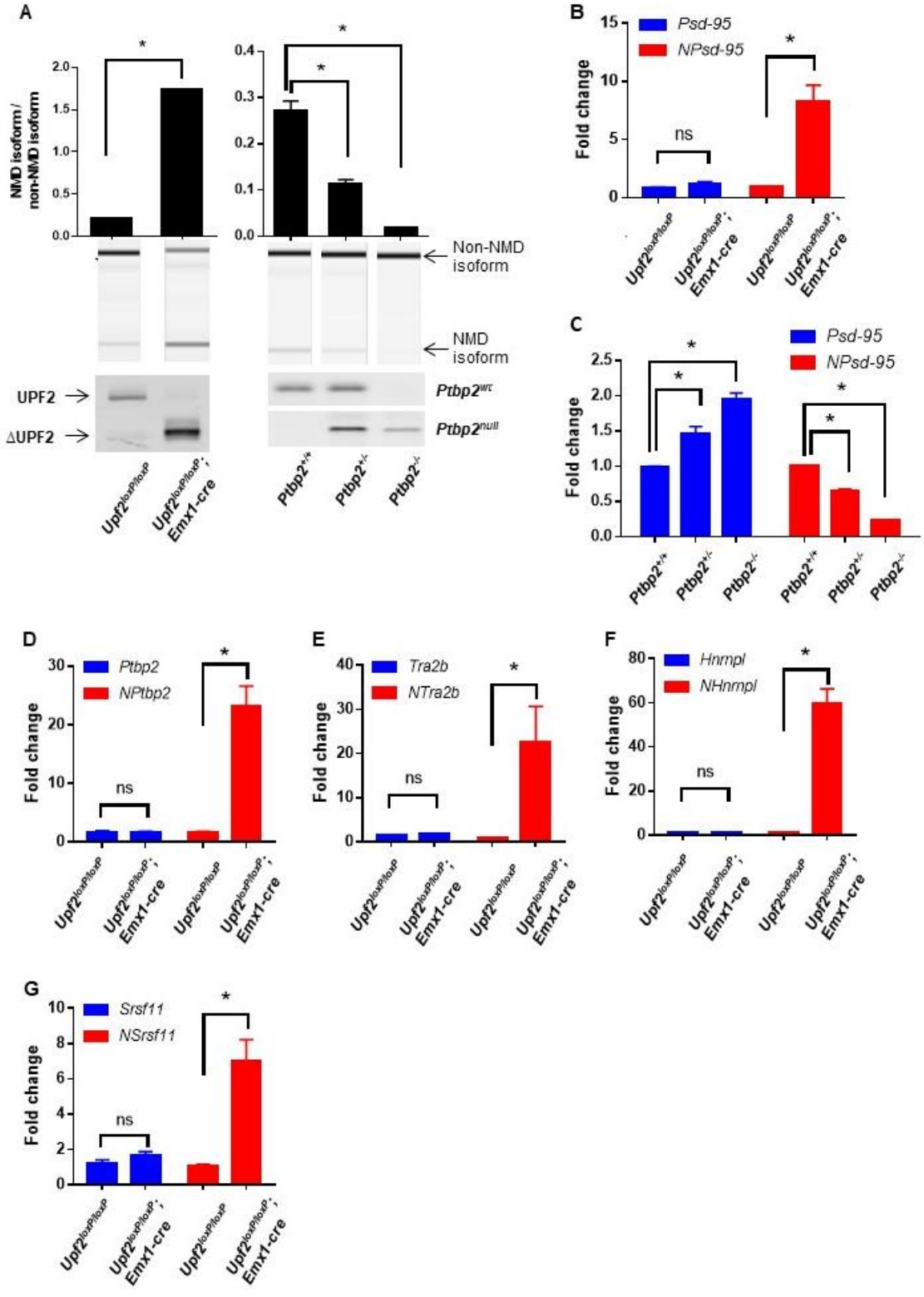
A
NMD isoform / non-NMD isoform
Non-NMD isoform
NMD isoform
UPF2
ΔUPF2
Ptbp2wt
Ptbp2null
Upf2loxPfloxP
Upf2loxPfloxP; Emx1-cre
Ptbp2+/+
Ptbp2+/-
Ptbp2-/-
B
Psd-95
NPsd-95
Fold change
ns
C
D
Ptbp2
NPtbp2
E
Tra2b
NTra2b
F
Hnrnpl
NHnrnpl
G
Srsf11
NSrsf11

Figure 4. The new AS-NMD method distinguishes NMD activity from alternative splicing regulation in animal samples. (*A*) Alternative splicing assay of the *Psd-95* NMD and non-NMD isoforms in *Upf2* conditional knockout cortices (*left* panel) and *Ptbp2* null cortices (*right* panel). (*Lower left* panel) Western blot of UPF2 in $Upf2^{loxP/loxP}$ and $Upf2^{loxP/loxP}$; *Emx1-cre* cortices. The *Upf2* conditional knockout cortices produce truncated UPF2 proteins (ΔUPF2). (*Lower right* panel) Genotyping of *Ptbp2* animals. Statistics were calculated using a two-tailed unpaired Student's *t*-test for the *Upf2* knockout samples ($N = 2$) and a one-way ANOVA test followed by Tukey's multiple comparison test for the *Ptbp2* mutant samples ($Ptbp2^{+/+}$ and $Ptbp2^{+/-}$, $N = 2$; $Ptbp2^{-/-}$, $N = 4$). (*B*, *C*) RT-qPCR analysis of the samples shown in *A* for individual expression of the *Psd-95* non-NMD isoform and *Psd-95* NMD (*NPsd-95*) isoform. (*D–G*) Expression levels of both NMD and non-NMD isoforms of *Ptbp2*, *Tra2b*, *Hnrnpl*, *and Srsf11* in *Upf2* knockout cortices relative to wild type. (*B–G*) A two-way ANOVA test followed by Dunnett's multiple comparison tests was used to determine significant expression changes between samples. (*) $P < 0.05$; (ns) not significant. Error bars represent mean ± SEM.

Application of the AS-NMD quantitative assay in NMD modulator screening

One direct application of this new AS-NMD method is unbiased screening for changes in cellular NMD activity with high confidence. A small panel of widely used chemical molecules and pharmacological inhibitors were tested at various concentrations for their effects on NMD (Figure 5 and 6). The expression of both the NMD and non-NMD isoforms of the endogenous reporter genes were simultaneously measured before and after drug treatment. The NMD isoform and non-NMD isoform expression levels under the treatment vs control conditions were matched with the AS-NMD expression profile (Figure 2A and B). When all five reporter gene profiles agree with each other via ANOVA analysis, the mode of regulation was then determined. Drugs affected the NMD isoforms across the board and minimally affected the non-NMD counterparts were of special interests as NMD modulators.

Na+/K+-ATPase inhibitor ouabain and ion chelator ionomycin were previously reported to inhibit NMD (Nickless et al. 2014). However, the mechanism of regulation remains unclear. Thus, candidates for the newly developed and sensitive AS-NMD assay. *C-fos* and *Pip92* are immediate early genes of ouabain (Taurin et al. 2002; Nakagawa, Rivera, and Larner 1992). RT-qPCR of these two genes showed five- and three-fold changes upon ouabain treatment respectively (Figure 5A and B). This indicated N2a cells were responsive to ouabain treatment. Interestingly, the subsequent AS-NMD assay using *Psd-95*, *Ptbp2*, and *Hnrnpl* of the same samples showed no uniform NMD

regulation changes, contradicting the Nickless et al. 2014 report (Figure 5C-E). *C-jun* and *Pip92* are known reliable immediate early genes of ionomycin (Chung et al. 2001). When applied ionomycin, *C-jun* and *Pip92* were upregulated in a dosage dependent manner (Figure 5F-G). However, ionomycin treatment in a range of 1 to 100 µM did not uniformly alter the levels of the NMD isoforms (Figure 5H-J). Ionomycin equally repressed both NMD and non-NMD isoforms of *Psd-95* (Figure 5H) but had no effect on *Ptbp2* expression (Figure I), suggesting that ionomycin inhibited *Psd-95* transcription. The other reporter gene *Hnrnpl* NMD isoform dramatically increased at 1 µM but decreased as the dosage increased (Figure 5J). This indicates an ionomycin linked *Hnrnpl* specific response at a lower dosage (Figure 5H-J). Therefore, it was concluded that despite previous reports, the AS-NMD method implied no NMD inhibition in N2a cells when treated with ouabain or ionomycin.

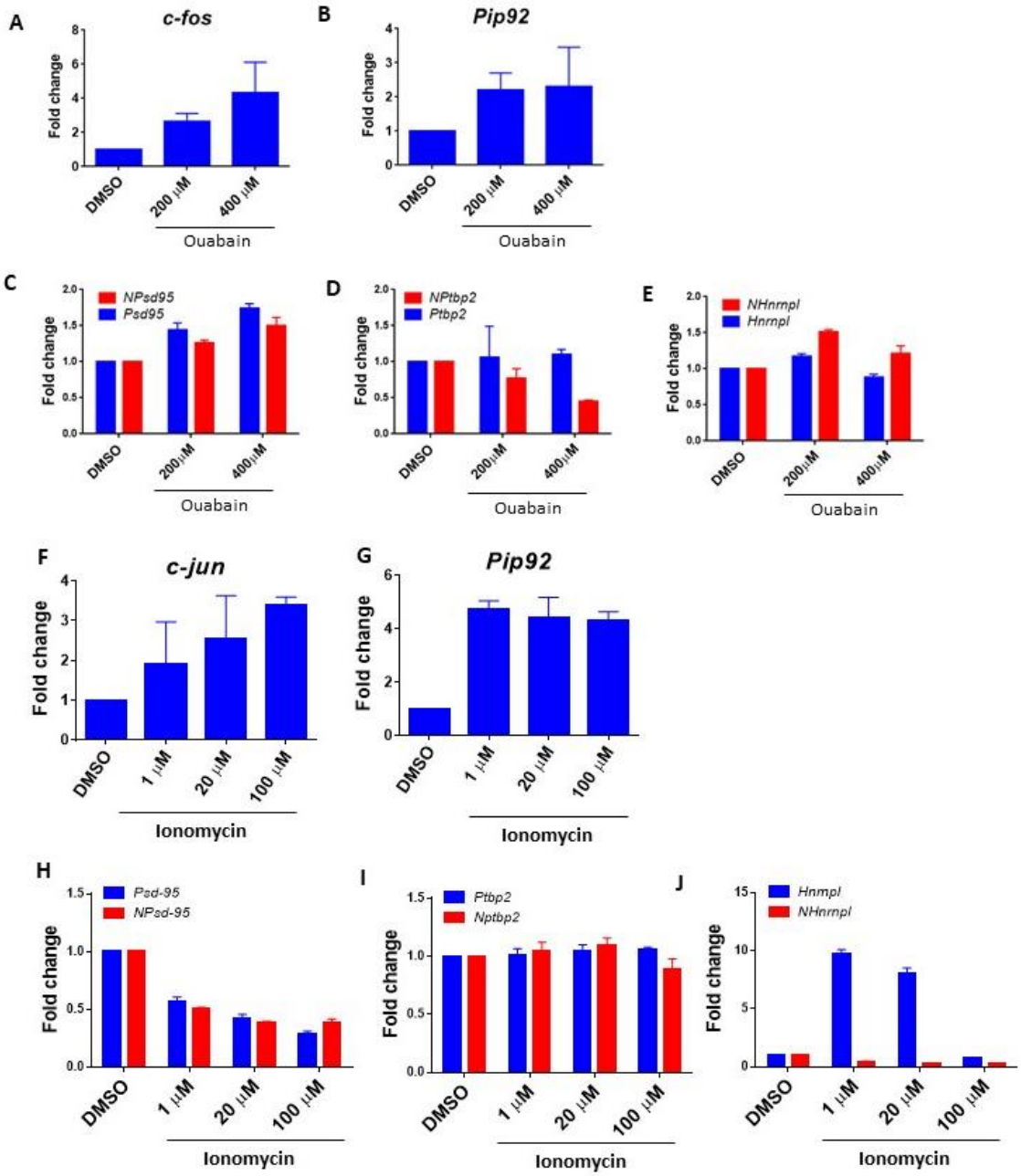
A
c-fos
Fold change
DMSO
200 μM
400 μM
Ouabain
B
Pip92
Fold change
DMSO
200 μM
400 μM
Ouabain
C
NPsd95
Psd95
Fold change
DMSO
200μM
400μM
Ouabain
D
NPtbp2
Ptbp2
Fold change
DMSO
200μM
400μM
Ouabain
E
NHnrnpl
Hnrnpl
Fold change
DMSO
200μM
400μM
Ouabain
F
c-jun
Fold change
DMSO
1 μM
20 μM
100 μM
Ionomycin
G
Pip92
Fold change
DMSO
1 μM
20 μM
100 μM
Ionomycin
H
Psd-95
NPsd-95
Fold change
DMSO
1 μM
20 μM
100 μM
Ionomycin
I
Ptbp2
Nptbp2
Fold change
DMSO
1 μM
20 μM
100 μM
Ionomycin
J
Hnrnpl
NHnrnpl
Fold change
DMSO
1 μM
20 μM
100 μM
Ionomycin

Figure 5. Ouabain and Ionomycin do not show NMD inhibition activities. RT-qPCR assay of (*A*-*B*) immediate early genes *c-fos* and *Pip92* as well as the NMD and non-NMD isoforms of *Psd-95* (*C*), *Ptbp2* (*D*) and *Hnrnpl* (*E*) in N2a cells treated with ouabain. Ouabain clearly induced *c-fos* and *Pip92 but* did not unequivocally affect NMD activity. RT-qPCR assay of immediate early genes *c-fos (F)* and *Pip92 (G)* along with the NMD and non-NMD isoforms of *Psd-95* (*H*), *Ptbp2* (*I*) and *Hnrnpl* (*J*) in N2a cells treated with ionomycin. Ionomycin clearly induced *c-fos* and *Pip92* but did not consistently change NMD isoforms. N = 3. Error bars represent mean ± SEM.

Additional chemicals including PKC inhibitor GF109203X, Cam Kinase II inhibitor KN-93, and protein kinase A inhibitor KT5720 were tested using validated reporter genes in accordance with the AS-NMD method (Figure 6). None of these chemical inhibitors had shown NMD regulations matching AS-NMD gene expression patterns from Figure 2A and 2B. Interestingly, one of the ER stress inducers, thapsigargin, was determined to have significant NMD inhibition property (results not shown). This finding encouraged an in-depth investigation of thapsigargin induced NMD inhibition which will be presented in detail using AS-NMD method in the next chapter, chapter three. It's NMD inhibition mechanism will also be revealed.

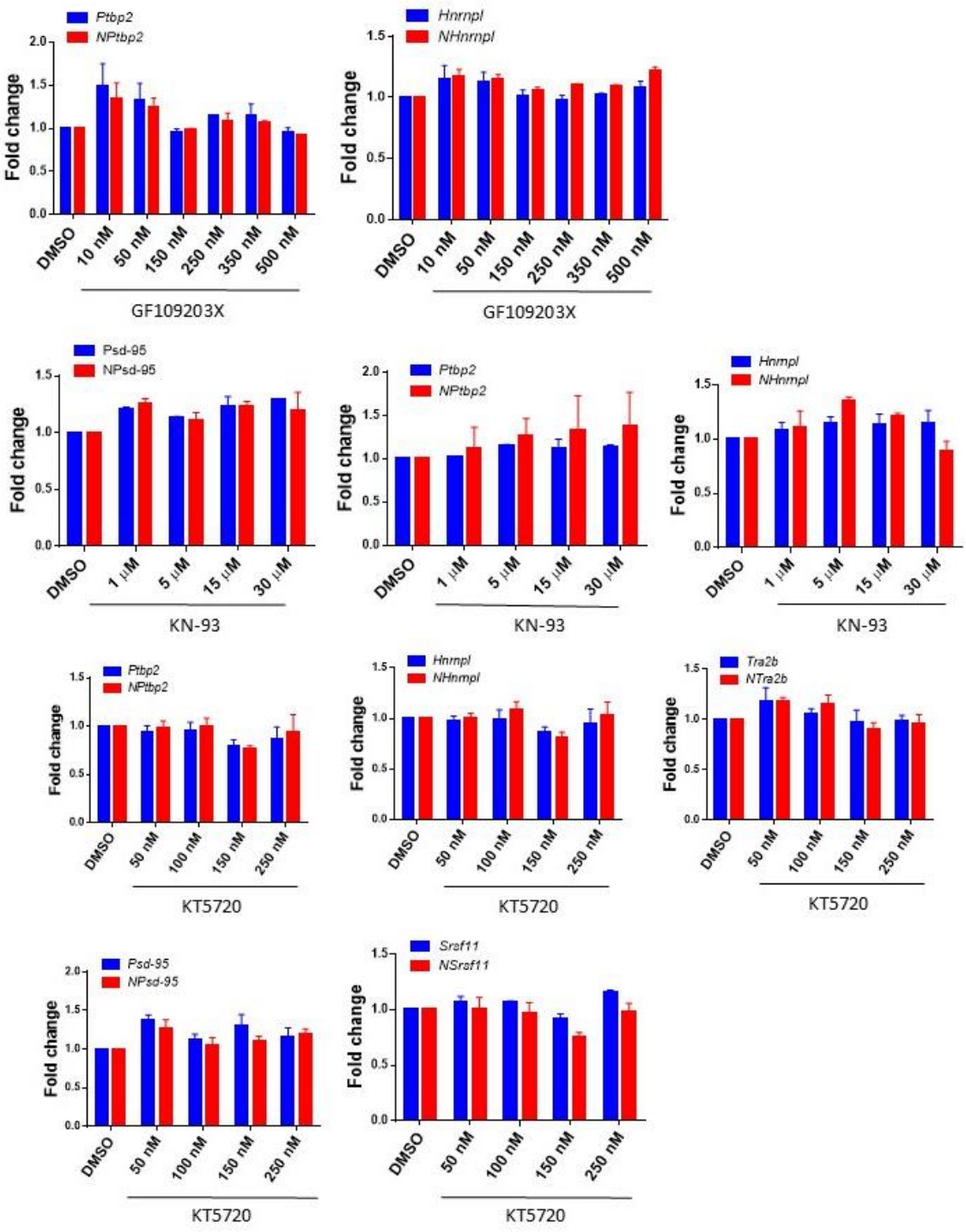
Ptbp2
NPtbp2
Fold change
DMSO
10 nM
50 nM
150 nM
250 nM
350 nM
500 nM
GF109203X
Hnrnpl
NHnrnpl
Fold change
DMSO
10 nM
50 nM
150 nM
250 nM
350 nM
500 nM
GF109203X
Psd-95
NPsd-95
Fold change
DMSO
1 μM
5 μM
15 μM
30 μM
KN-93
Ptbp2
NPtbp2
Fold change
DMSO
1 μM
5 μM
15 μM
30 μM
KN-93
Hnrnpl
NHnrnpl
Fold change
DMSO
1 μM
5 μM
15 μM
30 μM
KN-93
Ptbp2
NPtbp2
Fold change
DMSO
50 nM
100 nM
150 nM
250 nM
KT5720
Hnrnpl
NHnrnpl
Fold change
DMSO
50 nM
100 nM
150 nM
250 nM
KT5720
Tra2b
NTra2b
Fold change
DMSO
50 nM
100 nM
150 nM
250 nM
KT5720
Psd-95
NPsd-95
Fold change
DMSO
50 nM
100 nM
150 nM
250 nM
KT5720
Srsf11
NSrsf11
Fold change
DMSO
50 nM
100 nM
150 nM
250 nM
KT5720

Figure 6. Chemical inhibitors that did not have effects on NMD. N2a cells were treated with each inhibitor at the indicated concentrations for 5 hours. Expression of NMD and non-NMD isoforms was examined by RT-qPCR. KT5720: PKA inhibitor (Tocris Bioscience, 1288100U). KN-93: CamKII inhibitor (Fisher Scientific, NC0362431). GF109203X: PKC inhibitor (R&D, A00061). N = 3. Error bars represent mean ± SEM.

Discussion

In this study, a new method was developed to precisely monitor changes in cellular NMD activity through quantitative measurement of a panel of endogenous NMD isoforms and their corresponding non-NMD isoforms. It can be used on its own to assess changes in intracellular NMD activity with high specificity and sensitivity. This AS-NMD assay indicated that different NMD targets have varying sensitivity to NMD inactivation. For example, the NMD isoform of *Hnrnpl* was up-regulated by about 60-fold in the conditional Upf2 knockout cortices, whereas the *Psd-95* NMD isoform increased by about eightfold (Figure 3B and F). Of these tested AS-NMD reporter genes, *Hnrnpl* and *Tra2b* exhibiting much higher sensitivity towards NMD inhibition than *Psd-95* and *Srsf11*. The varying sensitivity of these NMD targets does not appear to be associated with the 3′ UTR length or the length between the PTC and the downstream exon–exon junction (Table 5). For example, the 3′ UTR of the *Hnrnpl* and *Psd-95* NMD isoforms are similar in length and both are much shorter than others. Therefore, the different sensitivities could be caused by innate NMD isoform expression due to splicing or transcription initiation factors. When NMD is active, the differential expression of NMD isoforms are masked by active degradation of the transcripts, making them “cryptic”.

Not only did AS-NMD assay show it's easy-to-use and robustness when evaluating NMD activities *in vitro*, it is also viable in hard-to-transfect *in vivo* animal samples. Traditional reporter plasmids must be delivered through viral or

non-viral methods such as lentiviral vector infection or electroporation. For example, in order to monitor NMD activities using foreign minigene reporters in embryonic stage mouse cortices, one could use *in utero* electroporation (IUE) to deliver the reporters (Pacary and Guillemot 2020). The procedure is time consuming and requires a large amount of plasmids with variable outcomes between experiments. When using lentiviral or adeno associated viral carriers, the scale of experiments can also be very expensive. Endogenous AS-NMD assay bypasses these issues. Figure 4 showed the AS-NMD assay was able to clearly distinguish alternative splicing and NMD inhibition events, consistent with the *in vitro* profiles.

One immediate application of the AS-NMD reporter assay is NMD modulator screening. In figure 5, ouabain, a cardiac glycoside, and ionomycin, an intracellular Ca2+ ionophore, were examined based on their reported role of NMD inhibition through intracellular calcium modulation (Nickless et al. 2014). Wide dosages of ouabain and ionomycin were used and the abundance of both NMD and non-NMD isoforms were measured at various time-points. However, no clear changes in cellular NMD efficiency were observed even at high concentrations (Figure 5). Immediate early genes *c-fos*, *c-jun*, and *Pip92* clearly showed cells were responsible for the treatments. Taken together, the results suggested that enhanced cytosolic Ca2+ signaling was not sufficient to inhibit NMD in N2a cells.

Nickless et al. used their exogeneous fluorophore reporter system to screen chemical molecules for novel NMD modulator. However, the AS-NMD system was unable to confirm cardiac glycosides or ionophore as NMD inhibitors. When disregarding the aforementioned shortfalls of exogenous reporter system vs endogenous the AS-NMD system, this disagreeing result could be explained by the different cell lines used between two studies. Nickless et al. conducted their study in human cell lines such as human osteosarcoma cell line (U2OS), human Calu-6 cell line, and human embryonic kidney (HEK) 293 while this study used mouse neuroblastoma N2a. However, one molecule, thapsigargin, was also reported to be a potent NMD inhibitor using both exogenous minigene and endogenous AS-NMD assay. This overlap sparked great interests and will be extensively discussed in the next chapter. Further, additional chemical inhibitors screened failed to identify novel NMD modulators. The panel of chemical inhibitors including KT5720, KN-93, and GF109203X was unable to alternate NMD activities in N2a cells.

In conclusion, the AS-NMD assay successfully distinguished NMD regulation from transcriptional regulation and alternative splicing control, which also affect the steady-state levels of NMD substrates. Five different NMD isoforms were used to strengthen the robustness of this new assay. These five isoforms responded consistently to the changes in NMD activity, albeit to varying degrees, indicating that fewer may suffice. To this end, the assay has proven its efficacy in both animal development and *in vitro* drug screen. The endogenous

nature of AS-NMD assay has demonstrated its advantages over exogenous reporter assays (Table 2). The high sensitivity and broad dynamic range allow for the detection of continual changes in NMD activity during development or in response to environmental changes, presenting a new approach to explore endogenous NMD modulation and the subsequent studies in development and genetic disorders. In the present analysis, only a small panel of widely used small molecule inhibitors were tested but showed potential for more future unbiased screening. With the aid of cataloged libraries, high-throughput robotic liquid handling systems and next-generation sequencing, this new AS-NMD method can be adapted to evaluate large scale libraries and *in vivo* samples.

Materials and Methods

Cell cultures, transfection, and drug treatments

Neuro-2a (N2a) cells were maintained in N2a complete media (L-glutamine-free Dulbecco's modified Eagle's medium DMEM, 10% FBS and 1× GlutaMAX) at 37°C, 5% CO2. 750,000 cells were plated on 35 mm BioLite TC plates and incubated with 2 mL of N2a complete media overnight before treatment with the drugs. For siRNA knockdown experiments, 350,000 cells were plated on 35 mm TC plates and incubated with RNAiMAX Lipofectamine (Life Technologies) and siRNAs (siPtbp1, cat. no. s72335 and s72336; siPtbp2, cat. no. s80148 and s80149; siUpf1, cat. no. s72879 and s72878) in 2 mL of N2a complete media for 48 hours before applying treatments. Lipofectamine 2000 (Life Technologies) was used to transfect the Flag-Ptbp1 plasmid and control GFP plasmid into N2a cells for 48 hours. Thapsigargin (VWR, cat. no. 89161-410), KT5720 (Tocris Bioscience, cat. no. 1288100U), KN-93 (Fisher Scientific, cat. no. NC0362431), GF109203X (R&D, cat. no. A00061), ionomycin (Fisher Scientific, cat. no. AG-CN2-0416-M001), and ouabain octahydrate (Fisher Scientific, cat. no. 80055-364) were added according to the indicated concentrations. The cells were collected at 5 h post-treatment unless otherwise specified. For L-glutamine deprivation, 750,000 N2a cells were plated overnight and switched to L-glutamine-free DMEM with 10% FBS.

Animals

Conditional *Upf2*$^{-/-}$ (that is, *Upf2*$^{loxP/loxP}$*; Emx1-cre*) mice were generated by first breeding *Upf2*$^{loxP/loxP}$ mice to *Emx1-cre* mice and subsequently breeding *Upf2*$^{loxP/+}$*; Emx1-cre* mice to *Upf2*$^{loxP/loxP}$ mice (Zheng et al. 2012). *Ptbp2*$^{-/-}$ mice were generated by breeding *Ptbp2*$^{+/-}$ mice to *Ptbp2*$^{+/-}$ mice (Li et al. 2014). All animal procedures were approved by the Institutional Animal Care and Use Committee at UCR.

RNA extraction, cDNA synthesis, and RT-qPCR

TRIzol (Life Technologies, cat. no. 15596-018) was directly added to the cells or mouse brain tissues to extract total RNA following the TRIzol reagent standard protocol. Isolated RNA was treated with 4 units of Turbo DNase (Ambion) at 37°C for 35 min to degrade all remaining genomic DNA. After the DNase treatment, RNA was purified using phenol-chloroform (pH 4.5, VWR cat. no. 97064-744). RNA concentrations were measured using a Nanodrop 2000c (Thermo Fisher). One microgram of freshly isolated DNA-free RNA was reverse transcribed to cDNA using 1 µL random hexamers (30 µM) and 200 units of Promega M-MLV reverse transcriptase (cat. no. M1705) following the Promega protocol in a 20 µL reaction. These 20 ul cDNA reactions were diluted with 180 ul (1:10) of nuclease free H2O before use. RT-qPCR primers were designed in house using Primer 3 software and purchased from IDT. For all qPCR primers, quality control was performed for their specificity, sensitivity, melting curves, and standard curves (Table 3). RT-qPCR assays were conducted using a

QuantStudio 6 Real-Time PCR instrument with 2× Power SYBR Green PCR master mix (Life Tech) following the Life Tech protocol. Each 10 µL reaction contained 0.3 µL cDNA, 5 µL 2× Power SYBR Green PCR master mix, 0.3 nM forward primer, and 0.3 nM reverse primer. The QuantStudio 6 RT-qPCR run program was as follows: 50°C for 2 min; 95°C for 15 sec and 60°C for 1 min, with the 95°C and 60°C steps repeated for 40 cycles; and a melting curve test from 60°C to 95°C at a 0.05°C/sec measuring rate. QuantStudio Real-Time PCR software was used for the analysis. All RT-qPCR reactions were conducted with three technical replicates along with a no template control (NTC, not amplified). Outliers were excluded when the coefficient of variation of Ct for the three technical replicates was larger than 0.3. Relative expression (fold changes) was calculated using the ΔΔCt method. For the splicing assays of the NMD exons, PCR was performed using New England Biolab Taq DNA polymerase (cat. no. M0267E). All statistical analysis was performed using GraphPad Prism 6.

Protein extraction, immunoblotting, and quantitative image analysis

Cells in six-well plates were washed twice with 1 mL cold 1× PBS and harvested with freshly prepared RIPA buffer. The BCA assay (Thermo Scientific) was performed to determine protein concentrations before loading equal amounts of the materials onto SDS-PAGE gels (4% stacking and 12% resolving) for Western blotting. Primary antibodies to PTBP1-NT (1:3000), PTBP2-IS2 (1:1000), UPF2l (Andersen Lab) (Singh, Rebbapragada, and Lykke-Andersen 2008) and GAPDH (1:1500, Ambion) were used. Specific Western blot bands

were quantified using ImageQuant TL and normalized with GAPDH to derive the relative protein levels.

Quantitative analysis of alternative splicing

PCR cycle numbers were optimized for *Psd-95* (28 cycles). Qiaxcel quantitative gel electrophoresis of PCR amplicons was conducted. Splicing of the exons was determined using the following formula. All statistical analysis was performed using GraphPad Prism 6.

Psd-95 splicing ratio = NMD exon skipping isoform / non−NMD exon inclusion isoform

All ratios were calculated using in nmol measured by Qiaxcel.

Table 3. AS-NMD reporter RT-qPCR primers

Splicing Primers	Forward	Reverse	Tm	Size (inclusion)	Size (exclusion)
Ptbp2	GCTGGTGGCAATACAGTCCT	CCCATCAGCCATCTGTATCA	60	156	122
Srsf11	TCCAGACTCAGCAGTTGTGG	GGTAAGTGGGTTGGGGGTAG	60	298	189
Tra2b	AGCGGCGAGCAGAACTAC	ATCCGTGAGCACTTCCACTT	60	343	67
Hnrnpl	CTACACGAACCCCAACCTCA	CATCATGGTAATGGCTGTGG	62	209	139
Xbp1	TGGCCGGGTCTGCTGAGTCCG	GTCCATGGGAAGATGTTCTGG	56	~98	~72
ALS associated cryptic exons NMD targets				Cryptic Inclusion	Cryptic exclusion
Ups15	CCAGGTGCATCCAATTTTTC	GCCTGGCTGTTCATTGTTTC	60	338	174
A230046K03Rik	CAGCAGCTGCCAAACTTCTA	CATTGCATCTGTTGGTGAGG	60	408	210
Mib1	CAGCAATGCAAGCTGCTAGT	TGGGATGACAACCAAAATCC	60	332	273
Genotyping Primers				Size	
Ptbp2 WT	TCTACTTCATTGTGTTGTTTTG	GATACAGCAGGCTCCCCTCA	60	184	
Ptbp2 Null	TCTACTTCATTGTGTTGTTTTG	AAATAAGCATTTTCTAGCACCAA	60	455	

Table 4. Splicing primers

Psd95_qPCR	TCCAGTCTGTGCGAGAGGTA	ACGGATGAAGATGGCGATAG	116	-3.275	32.001	0.990	100%	22.007 - 32.139	0.2
NPsd95_qPCR	CGAGAGGTAGCAGAGCAGAGA	AAGCACTCCGTGAACTCCTG	105	-3.296	31.473	0.990	100%	21.050 - 27.916	0.1
Ptbp2_qPCR	TTACGCCCCAAAGTCTGTTT	CCCATCAGCCATCTGTATCA	107	-3.417	30.309	0.988	96%	20.029 - 26.873	0.389
Ptbp2_NMD_qPCR	GAGTCTCAGCTGGTGGCAAT	TGCACATCTCCATAAACACCTC	72	-3.346	34.659	0.990	99%	24.604 - 31.296	0.586
Srsf11_qPCR	TCCAGACTCAGCAGTTGTGG	TCTCATCAGGAATAACTCTTCAGC	100	-3.418	29.948	0.998	96%	19.755 - 30.042	0.07
Srsf11_NMD_qPCR	TCCAGACTCAGCAGTTGTGG	GGCTGAACCAGGGAAAAGA	102	-3.397	35.431	0.994	97%	25.036 - 31.648	0.234
Tra2b_qPCR	GGAGCTTGACAGCTTCAGGA	AAGCAGAACGGGATTCCC	105	-3.340	29.231	0.998	100%	19.217 - 25.841	0.043
Tra2b_NMD_qPCR	TGGAATCAGAAAGCACTACGC	GAGTCTTCCTTGGAGCGAGA	116	-3.458	35.032	0.998	95%	24.690 - 31.606	0.248
Hnrnpl_qPCR	CAACCTCAGTGGACAAGGTG	CCTCATATTCTGCGGGATGA	92	-3.211	28.059	0.999	104%	18.394 - 24.832	0.117
Hnrnpl_NMD_qPCR	GGTCGCAGTGTATGTTTGATG	GGCGTTTGTTGGGGTTACT	100	-3.394	34.321	0.996	97%	24.209 - 30.801	0.313
ER stress reporter									
Xbp1s_qPCR	CTGAGTCCGCAGCAGGTG	GGCAACAGTGTCAGAGTCCA	74	-3.226	34.042	0.975	104%	24.113 - 30.566	0.447
Bip_qPCR	CTGAGGCGTATTTGGGAAAG	CAGCATCTTTGGTTGCTTGT	93	-3.647	30.698	0.996	88%	19.634 - 26.928	0.051
Ern1_qPCR	TCCTAACAACCTGCCCAAAC	AGATACGGTGGTCGGTGTGT	121	-3.766	32.98	0.997	84%	21.711 - 29.303	0.244
Atf6a_qPCR	GCAGGAGGGGAGATACGTT	GTGGTCTTGTTGTGGGTGGT	82	-3.853	34.269	0.986	82%	22.918 - 30.624	0.48
Immediate early genes									
Pip92	CCGACAATATGCTCAACGTG	CTCGAAAGAAGCCACCAGAG	70	-3.271	33.069	0.995	102%	23.076 - 33.004	0.012
c-fos	GCAGAAGGGGCAAAGTAGAG	GCAGCCATCTTATTCCGTTC	82	-3.260	35.667	0.994	102%	26.013 - 35.993	0.003
c-jun	GAAAAGTAGCCCCCAACCTC	GGGACACAGCTTTCACCCTA	102	-3.377	33.839	0.994	98%	23.605 - 30.308	0.02
Others									
Tardbp (Tdp43)	GGGGCAATCTGGTATATGTTG	TTCACTGCAGAGGAAGCATCT	82	-3.144	27.647	0.998	108%	18.262 - 24.55	0.102
eIF2ak3 (Perk)	GGTCTGGTTCCTTGGTTTCA	GGTCCCACTGGAAGAGGTC	99	-3.169	32.367	1.000	106%	22.886 - 29.224	0.033
Upf1	CCAGCGCTCTTACTTGGTG	ACGCAGGACAGAATGATGAAG	132	-3.405	30.229	0.998	97%	19.99 - 30.229	0.27
Upf2	TGTCCGCTTTATTGGAGAGC	TGCATGCCATTTCAATATGAT	116	-3.431	32.039	0.997	96%	21.756 - 28.617	0.264
Upf3a	GGAGACGAGAAGCAGGAAGA	CGAGATCTCTTGTCCCTTGG	104	-3.366	33.887	0.999	98%	23.75 - 30.556	0.01
Upf3b	GATAGGCAGGATCGCAACAG	TCCTGAAGCTGTTCCTTGGT	95	-3.329	33.615	0.995	100%	23.451 - 30.464	0.306
U6	CGCTTCGGCAGCACATATAC	ACGAATTTGCGTGTCATCCT	84	-3.415	29.4	0.999	96%	19.124 - 29.378	0.233
Gapdh	TGCGACTTCAACAGCAACTC	CTTGCTCAGTGTCCTTGCTG	200	-3.32	24.06	0.999	100%	13.54 - 21.84	0.08
Sdha	GCTTGCGAGCTGCATTTGG	CATCTCCAGTTGTCCTCTTCCA	145	-3.3	28.62	0.99	100%	18.32 - 25.26	0.15

Table 5. Relative position of PTC and 3' UTR length

Gene/isoform	3'UTR length	Distance to the first downstream splice junction (>50bp)	Rank (upregulation in Upf2KO)	Rank (upregulation after TG treatment)
NHnrnpl	1244	83	1	1
NTra2b	3333	195	2	1
Nptbp2	2077	66	2	3
NSrsf11	2854	86	4	4
NPsd95 (Dlg4)	1024	80	4	5

References

Andreassi, Catia, Hamish Crerar, and Antonella Riccio. 2018. “Post-Transcriptional Processing of mRNA in Neurons: The Vestiges of the RNA World Drive Transcriptome Diversity.” *Frontiers in Molecular Neuroscience* 11 (August): 304.

Bonifacino, Juan S., Mary Dasso, Joe B. Harford, Jennifer Lippincott-Schwartz, and Kenneth M. Yamada, eds. 2001. “Analysis of Nonsense-Mediated mRNA Decay in Mammalian Cells.” In *Current Protocols in Cell Biology*, 64:5245. Hoboken, NJ, USA: John Wiley & Sons, Inc.

Boutz, Paul L., Peter Stoilov, Qin Li, Chia-Ho Lin, Geetanjali Chawla, Kristin Ostrow, Lily Shiue, Manuel Ares Jr, and Douglas L. Black. 2007. “A Post-Transcriptional Regulatory Switch in Polypyrimidine Tract-Binding Proteins Reprograms Alternative Splicing in Developing Neurons.” *Genes & Development* 21 (13): 1636–52.

Chang, Yao-Fu, J. Saadi Imam, and Miles F. Wilkinson. 2007. “The Nonsense-Mediated Decay RNA Surveillance Pathway.” *Annual Review of Biochemistry* 76: 51–74.

Chapin, Alex, Hao Hu, Shawn G. Rynearson, Julie Hollien, Mark Yandell, and Mark M. Metzstein. 2014. “In Vivo Determination of Direct Targets of the Nonsense-Mediated Decay Pathway in Drosophila.” *G3* 4 (3): 485–96.

Chung, Kwang Chul, Jee Young Sung, Wooin Ahn, Hyewhon Rhim, Tae Hwan Oh, Min Goo Lee, and Young Soo Ahn. 2001. “Intracellular Calcium Mobilization Induces Immediate Early Genepip92 via Src and Mitogen-Activated Protein Kinase in Immortalized Hippocampal Cells.” *The Journal of Biological Chemistry* 276 (3): 2132–38.

Colombo, Martino, Evangelos D. Karousis, Joël Bourquin, Rémy Bruggmann, and Oliver Mühlemann. 2017. “Transcriptome-Wide Identification of NMD-Targeted Human mRNAs Reveals Extensive Redundancy between SMG6- and SMG7-Mediated Degradation Pathways.” *RNA* 23 (2): 189–201.

Gerbracht, Jennifer V., Volker Boehm, and Niels H. Gehring. 2017. “Plasmid Transfection Influences the Readout of Nonsense-Mediated mRNA Decay Reporter Assays in Human Cells.” *Scientific Reports* 7 (1): 10616.

Han, Xin, Yanling Wei, Hua Wang, Feilong Wang, Zhenyu Ju, and Tangliang Li. 2018. “Nonsense-Mediated mRNA Decay: A ‘Nonsense’ Pathway Makes Sense in Stem Cell Biology.” *Nucleic Acids Research* 46 (3): 1038–51.

Huang, Lulu, Chih-Hong Lou, Waikin Chan, Eleen Y. Shum, Ada Shao, Erica Stone, Rachid Karam, Hye-Won Song, and Miles F. Wilkinson. 2011. “RNA Homeostasis Governed by Cell Type-Specific and Branched Feedback Loops Acting on NMD.” *Molecular Cell* 43 (6): 950–61.

Isken, Olaf, and Lynne E. Maquat. 2007. “Quality Control of Eukaryotic mRNA: Safeguarding Cells from Abnormal mRNA Function.” *Genes & Development* 21 (15): 1833–56.

Jaffrey, Samie R., and Miles F. Wilkinson. 2018. “Nonsense-Mediated RNA Decay in the Brain: Emerging Modulator of Neural Development and Disease.” *Nature Reviews. Neuroscience* 19 (12): 715–28.

Kurosaki, Tatsuaki, and Lynne E. Maquat. 2016. “Nonsense-Mediated mRNA Decay in Humans at a Glance.” *Journal of Cell Science* 129 (3): 461–67.

Kurosaki, Tatsuaki, Maximilian W. Popp, and Lynne E. Maquat. 2019. “Quality and Quantity Control of Gene Expression by Nonsense-Mediated mRNA Decay.” *Nature Reviews. Molecular Cell Biology* 20 (7): 406–20.

Lareau, Liana F., Angela N. Brooks, David A. W. Soergel, Qi Meng, and Steven E. Brenner. n.d. “The Coupling of Alternative Splicing and Nonsense-Mediated mRNA Decay.” http://compbio.berkeley.edu/people/brenner/pubs/lareau-2007-landes-nmd.pdf.

Lindeboom, Rik G. H., Fran Supek, and Ben Lehner. 2016. “The Rules and Impact of Nonsense-Mediated mRNA Decay in Human Cancers.” *Nature Genetics* 48 (10): 1112–18.

Lykke-Andersen, J., M. D. Shu, and J. A. Steitz. 2000. “Human Upf Proteins Target an mRNA for Nonsense-Mediated Decay When Bound Downstream of a Termination Codon.” *Cell* 103 (7): 1121–31.

Lykke-Andersen, Søren, and Torben Heick Jensen. 2015. “Nonsense-Mediated mRNA Decay: An Intricate Machinery That Shapes Transcriptomes.” *Nature Reviews. Molecular Cell Biology* 16 (11): 665–77.

Maquat, Lynne E., Woan-Yuh Tarn, and Olaf Isken. 2010. “The Pioneer Round of Translation: Features and Functions.” *Cell* 142 (3): 368–74.

Nakagawa, Y., V. Rivera, and A. C. Larner. 1992. “A Role for the Na/K-ATPase in the Control of Human c-Fos and c-Jun Transcription.” *The Journal of Biological Chemistry* 267 (13): 8785–88.

Nickless, Andrew, Erin Jackson, Jayne Marasa, Patrick Nugent, Robert W. Mercer, David Piwnica-Worms, and Zhongsheng You. 2014. “Intracellular Calcium Regulates Nonsense-Mediated mRNA Decay.” *Nature Medicine* 20 (8): 961–66.

Nickless, Andrew, and Zhongsheng You. 2018. “Studying Nonsense-Mediated mRNA Decay in Mammalian Cells Using a Multicolored Bioluminescence-Based Reporter System.” In *mRNA Decay: Methods and Protocols*, edited by Shireen R. Lamandé, 213–24. New York, NY: Springer New York.

Nott, Ajit, Shlomo H. Meislin, and Melissa J. Moore. 2003. “A Quantitative Analysis of Intron Effects on Mammalian Gene Expression.” *RNA* 9 (5): 607–17.

Pacary, Emilie, and François Guillemot. 2020. “In Utero Electroporation to Study Mouse Brain Development.” In *Brain Development: Methods and Protocols*, edited by Simon G. Sprecher, 513–23. New York, NY: Springer New York.

Paillusson, Alexandra, Nadine Hirschi, Claudio Vallan, Claus M. Azzalin, and Oliver Mühlemann. 2005. “A GFP-Based Reporter System to Monitor Nonsense-Mediated mRNA Decay.” *Nucleic Acids Research* 33 (6): e54.

Pan, Qun, Arneet L. Saltzman, Yoon Ki Kim, Christine Misquitta, Ofer Shai, Lynne E. Maquat, Brendan J. Frey, and Benjamin J. Blencowe. 2006. “Quantitative Microarray Profiling Provides Evidence against Widespread Coupling of Alternative Splicing with Nonsense-Mediated mRNA Decay to Control Gene Expression.” *Genes & Development* 20 (2): 153–58.

Pereverzev, Anton P., Nadya G. Gurskaya, Galina V. Ermakova, Elena I. Kudryavtseva, Nadezhda M. Markina, Alexey A. Kotlobay, Sergey A. Lukyanov, Andrey G. Zaraisky, and Konstantin A. Lukyanov. 2015. “Method for Quantitative Analysis of Nonsense-Mediated mRNA Decay at the Single Cell Level.” *Scientific Reports* 5 (January): 7729.

Popp, Maximilian Wei-Lin, and Lynne E. Maquat. 2013. “Organizing Principles of Mammalian Nonsense-Mediated mRNA Decay.” *Annual Review of Genetics* 47: 139–65.

Rehwinkel, Jan, Ivica Letunic, Jeroen Raes, Peer Bork, and Elisa Izaurralde. 2005. “Nonsense-Mediated mRNA Decay Factors Act in Concert to Regulate Common mRNA Targets.” *RNA* 11 (10): 1530–44.

Saltzman, Arneet L., Yoon Ki Kim, Qun Pan, Matthew M. Fagnani, Lynne E. Maquat, and Benjamin J. Blencowe. 2008. “Regulation of Multiple Core Spliceosomal Proteins by Alternative Splicing-Coupled Nonsense-Mediated

mRNA Decay.” *Molecular and Cellular Biology* 28 (13): 4320–30.

Singh, Guramrit, Indrani Rebbapragada, and Jens Lykke-Andersen. 2008. “A Competition between Stimulators and Antagonists of Upf Complex Recruitment Governs Human Nonsense-Mediated mRNA Decay.” *PLoS Biology* 6 (4): e111.

Soergel, David A. W., Liana F. Lareau, and Steven E. Brenner. 2013. *Regulation of Gene Expression by Coupling of Alternative Splicing and NMD*. Landes Bioscience.

Spellman, Rachel, Miriam Llorian, and Christopher W. J. Smith. 2007. “Crossregulation and Functional Redundancy between the Splicing Regulator PTB and Its Paralogs nPTB and ROD1.” *Molecular Cell* 27 (3): 420–34.

Stoilov, Peter, Rosette Daoud, Oliver Nayler, and Stefan Stamm. 2004. “Human tra2-beta1 Autoregulates Its Protein Concentration by Influencing Alternative Splicing of Its Pre-mRNA.” *Human Molecular Genetics* 13 (5): 509–24.

Tani, Hidenori, Naoto Imamachi, Kazi Abdus Salam, Rena Mizutani, Kenichi Ijiri, Takuma Irie, Tetsushi Yada, Yutaka Suzuki, and Nobuyoshi Akimitsu. 2012. “Identification of Hundreds of Novel UPF1 Target Transcripts by Direct Determination of Whole Transcriptome Stability.” *RNA Biology* 9 (11): 1370–79.

Taurin, Sebastien, Nickolai O. Dulin, Dimitri Pchejetski, Ryszard Grygorczyk, Johanne Tremblay, Pavel Hamet, and Sergei N. Orlov. 2002. “C-Fos Expression in Ouabain-Treated Vascular Smooth Muscle Cells from Rat Aorta: Evidence for an Intracellular-Sodium-Mediated, Calcium-Independent Mechanism.” *The Journal of Physiology* 543 (Pt 3): 835–47.

Wang, Ding, Jiri Zavadil, Leenus Martin, Fabio Parisi, Eugene Friedman, David Levy, Heather Harding, David Ron, and Lawrence B. Gardner. 2011. “Inhibition of Nonsense-Mediated RNA Decay by the Tumor Microenvironment Promotes Tumorigenesis.” *Molecular and Cellular Biology* 31 (17): 3670–80.

Yepiskoposyan, Hasmik, Florian Aeschimann, Daniel Nilsson, Michal Okoniewski, and Oliver Mühlemann. 2011. “Autoregulation of the Nonsense-Mediated mRNA Decay Pathway in Human Cells.” *RNA* 17 (12): 2108–18.

Zheng, S. 2016. “Chapter Twelve - IRAS: High-Throughput Identification of Novel Alternative Splicing Regulators.” In *Methods in Enzymology*, edited by Grigory S. Filonov and Samie R. Jaffrey, 572:269–89. Academic Press.

Zheng, Sika. 2016. “Alternative Splicing and Nonsense-Mediated mRNA Decay Enforce Neural Specific Gene Expression.” *International Journal of Developmental Neuroscience: The Official Journal of the International Society for Developmental Neuroscience*, March. https://doi.org/10.1016/j.ijdevneu.2016.03.003.

Zheng, Sika, Robert Damoiseaux, Liang Chen, and Douglas L. Black. 2013. “A Broadly Applicable High-Throughput Screening Strategy Identifies New Regulators of Dlg4 (Psd-95) Alternative Splicing.” *Genome Research* 23 (6): 998–1007.

Zheng, Sika, Erin E. Gray, Geetanjali Chawla, Bo Torben Porse, Thomas J. O’Dell, and Douglas L. Black. 2012. “PSD-95 Is Post-Transcriptionally Repressed during Early Neural Development by PTBP1 and PTBP2.” *Nature Neuroscience* 15 (3): 381–88, S1.

Chapter 3: ER stress inhibits nonsense-mediated RNA decay

Abstract

Thapsigargin has been reported as a potent nonsense-mediated RNA decay (NMD) inhibitor through intracellular calcium modulation. However, the detailed signaling mechanism remains unclear. The high sensitivity and broad dynamic range of AS-NMD reporter assay revealed a strong correlation between NMD inhibition, endoplasmic reticulum (ER) stress, and polysome disassembly upon thapsigargin treatment in a temporal and dose-dependent manner. Little evidence was found of calcium signaling mediating thapsigargin-induced NMD inhibition. Instead, one of the three unfolded protein response (UPR) pathways activated by thapsigargin, the protein kinase RNA-like endoplasmic reticulum kinase (PERK) pathway was required for NMD inhibition. Finally, thapsigargin induced ER stress compounded TDP-43 deficiency upregulated NMD isoforms that had been implicated in the pathogenic mechanisms of amyotrophic lateral sclerosis and frontotemporal dementia (ALS - FTD). The additive effect of ER stress was completely blocked by PERK depletion, as predicted. This chapter further revealed the intricate network of NMD with cellular stress and the implications of such interactions in a neurodegenerative disease model.

Introduction

Nonsense-mediated RNA decay (NMD) is a post transcriptional surveillance mechanism that degrades faulty and aberrant transcripts containing premature termination codons (PTCs) (L. E. Maquat et al. 1981; Lykke-Andersen and Jensen 2015). Moreover, NMD actively regulates endogenous genes and is integrated into a variety of physiological settings including the fine-tuning of the unfolded protein response (UPR), coupling with alternative splicing, neural differentiation and more (Lynne E. Maquat and Gong 2009; Sakaki et al. 2012; Lou et al. 2014; Oren et al. 2014; Karam et al. 2015). Despite extensive studies on the molecular mechanisms of target recognition and its integration with other processes, less is known about the modulation of NMD itself. Only a few studies showed that NMD was inhibited as an adaptive response to hypoxia and calcium signaling (Gardner 2008; Nickless et al. 2014) or in the tumor microenvironment (Wang et al. 2011).

In the last chapter, a robust alternative splicing and NMD (AS-NMD) coupling assay to quantitatively and accurately monitor NMD activity was developed. Its readouts are consistent in both *in vitro* and *in vivo* validations, without using foreign plasmid reporters such as PTC harboring minigenes or fluorescent tagged constructs. It was then used to screen a small panel of inhibitors and chemical molecules, hoping to identify novel NMD modulators that could be used in future NMD manipulation or suppression therapy. Out of all six compounds tested, thapsigargin (TG) had previously been reported as a potent

NMD inhibitor (Nickless et al. 2014). Thapsigargin is also a noncompetitive inhibitor of the sarco/endoplasmic reticulum Ca2+ ATPase. Its treatment increases intracellular Ca2+ concentration, which stimulates various calcium dependent signaling pathways. In fact, Nickless et al. (2014) recently showed that intracellular calcium inhibited NMD after administration of thapsigargin. In addition, thapsigargin also induces ER stress. Some cellular stresses including hypoxia is known to inhibit NMD via phosphorylation of eukaryotic initiation factor 2α (eIF2α) (Gardner 2008; Wang et al. 2011), although the exact mechanism underlying NMD inhibition by eIF2α phosphorylation remains to be determined (Karam et al. 2015). Nevertheless, the diverging mechanisms reported by these studies were both based on the exogenous NMD reporter approach and gene-centric validations. Therefore, an independent investigation using the new AS-NMD assay could help verify the molecular mechanisms of thapsigargin induced NMD inhibition.

Given the active role of NMD interacting with stresses and other biological networks, NMD has been linked to many genetic diseases. For example, RNA binding protein TDP-43 is commonly found in the cytoplasmic inclusion bodies of amyotrophic lateral sclerosis (ALS) and frontotemporal dementia (FTD), and its genetic mutations are linked to familial ALS - FTD (Neumann et al. 2006; Arai et al. 2006; Guo et al. 2011; S.-C. Ling, Polymenidou, and Cleveland 2013; Lagier-Tourenne et al. 2012). Increased cryptic splicing in TDP-43-deficient cells has recently been proposed as one of the pathogenic mechanisms (J. P. Ling et al.

2015). These cryptic isoforms are presumably subjected to NMD regulation. Enhanced NMD activity via UPF1 overexpression was found to improve cellular protection against TDP-43-induced toxicity (Barmada et al. 2015). On the other hand, attenuated NMD activity may have therapeutic benefits for other inherited diseases where nonsense mutations are detrimental and manifest worse symptoms than missense mutations (Palacios 2013; Linde et al. 2007; Ramalho et al. 2002; Lee and Dougherty 2012; Welch et al. 2007). Therefore, monitoring and understanding the mechanisms of NMD modulators could be the key to precise NMD manipulation tailored toward each specific scenario and disease. The later part of this chapter will also examine the potential effects of NMD inhibition based on the recent TDP-43 induced ALS–FTD model.

Results

Thapsigargin specifically enhances the endogenous NMD targets

N2a cells were treated with 0.2 μM of thapsigargin for the indicated time period. NMD activities were measured using the new AS-NMD method described in the last chapter. The NMD isoform transcripts increased as early as one hour after thapsigargin treatment and continued to increase gradually for all reporter genes (Figure 7). At 5 hrs, the NMD isoform levels were enhanced by three- to 10-fold whereas the non-NMD isoform levels barely changed for *Srsf11*, *Tra2b*, and *Hnrnpl*. *Ptbp2* and *Psd-95* non-NMD isoforms increased slightly to around 1.8-fold. Although transcription and alternative splicing regulation might have

modestly contributed to the changes in *Ptbp2* and *Psd-95*, the dramatic increase in the levels of the NMD isoforms for all five genes were not nearly proportional to transcriptional stimulation or splicing changes. Rather, the changes were consistent with attenuation of the NMD pathway specific to these NMD isoforms.

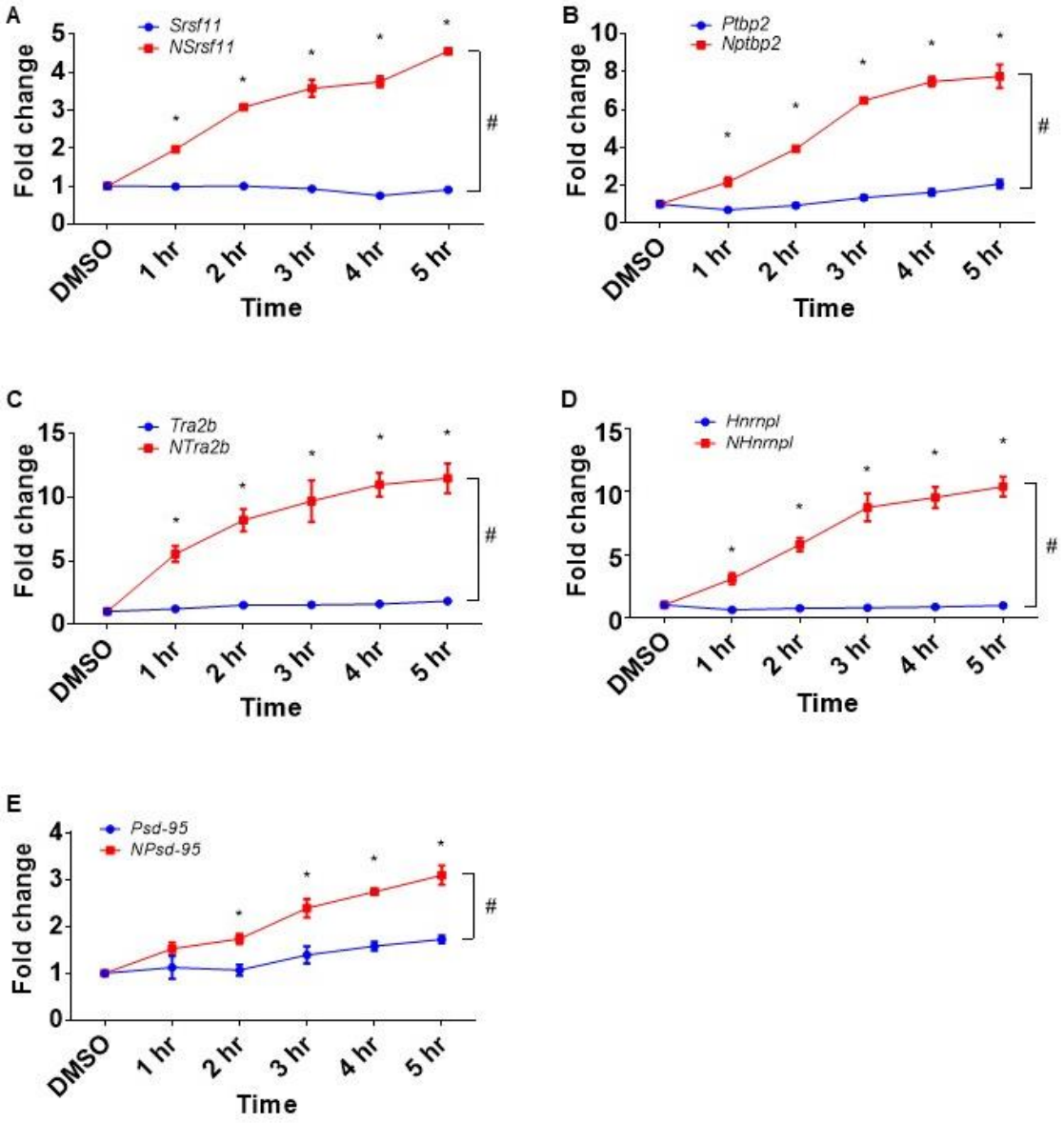

Figure 7. Thapsigargin specifically enhances the endogenous NMD targets. (A–E) Temporal expression of NMD isoforms (red lines) and non-NMD isoforms (blue lines) of *Srsf11, Ptbp2, Tra2b, Hnrnpl*, and *Psd-95* upon 0.2 µM thapsigargin treatment. Expression levels are normalized to DMSO-treated samples. A two-way ANOVA test was used to determine significant difference of expression between the two isoforms. (#) $P < 0.05$. Dunnett's multiple comparison tests were used to determine significant expression changes of individual isoforms over time relative to DMSO treatment. (*) $P < 0.05$. N = 3. Error bars represent mean ± SEM.

The AS-NMD method reveals a strong correlation between ER stress, polysome disassembly, and NMD inhibition in a thapsigargin dose-dependent manner

Since thapsigargin-induced NMD inhibition occurred as early as one hour post-treatment, it is suspected that such NMD inhibition may be coupled with the unfolded protein response (UPR) triggered by thapsigargin-induced ER stress. As a part of UPR, the serine/threonine protein kinase/endoribonuclease inositol-requiring enzyme 1 (IRE1α) oligomerizes and activates its ribonuclease activity through trans-autophosphorylation (Samali et al. 2010; Rubio et al. 2011; Hetz 2012; van Schadewijk et al. 2012). Activated IRE1α excises a 26-nt intron of *Xbp1* mRNA, resulting in a shorter isoform (*Xbp1s*) that encodes a potent transcriptional activator for the expression of chaperones and were used to measure cellular stress level (Figure 8A-B). RT-PCR splicing assay of *Xbp1* with primers flanking the 26-nt intron detected *Xbp1s* at one-hour after thapsigargin treatment with the intron excision continuously enhanced thereafter, indicating increased ER stress and UPR activity (Figure 8A). These results confirmed NMD inhibition and *Xbp1* intron excision happened almost simultaneously in the early phase of thapsigargin treatment.

To further evaluate the association between ER stress and NMD inhibition, a dosage titration of thapsigargin was performed. Cells were treated with thapsigargin at concentrations of 0.002, 0.005, 0.01, 0.02, 0.05, 0.1, and 0.2 μM and harvested at 5 hrs post-treatment for analysis. As expected, *Xbp1s*

increased in a dosage dependent manner (Figure 8B). At the same time, the NMD isoforms of *Srsf11*, *Ptbp2*, *Tra2b*, *Hnrnpl*, and *Psd-95* were uniformly upregulated at a concentration as low as 0.02 μM and escalated in a dose-dependent manner (Figure 8C). Concentrations above 0.2 μM did not further increase NMD inhibition (data not shown). Together, *Xbp1s* splicing and NMD repression exhibited the same kinetics toward thapsigargin. These data support a strong positive correlation between ER stress and NMD inhibition.

In addition to altering gene expression via the IRE1-Xbp1s signaling to retain homeostasis, ER stress also reduces global protein synthesis (Harding, Zhang, and Ron 1999; Ron 2002; Wek, Jiang, and Anthony 2006). Global translation activity is important for triggering NMD (Raimondeau, Bufton, and Schaffitzel 2018). However, the evidence of thapsigargin inhibiting NMD started as low as 20 nM while literatures often used at least 1 μM to induce ER stress (Oslowski and Urano 2011; Ding et al. 2007). Thus, ribosome fractionation assays were performed to determine the NMD-inhibiting thapsigargin doses also repressed translation. Sucrose density-gradient centrifugation was used to examine polysome integrity as an indicator of translational activity. Control cells treated with DMSO showed a typical polysome profile consisting of peaks of individual ribosome subunits (40S and 60S), monosomes (80S), and polysomes (2, 3, 4, 5, and ≥6 ribosomes). Under this normal condition, the heights of the polysome peaks steadily increased with the number of ribosomes (DMSO, Figure 8D). Thapsigargin, on the other hand, effectively reduced the heights of the

polysome peaks. The heavier polysomes (≥4 ribosomes) were affected the most and further collapsed with increasing doses of thapsigargin (Figure 8D). Polysome disintegration was also accompanied by increasing optical density values of 80S. To better visualize and quantify the dose effect of thapsigargin, a line was drawn from the peak of the disome (1st peak after 80S) to the peak of the polysome consisting of roughly eight ribosomes based on relative elution time. The geometric angle created by this line relative to a horizontal line through the disome peak was an indicator of polysome integrity. This angle was 30 for DMSO-treated cells and decreased to 0, −18, −20, −30, and −40 in response to increasing thapsigargin concentrations of 0.01, 0.02, 0.05, 0.1, and 0.2 μM, respectively (Figure 8D). Interestingly, heavy polysomes began to disintegrate from 0.01 μM thapsigargin with minor NMD repression. Yet, the results showed that polysome disassembly was positively correlated with and appeared to lead NMD inhibition. In summary, these data supported that the NMD isoforms were undergoing translation at the onset of thapsigargin treatment and could therefore readily respond to NMD inhibition.

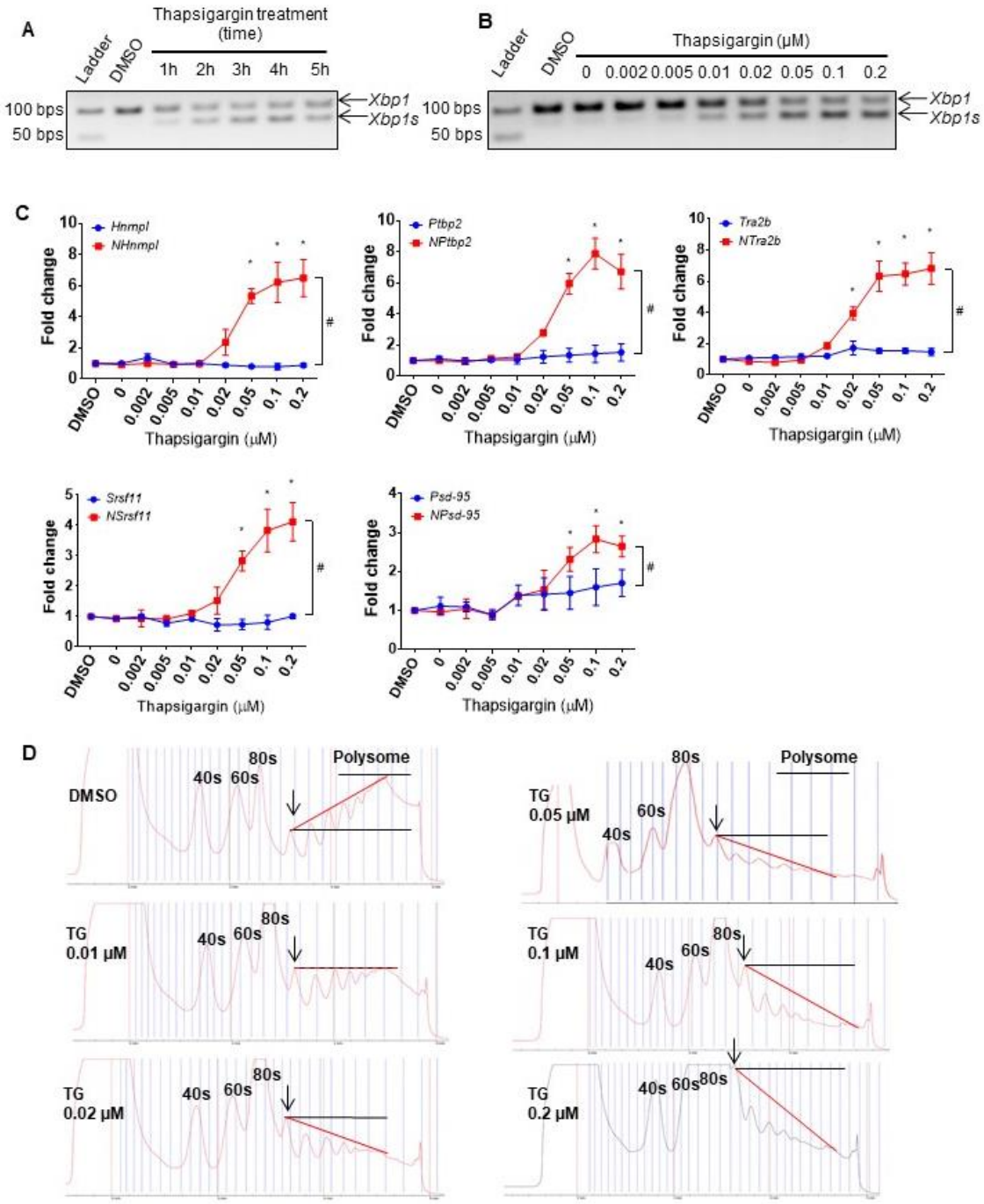
A
Ladder
DMSO
Thapsigargin treatment (time)
1h 2h 3h 4h 5h
100 bps
50 bps
Xbp1
Xbp1s
B
Ladder
DMSO
Thapsigargin (μM)
0 0.002 0.005 0.01 0.02 0.05 0.1 0.2
100 bps
50 bps
Xbp1
Xbp1s
C
Hnrnpl
NHnrnpl
Ptbp2
NPtbp2
Tra2b
NTra2b
Srsf11
NSrsf11
Psd-95
NPsd-95
Fold change
Thapsigargin (μM)
D
DMSO
TG 0.01 μM
TG 0.02 μM
TG 0.05 μM
TG 0.1 μM
TG 0.2 μM
40s
60s
80s
Polysome

Figure 8. Dose-dependent correlation between ER stress, polysome disassembly, and NMD inhibition upon thapsigargin treatment. (A) *Xbp1* splicing when treated with 0.2 µM thapsigargin in N2a cells for the indicated time points. N = 3. (B) Thapsigargin dose-dependent Xbp1 splicing in N2a cells collected at 5 hr. N = 3. (C) Thapsigargin dose-dependent expression of the NMD (red lines) and non-NMD (blue lines) isoforms of *Srsf11, Ptbp2, Tra2b, Hnrnpl*, and *Psd-95* in N2a cells at 5 h after treatment. A two-way ANOVA test was used to determine the significant difference between the two isoforms. (#) $P < 0.05$. Dunnett's multiple comparison tests were used to determine significant expression changes of individual isoforms after thapsigargin treatment in comparison to DMSO treatment. (*) $P < 0.05$. N = 3. Error bars represent mean ± SEM. (D) Polysome fractionation graphs of N2a cells at 5 h after treatment with DMSO, 0.01 µM, 0.02 µM, 0.05 µM, 0.1 µM, and 0.2 µM thapsigargin (TG). 40S, 60S, 80S, disome (black arrow) and polysome are labeled accordingly. In each graph, a red line is drawn from the disome peak to the peak of the eight-ribosome fraction.

Two of the UPR pathways are not responsible for ER stress induced NMD inhibition

Since the degree of NMD inhibition was strongly correlated with the extent of ER stress measured by Xbp1 splicing and polysome disassembly, the following experiments aimed to check which signaling pathway directly led to NMD inhibition. ER stress stimulates three branches of the unfolded protein response (UPR): the IRE1, activating transcription factor 6α (ATF6α), and protein kinase RNA-like endoplasmic reticulum kinase (PERK) pathways (Hiderou Yoshida et al. 1998; H. Yoshida et al. 2001; Harding, Zhang, and Ron 1999; Calfon et al. 2002; Han et al. 2013). These three stress sensors bind to chaperone protein BIP and are quiescent under non-stress conditions. During ER stress, misfolded proteins sequester BIP from continually interacting with these three proteins. Upon release from BIP binding, PERK is activated via autophosphorylation, similar to IRE1α. ATF6α is activated by intramembrane proteolysis and is translocated into the nucleus to induce the transcription of chaperones, such as *Bip*.

To test which pathway mediates NMD activity, RNAi was used to knock down the stress sensors for 48 hours before thapsigargin treatment for 5 hours and examined whether any thapsigargin-inhibited NMD activity could be restored. IRE1α was reported to be targeted by NMD (Oren et al. 2014; Karam et al. 2015), and thapsigargin treatment also enhanced *Ire1*α expression in this study (Figure 9F). However, the AS-NMD assay showed uniformed downregulation of

both the NMD and the non-NMD isoforms for all reporter genes when *Ire1*α was knocked down using silencer select siRNA system (Figure 9A-E). This does not match the normal NMD inhibition profile of the AS-NMD assay, instead, a transcription slowdown. For the *Atf6* pathway, the same reporter genes were examined using AS-NMD assay. *Psd-95* and *Ptbp2* isoforms showed no response to thapsigargin treatment at all, whereas *Tra2b*, *Hnrnpl*, and *Srsf11* were repressed in both non-NMD and NMD isoforms (Figure 9G-K). This ununiformed regulation was inconclusive in concluding the ATF6 pathway responsible for NMD inhibition. In summary, *Ire1α* and *Atf6* were not responsible for NMD inhibition induced by thapsigargin and ER stress described in this study.

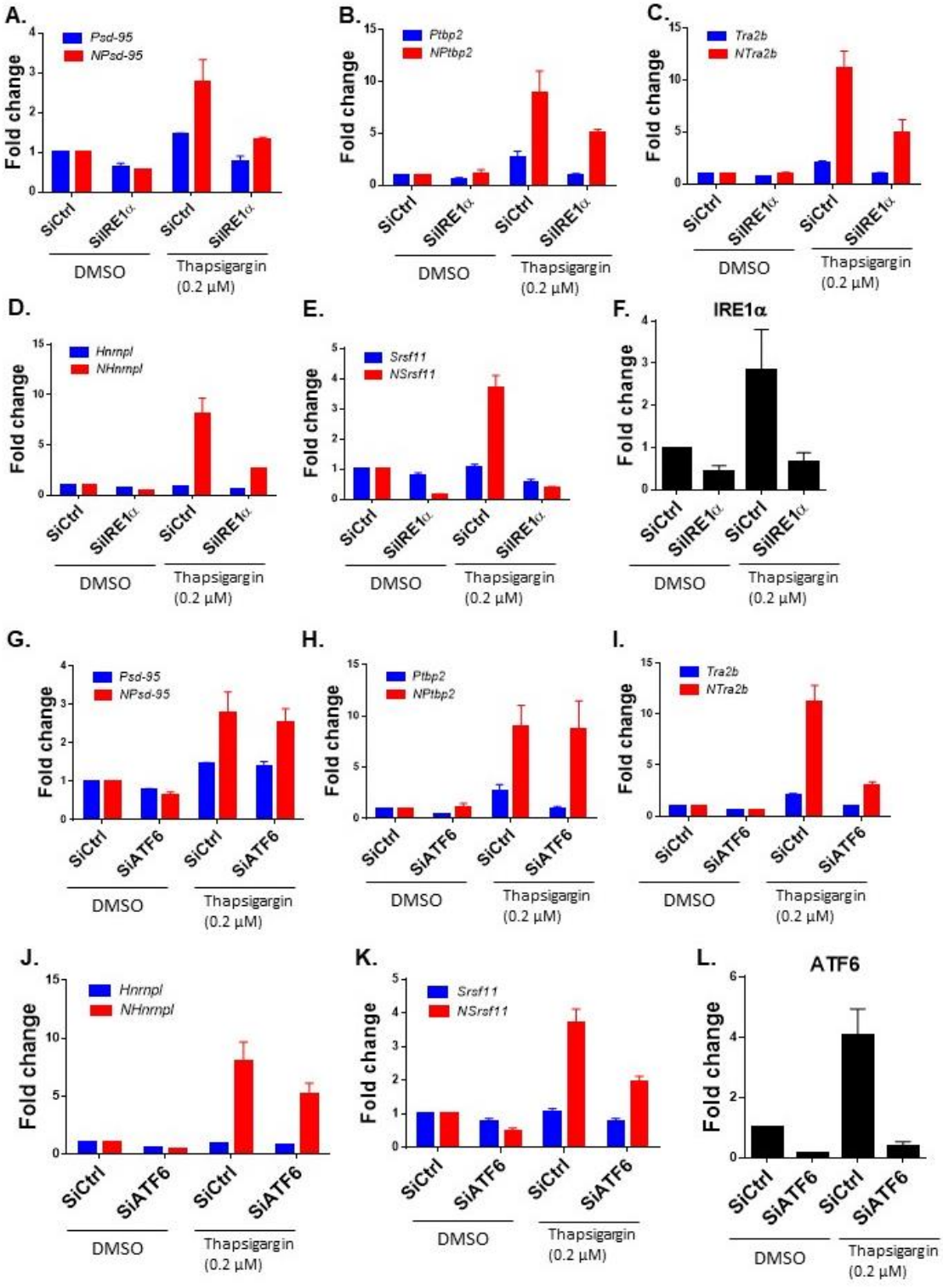
A.
Psd-95
NPsd-95
Fold change
SiCtrl
SiIRE1α
SiCtrl
SiIRE1α
DMSO
Thapsigargin (0.2 μM)
B.
Ptbp2
NPtbp2
Fold change
SiCtrl
SiIRE1α
SiCtrl
SiIRE1α
DMSO
Thapsigargin (0.2 μM)
C.
Tra2b
NTra2b
Fold change
SiCtrl
SiIRE1α
SiCtrl
SiIRE1α
DMSO
Thapsigargin (0.2 μM)
D.
Hnrnpl
NHnrnpl
Fold change
SiCtrl
SiIRE1α
SiCtrl
SiIRE1α
DMSO
Thapsigargin (0.2 μM)
E.
Srsf11
NSrsf11
Fold change
SiCtrl
SiIRE1α
SiCtrl
SiIRE1α
DMSO
Thapsigargin (0.2 μM)
F.
IRE1α
Fold change
SiCtrl
SiIRE1α
SiCtrl
SiIRE1α
DMSO
Thapsigargin (0.2 μM)
G.
Psd-95
NPsd-95
Fold change
SiCtrl
SiATF6
SiCtrl
SiATF6
DMSO
Thapsigargin (0.2 μM)
H.
Ptbp2
NPtbp2
Fold change
SiCtrl
SiATF6
SiCtrl
SiATF6
DMSO
Thapsigargin (0.2 μM)
I.
Tra2b
NTra2b
Fold change
SiCtrl
SiATF6
SiCtrl
SiATF6
DMSO
Thapsigargin (0.2 μM)
J.
Hnrnpl
NHnrnpl
Fold change
SiCtrl
SiATF6
SiCtrl
SiATF6
DMSO
Thapsigargin (0.2 μM)
K.
Srsf11
NSrsf11
Fold change
SiCtrl
SiATF6
SiCtrl
SiATF6
DMSO
Thapsigargin (0.2 μM)
L.
ATF6
Fold change
SiCtrl
SiATF6
SiCtrl
SiATF6
DMSO
Thapsigargin (0.2 μM)

Figure 9. *Ire1α* and *Atf6* pathways are not responsible for NMD inhibition caused by thapsigargin. (A-E) Expression of AS-NMD targets in *Ire1α*-depleted N2a cells at 5 hours after treatment with DMSO or 0.2 µM thapsigargin. (F) *Ire1α* (*Ern1*) expressions in control vs *Ire1α*-depleted N2a cells at 5 hours after treatment with DMSO or 0.2 µM thapsigargin by RT-qPCR. (G-K) Expression of AS-NMD targets in *Atf6*-depleted N2a cells at 5 hours after treatment with DMSO or 0.2 µM thapsigargin. (L) *Atf6* expression in cells treated with Silencer Select siRNA targeting *Atf6* and 0.2 µM thapsigargin simultaneously. N = 3. Error bars represent mean ± SEM.

Thapsigargin inhibits NMD by activating the PERK pathway

Interestingly, the depletion of only PERK completely prevented thapsigargin from repressing NMD. Two independent siRNAs reduced the endogenous *Perk* transcripts to around 20% (Figure 10A). PERK knockdown did not significantly affect the steady-state levels of either the NMD or non-NMD isoforms of *Psd-95*, *Ptbp2*, and *Tra2b* (Figure 10B–D). Thapsigargin application in control siRNA-pretreated cells induced only the NMD isoforms of these genes along with *Xbp1s* and *Bip* (Figure 10B-F) and also surprisingly increased *Perk* transcript levels (Figure 10A). In siPerk-pretreated cells, none of the NMD isoforms were upregulated by thapsigargin (Figure 10B-D).

Xbp1s levels, which are indicative of IRE1α activity, were still six- to eightfold higher in the thapsigargin-treated siPerk cells than in DMSO-treated cells (Figure 10E). Similarly, *Bip* transcript levels, which are widely used as a reporter of ATF6α activity, were unchanged by control siRNA, *Perk* siRNAs or DMSO treatment, but remained high after thapsigargin treatment regardless of siPerk application (Figure 10F). Further validating the activation of IRE1α and ATF6α by thapsigargin was not sufficient to inhibit NMD.

Because RNAi-mediated depletion could not resolve whether it was the physical scaffold or enzymatic activity of PERK that was essential for NMD inhibition, a small molecule PERK inhibitor, GSK2606414, that inhibits the specific enzymatic activity of PERK was used for further evaluation (Axten et al. 2012). Application of GSK2606414, like siPerk alone, did not affect NMD activity

in DMSO-treated cells (Figure 10G-I). In thapsigargin-treated cells, however, pretreatment of GSK2606414 for one hour effectively reversed the up-regulation of the NMD isoforms in a dose-dependent manner (Figure 10G-I). GSK2606414 phenocopied *Perk* siRNA treatment in attenuating thapsigargin-induced Xbp1s but to a level still well above that in DMSO-treated cells (Figure 10J). Similar to RNAi depletion of Perk, GSK2606414 did not down-regulate *Bip* transcripts (Figure 10K). These data further show that of the three UPR branches only PERK activity was required for thapsigargin to inhibit NMD.

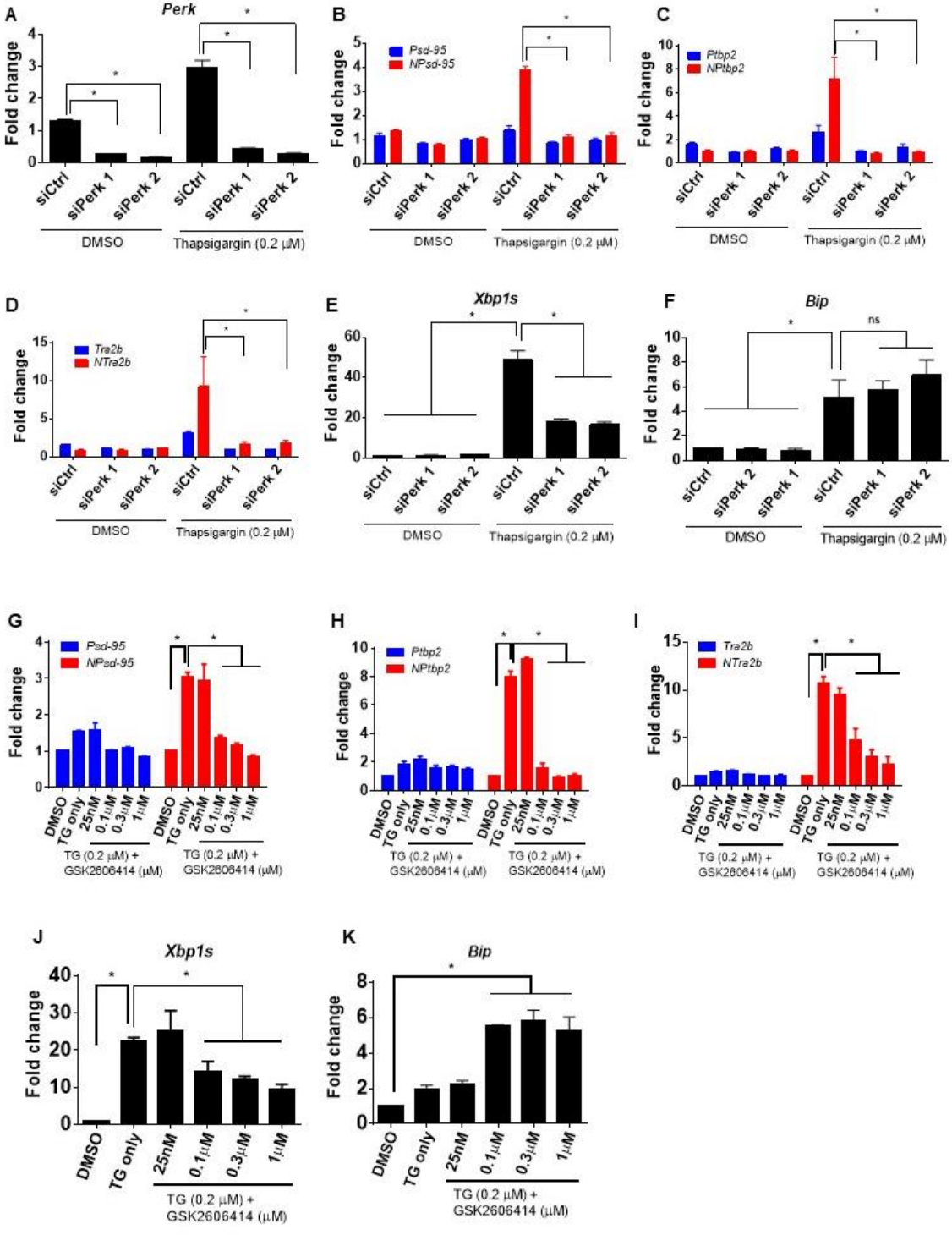
A
Perk
Fold change
siCtrl
siPerk 1
siPerk 2
DMSO
Thapsigargin (0.2 μM)
B
Psd-95
NPsd-95
C
Ptbp2
NPtbp2
D
Tra2b
NTra2b
E
Xbp1s
F
Bip
ns
G
H
I
J
K
DMSO
TG only
25nM
0.1μM
0.3μM
1μM
TG (0.2 μM) +
GSK2606414 (μM)

Figure 10. PERK is necessary for thapsigargin-induced NMD inhibition. Expression levels of *Perk* (*A*); the NMD (red) and non-NMD (blue) isoforms of *Psd-95* (*B*), *Ptbp2* (*C*), and *Tra2b* (*D*); *Xbp1s* (*E*); and *Bip* (*F*) after *siPerk* knockdown and thapsigargin treatment. Control siRNA and two different siRNAs targeting *Perk* were transfected into N2a cells for 48 h before thapsigargin application. Note that the thapsigargin effect on the NMD isoforms was completely blocked by *siPerk* transfection (*B*–*D*). Expression levels of the NMD (red) and non-NMD (blue) isoforms of *Psd-95* (*G*), *Ptbp2* (*H*), and *Tra2b* (*I*) as well as *Xbp1s* (*J*) and *Bip* (*K*) in N2a cells treated with DMSO, thapsigargin, or thapsigargin plus PERK inhibitor GSK2606414 at indicated concentrations. A dosage of 0.1 μM GSK2606414 or above was sufficient to revert the effect of thapsigargin on the NMD isoforms (*G*–*I*). A one-way ANOVA test was used for *A*, *E*, *F*, *J*, and *K*. A two-way ANOVA test followed by Dunnett's multiple comparison tests was used for *B*, *C*, *D*, *G*, *H*, and *I*. (*) $P < 0.05$; (ns) not significant. $N = 3$. Error bars represent mean ± SEM.

PERK activation induced polysome disassembly is responsible for NMD inhibition

Activated PERK phosphorylates eIF2α at serine 51, leading to attenuation of protein synthesis and polysome disassembly (Harding, Zhang, and Ron 1999; Wek, Jiang, and Anthony 2006). To test whether eIF2α was part of the signaling cascade, quantitative immunoblots on total eIF2α and phosphor-eIF2α (Ser51) in cells treated with thapsigargin and PERK inhibitor GSK2606414 were made. As expected, DMSO did not alter the level of phosphorylation. An increase in phosphor-eIF2α at one and a half hours after thapsigargin treatment was observed, which was completely diminished by GSK2606414 (Figure 11A). Meanwhile, total eIF2α levels remained constant across all conditions (Figure 11A). At the same time, the polysome profile graphs also confirmed that GSK2606414 could partially restore polysome integrity which was sufficient to also reverse the NMD inhibition caused by thapsigargin (Figure 11B). These data supported the mechanism that thapsigargin inhibits NMD via PERK activation and subsequent attenuation of global protein translation through eIF2α phosphorylation (Fig. 11C).

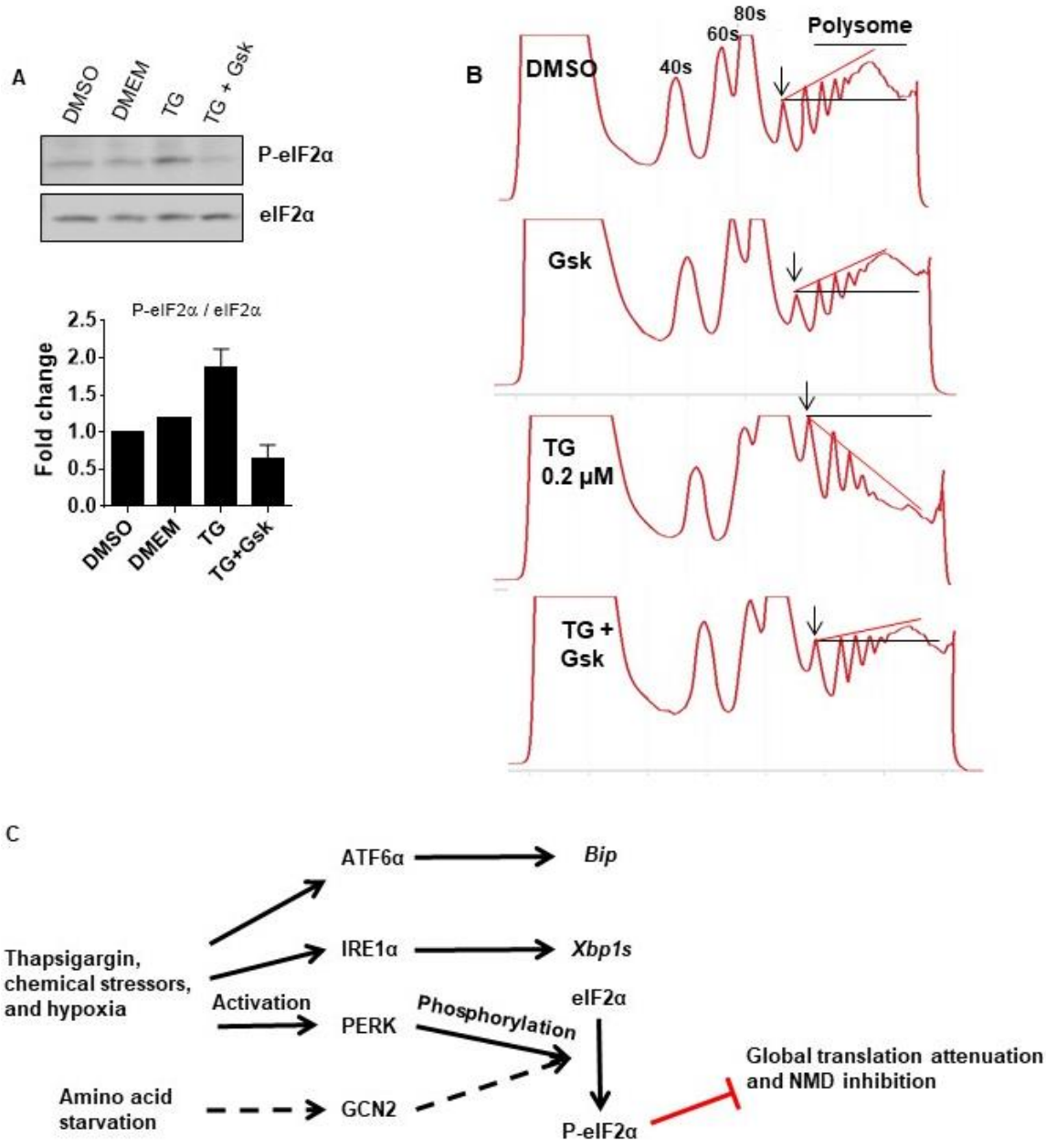
A
DMSO
DMEM
TG
TG + Gsk
P-eIF2α
eIF2α
P-eIF2α / eIF2α
Fold change
2.5
2.0
1.5
1.0
0.5
0.0
DMSO
DMEM
TG
TG+Gsk
B
DMSO
40s
60s
80s
Polysome
Gsk
TG
0.2 μM
TG +
Gsk
C
ATF6α
Bip
Thapsigargin,
chemical stressors,
and hypoxia
IRE1α
Xbp1s
Activation
PERK
Phosphorylation
eIF2α
Amino acid
starvation
GCN2
P-eIF2α
Global translation attenuation
and NMD inhibition

Figure 11. Inhibiting PERK rescues thapsigargin-induced NMD attenuation by restoring polysome integrity and translation. *(A)* Western blots and quantification of phosphorylated eIF2α (P-eIF2α) and eIF2α when treated with thapsigargin and Gsk (0.3 μM) treatments. Bands are quantified via Image Quant and normalized with eIF2α to obtain fold changes. N = 2. Error bars represent mean ± SEM. (*B*) Polysome fractionation graphs of N2a cells at 5 h after treatment with DMSO, Gsk, 0.2 μM thapsigargin, or Gsk (0.5 μM) and thapsigargin (0.2 μM) double treatments. 40S, 60S, 80S, disome (black arrow) and polysome are labeled accordingly. In each graph, a red line is drawn from the disome peak to the estimated peak of the eight-ribosome fraction. (*C*) Proposed mechanism of thapsigargin and other stressors leading to NMD inhibition.

NMD inhibition is not ubiquitous under various cellular stresses

While investigating stress and NMD regulation, a question arose whether NMD could be ubiquitously inhibited under different cellular stresses. The AS-NMD reporter assay enabled the systematic study into stress and NMD. Various stress tests were conducted In N2a cells to observe changes in NMD activities such as high temperatures (up to 45°C for 2 hours) or serum deprivation (as low as 0% fetal bovine serum for up to 24 hours). Yet, NMD inhibition was only observed after culturing N2a cells in L-glutamine-free media (Figure 12). The NMD isoform levels of *Psd-95*, *Ptbp2*, and *Tra2b* were not altered during the first 6 hours of switching to L-glutamine-free media, possibly due to residual cellular glutamine sustaining cell metabolism. These NMD isoforms were clearly up-regulated at 12 hours and further enhanced at 15 hours (Figure 12A-C). These data show that amino acid deprivation could also lead to NMD inhibition, likely through the GCN2 pathway (Zhang et al. 2002). The cellular stress NMD inhibition was not limited to stress caused by thapsigargin but also not ubiquitous under all cellular stresses.

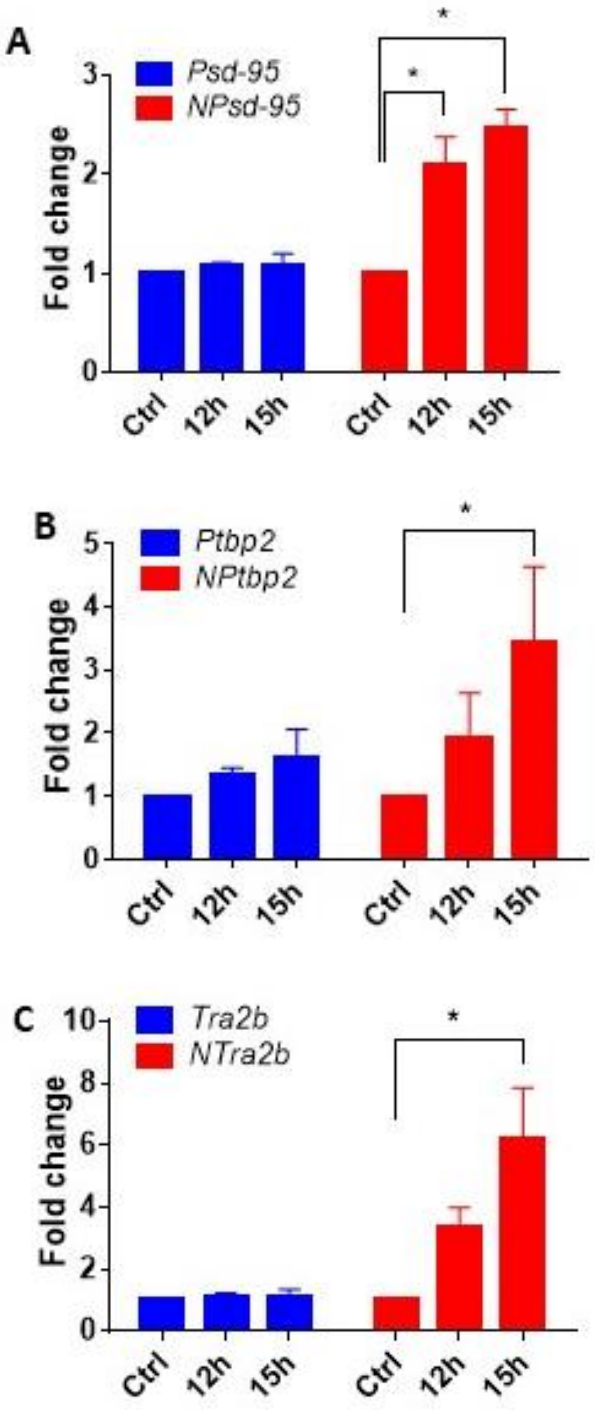
A
Psd-95
NPsd-95
Fold change
0
1
2
3
*
*
Ctrl
12h
15h
Ctrl
12h
15h
B
Ptbp2
NPtbp2
Fold change
0
1
2
3
4
5
*
Ctrl
12h
15h
Ctrl
12h
15h
C
Tra2b
NTra2b
Fold change
0
2
4
6
8
10
*
Ctrl
12h
15h
Ctrl
12h
15h

Figure 12. Amino acid deprivation inhibits NMD in a temporal manner. Expression levels of the NMD and non-NMD isoforms of *Psd-95 (A)*, *Ptbp2 (B)*, and *Tra2b (C)* in N2a cells cultured in L-glutamine-free media for 12 and 15 hours. The NMD isoforms but not the non-NMD isoforms were significantly upregulated by L-glutamine deprivation. A two-way ANOVA followed by Dunnett's multiple comparison tests was used to determine significant changes in gene expression. *, $P < 0.05$. N=3. Error bars represent mean ± SEM.

ER stress enhances TDP-43-controlled NMD isoforms through PERK

NMD plays critical roles in physiology and pathogenesis; therefore, the modulation of NMD activity may impact NMD-associated diseases. The recent discovery implicating NMD regulation in the pathogenic mechanisms of amyotrophic lateral sclerosis (ALS) and frontotemporal dementia (FTD) could be a good model to demonstrate the relevance of NMD modulation (Barmada et al. 2015; J. P. Ling et al. 2015). Ling et al. proposed that TDP-43-deficient cells produce many cryptically spliced gene isoforms could be one of the pathogenic mechanisms (J. P. Ling et al. 2015). Because many of these cryptic isoforms are subjected to NMD regulation, it is reasoned that ER stress might aggravate TDP-43 deficiency in the up-regulation of these NMD isoforms.

To investigate the possible compounding effect of ER stress on TDP-43-mediated NMD isoforms, the expression of TDP-43-repressed cryptic exons were examined with and without thapsigargin treatment. Specific PCR primers flanking the previously reported cryptic exons of *A230046K03Rik*, *Mib1*, and *Usp15* were designed to measure the ratios of the NMD isoforms to their corresponding translational isoforms. The splicing of cryptic exons was not detected in cells treated with control siRNA or DMSO but was drastically boosted by RNAi-mediated depletion of *Tdp-43* (Figure 13). Subsequent thapsigargin treatment further increased the level of the NMD sensitive cryptic isoforms in TDP-43-deficient cells but had no effect in the mock-transfected or control siRNA-transfected cells (Figure 13).

To test whether the thapsigargin compounding effect was due to PERK-mediated NMD inhibition, *Perk* was knocked down using RNAi prior to the drug treatment. As shown by two independent *Perk* siRNAs, loss of *Perk* did not cause cryptic splicing on its own nor interfere with the activity of TDP-43 in DMSO-treated cells (Figure 13). However, PERK knockdown completely eliminated thapsigargin's additive effects to TDP-43 depletion, resulting in similar isoform ratios between the DMSO and thapsigargin treatments. These results confirmed that ER stress exacerbated the cryptically spliced NMD isoforms buildup through PERK activation in TDP-43-deficient cells, identical with the ER stress-NMD inhibition pathway.

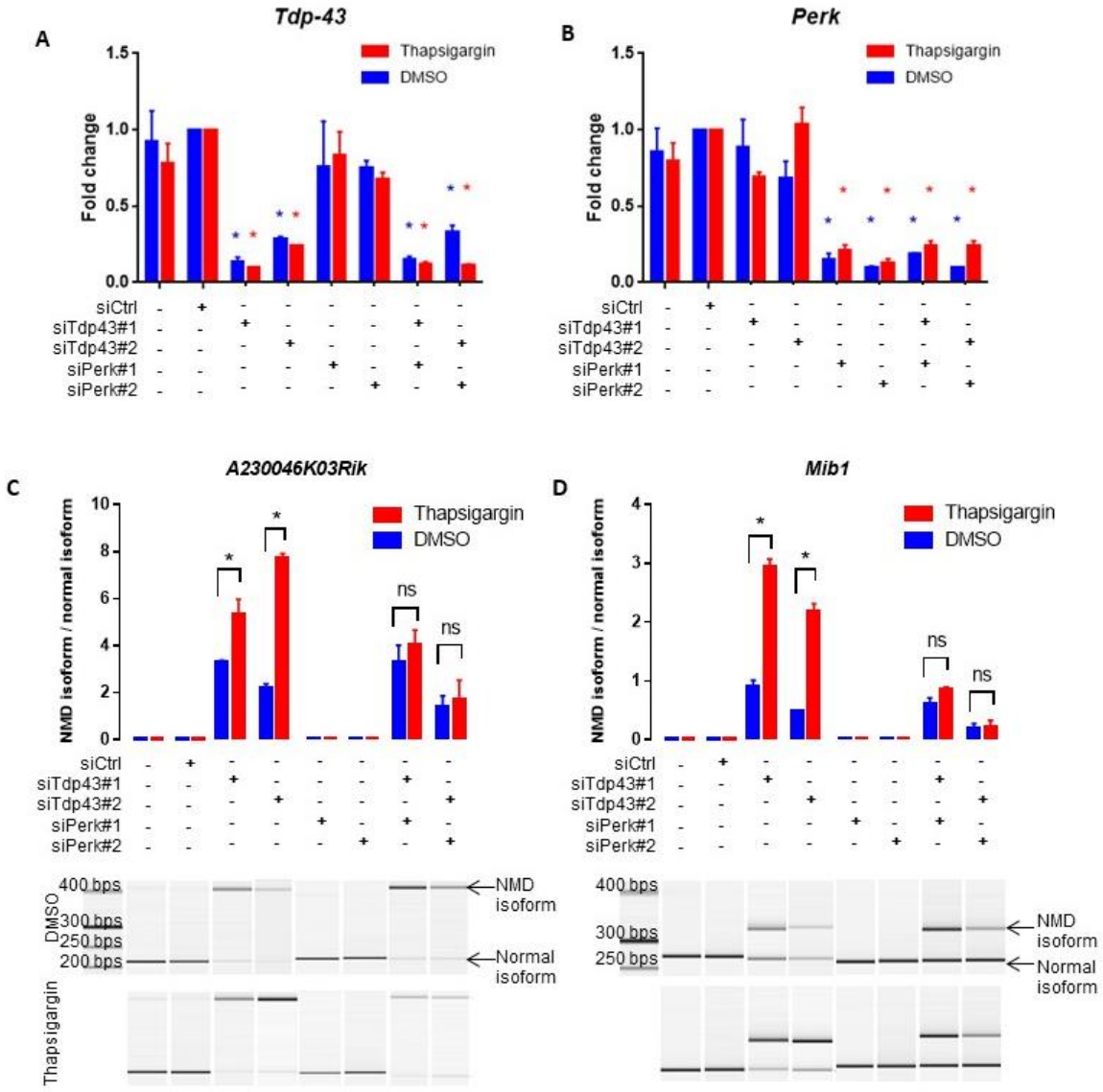
A
Tdp-43
Thapsigargin
DMSO
Fold change
1.5
1.0
0.5
0.0
siCtrl
siTdp43#1
siTdp43#2
siPerk#1
siPerk#2
B
Perk
Thapsigargin
DMSO
Fold change
C
A230046K03Rik
NMD isoform / normal isoform
Thapsigargin
DMSO
ns
400 bps
300 bps
250 bps
200 bps
NMD isoform
Normal isoform
DMSO
Thapsigargin
D
Mib1
NMD isoform / normal isoform
Thapsigargin
DMSO
ns
400 bps
300 bps
250 bps
NMD isoform
Normal isoform

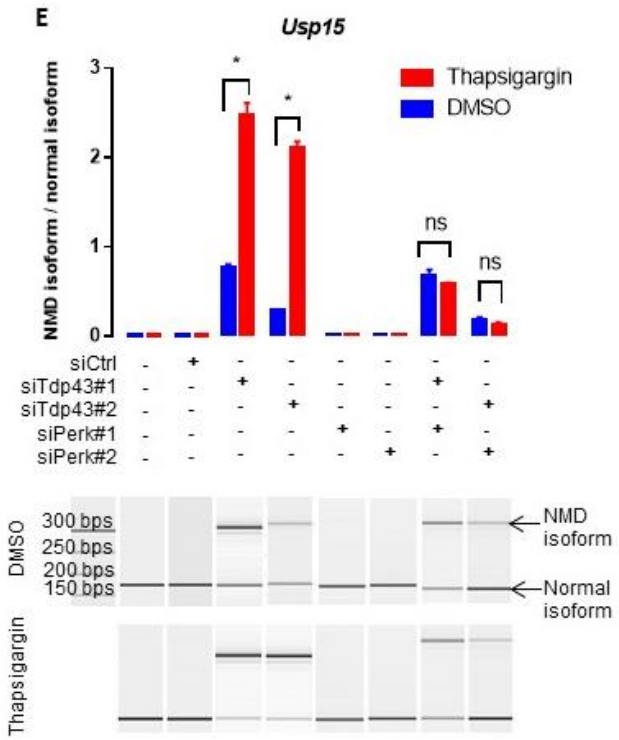

Figure 13. Thapsigargin enhances TDP-43-repressed NMD isoforms through PERK. The expression levels of *Tdp-43* (*A*) and *Perk* (*B*) in N2a cells transfected with control siRNA, siTdp43, and/or siPerk and subsequently treated with DMSO or 0.2 µM thapsigargin. These cells were also assayed for the expression of the normal and NMD isoforms of *A230046K03Rik* (*C*), *Mib1* (*D*), and *Ups15* (*E*). Representative digital gels are shown in the *lower* panels. Arrows point to the NMD and normal isoforms. The ratio of the NMD isoform relative to the normal isoform was quantified for each gene under each experimental condition (*upper* panels). In siTdp43 cells, thapsigargin further increased the ratios. In siTdp43 and siPerk double-knockdown cells, thapsigargin had no effect on the ratios compared to DMSO. (ns) $P \geq 0.05$; (*) $P < 0.05$ (two-way ANOVA followed by Dunnett's multiple comparison tests). All error bars represent mean ± SEM. $N = 3$.

Discussion

AS-NMD assay is sensitive and has a broad dynamic range thanks to the high resolution and wide range of RT-qPCR. It can determine the efficiency and dynamics of NMD activity regulated by cellular pathways or during development, for analyzing the kinetics of drug response, and for dissecting the underlying molecular mechanisms. While the repressive effect of thapsigargin on NMD started to plateau at a concentration of 0.2 µM and above, NMD inhibition was already detected at treatment levels as low as 0.02 µM (Figure 8). At this low concentration, the NMD isoform up-regulation was only about 20% of the maximal up-regulation but was nevertheless consistently detected by the method (Figure 8). Similarly, in the time course experiment, 20%–30% of full inhibition (typically achieved at 5 h post-treatment) was readily detectable at 1 h post-treatment (Figure 7).

Before the AS – NMD screening, initial experiments were done to test whether core NMD factors were affected after 5 hours of thapsigargin treatment. No changes were found in the NMD factors expression (data not shown). A previous study reported a 1.5- to 2.5-fold increase in *Upf1* mRNA in HeLa cells 4 days after chronic depletion of various NMD factors (Yepiskoposyan et al. 2011). The apparent contrast may be due to the difference in the time scale of the treatment and changes in NMD activities observed in this study were not due to changes in core NMD factors.

Strong correlation between NMD inhibition, endoplasmic reticulum (ER)

stress and polysome disassembly upon thapsigargin treatment was discovered in a temporal and dose dependent manner. Previous studies have reported a UPR gene *Ire1*α to be targeted by NMD (Oren et al. 2014; Karam et al. 2015), and thapsigargin indeed enhanced *Ire1*α expression (Figure 9F). However, *Ire1*α expression remained unchanged at one hour when *Xbp1s* was first detected, suggesting that the initial *Xbp1* splicing was due to oligomerization-induced activation of IRE1α protein. Subsequent *Ire1*α induction may potentiate more *Xbp1* intron excision. *Ire1*α induction occurred at 0.01 μM and intensified with increasing concentration also suggesting that the initial *Xbp1* splicing was due to oligomerization-induced activation of IRE1α protein (data not shown).

Depletion of *Ire1α* or *Atf6* alone was not enough to fully rescue thapsigargin-induced inhibition of NMD activity. Both *Ire1α* and *Atf6α* were upregulated by thapsigargin while RNAi treatment efficiently reduced thapsigargin effects (Figure 9F and L). Depletion of *Ire1α* dampened thapsigargin-enhanced NMD isoforms by about twofold but did not revert their levels to those of pre-thapsigargin treatment (Figure 9A-E). Reduction of *Atf6α* did not alter the effect of thapsigargin on the NMD isoforms (Figure 9G–K). In the following *Perk* inhibition and knockdown experiments, a strong correlation of PERK activation, polysome disassembly, and NMD inhibition was observed (Figure 10 and 11). NMD inhibition successfully was rescued using PERK inhibitor and RNAi methods, along with the rescue of polysome integrity. The findings are therefore consistent with previous reports and support the

hypothesis that NMD inhibition is specific to PERK-eIF2α-translation repression signaling (Chiu et al. 2004; Gardner 2008, 2010; Hu et al. 2010; Wang et al. 2011).

On the other hand, the AS-NMD assay did not detect a role of intracellular Ca2+ signaling in NMD inhibition. Downstream from thapsigargin treatment, PERK inhibition via a specific drug inhibitor or *siRNA* depletion did not reverse the increase in cytosolic Ca2+ but did completely restore NMD activity. Furthermore, other chemicals increasing intracellular Ca2+ failed to attenuate NMD. Therefore, increased intracellular Ca2+ was not enough to inhibit NMD in our system, contradicting a recent study reporting calcium's sufficient role (Nickless et al. 2014). One possible explanation is that this study used mouse N2a cells, whereas Nickless et al. used human osteosarcoma cells (U2OS). Additionally, the use of exogenous fluorescent mini-gene reporters to measure NMD activity may be jeopardized due to the nature of thapsigargin translational inhibition from ER stress (Figure 11). The unintended translational attenuation could interfere with fluorescence and increase background signals that could alter the NMD ratio, leading to inaccurate interpretations.

Another stress, glutamine deprivation, also inhibited NMD in this study, while heat shock or serum withdrawal did not. This result was consistent with a previous study reporting NMD attenuation upon deprivation of all amino acids (Mendell et al. 2004). Although the mechanism of NMD inhibition by amino acid starvation remains unclear, it is probably due to translation interference. Amino

acid starvation activates general control nonderepressible 2 (GCN2), which can phosphorylate eIF2α (Dever et al. 1992) to slow down translation just like PERK activation (Pain 1994).

Finally, evidence of ER stress compounding TDP-43 depletion upregulated cryptic NMD isoforms was presented. These cryptic isoforms have been implicated in the pathogenic mechanisms of amyotrophic lateral sclerosis and frontotemporal dementia (J. P. Ling et al. 2015; Barmada et al. 2015). This study showed an adverse effect of ER stress on TDP-43 proteinopathy enhancing TDP-43-repressed NMD substrates (Figure 13). ER stress-stimulating episodes could thus restrain TDP-43 defective cells from clearing up these unwanted transcripts in a timely manner and could even possibly accelerate progressive loss of neurons in ALS and FTD patients. PERK inhibition completely blocked the undesirable effect of ER stress, providing a possible target of therapeutics to ameliorate the ill influence of ER stress on TDP-43 deficiency (Figure 13C-E).

As a proof-of-principle study, the AS-NMD method not only proved that thapsigargin induced NMD inhibition is caused through PERK activation and ER stress instead of intracellular calcium, it also demonstrated its utility in a genetic disease model like ALS - FTD. Increasing evidence suggests NMD can actively integrate into various cellular processes such as alternative splicing, unfolded protein responses, amino acid deprivation, and cellular stresses. This

endogenous assay could monitor and reveal more about NMD in the future with minimum invasion.

Materials and Methods

Cell cultures and drug treatments

Neuro-2a (N2a) cells were cultured in N2a complete media (L-glutamine-free Dulbecco's modified Eagle's medium (DMEM), 10% FBS and 1× GlutaMAX) at 37°C and 5% CO2. 750,000 cells were plated on 35 mm BioLite TC plates or 6 well dishes and incubated with 2 mL of N2a complete media overnight before thapsigargin treatments (VWR, cat. no. 89161-410). The cells were collected at 5 h post-treatment unless otherwise specified. The PERK inhibitor GSK2606414 (Thermo Fisher, cat. no. 501016108) was dissolved in DMSO. N2a cells were incubated with GSK2606414 for 1 h before thapsigargin treatment. For L-glutamine deprivation, 750,000 N2a cells were plated overnight and switched to L-glutamine-free DMEM with 10% FBS. SiRNA knockdown experiments were conducted using Lipofectamine RNAiMax and Silencer Select siRNAs (siTdp-43, cat. no. s106688 and s106686; siPerk, cat. no. s201280 and s65405; siIre1 cat. no. s95859; siAtf6, cat. no. s105470) according to the manufacturer's instructions. Silencer Negative Control siRNA (AM4615) was used as the siRNA control. Cells were incubated for 48 h for optimal knockdown efficiency or overexpression before downstream treatments.

RNA extraction, cDNA synthesis, and RT-qPCR

TRIzol (Life Technologies, cat. no. 15596-018) was directly added to the cells to extract total RNA following the TRIzol reagent standard protocol. Isolated RNA was treated with 4 units of Turbo DNase (Ambion) at 37°C for 35 min to degrade all remaining genomic DNA. After the DNase treatment, RNA was purified again using phenol-chloroform (pH 4.5, VWR cat. no. 97064-744). RNA concentrations were measured using a Nanodrop 2000c (Thermo Fisher). One microgram of freshly isolated DNA-free RNA was converted to cDNA using 1 µL random hexamers (30 µM) and 200 units of Promega M-MLV reverse transcriptase (cat. no. M1705) following the Promega protocol in a 20 µL reaction. For all qPCR primers, quality control was performed for their specificity, sensitivity, melting curves, and standard curves (Table 3). RT-qPCR experiments were conducted using a QuantStudio 6 Real-Time PCR instrument with 2× Power SYBR Green PCR master mix (Life Tech) following the Life Tech protocol. Each 10 µL reaction contained 0.3 µL cDNA, 5 µL 2× Power SYBR Green PCR master mix, 0.3 nM forward primer, and 0.3 nM reverse primer. The QuantStudio 6 RT-qPCR run program was as follows: 50°C for 2 min; 95°C for 15 sec and 60°C for 1 min, with the 95°C and 60°C steps repeated for 40 cycles; and a melting curve test from 60°C to 95°C at a 0.05°C/sec measuring rate. QuantStudio Real-Time PCR software was used for the analysis. All RT-qPCR reactions were conducted with three technical replicates along with a no template control (NTC, not amplified). Outliers were excluded when the coefficient of

variation of Ct for the three technical replicates was larger than 0.3. Relative expression (fold changes) was calculated using the ΔΔCt method. For the splicing assays of the NMD exons, PCR was performed using New England Biolab Taq DNA polymerase (cat. no. M0267E). All statistical analysis was performed using GraphPad Prism 6.

Protein extraction, immunoblotting, and quantitative image analysis

Cells in six-well plates were washed twice with 1 mL cold 1× PBS and harvested with freshly prepared RIPA buffer. The BCA assay (Thermo Scientific) was performed to determine protein concentrations before loading equal amounts of the materials onto SDS-PAGE gels (4% stacking and 12% resolving) for Western blotting. Primary antibodies P-eIF2 (1:333, Thermo Fisher), eIF2 (1:1000, Thermo Fisher), and GAPDH (1:1500, Ambion). Specific Western blot bands were quantified using ImageQuant TL and normalized with GAPDH to derive the relative protein levels.

Quantitative analysis of cryptic exon splicing

Optimized RT-PCR cycles were A230046K03Rik (29 cycles), Mib1 (29 cycles), and Usp15 (29 cycles) (Table 4). Quantitative gel electrophoresis of PCR amplicons was conducted. Splicing of the exons was determined using the following formula. All statistical analysis was performed using GraphPad Prism 6.

Cryptic splicing ratio = isoform including the cryptic exon / isoform skipping the cryptic exon

All ratios were calculated using in nmol measured by Qiaxcel.

Polysome fractionation

For polysome fractionation, 1.5×10^7 N2a cells in 20 mL N2a complete media were plated on 150 mm petri dishes overnight and treated with varying concentrations of thapsigargin the next day. Cycloheximide (Fisher Scientific, cat. no. 50490338) was added at a concentration of 100 µg/mL, and the cells were incubated for 10 min at 37°C before lysate collection. The cells were washed twice with 10 mL cold 1× PBS containing 100 µg/mL cycloheximide then collected in 4 mL of the same cold PBS solution. The cells were lysed with 0.5 mL lysis buffer (20 mM Tris pH 7.5, 100 mM KCl, 5 mM MgCl2, 2 mM DTT, 100 µg/mL cycloheximide, 1% Triton X-100, 50 µ/mL RNaseout, and 1× EDTA-free protease inhibitor cocktail). Roughly 400 µL (6000 optical units) of lysate was loaded onto premade sucrose gradients (60% to 15%) and balanced (within 0.5 mg) before ultracentrifugation at 4°C and 237,000g (50,000 rpm for a SW55 Ti rotor) for 1.5 h. Products were carefully removed from the ultracentrifuge and fractionated with the apparatus consisting of the gradient fractionator (Brandel SYN-202), the ISCO absorbance detector (ISCO # UA-6), and the fraction collector (R1 Fraction Collector) at 2.0 sensitivity and 150 cm/h chart speed to record absorbance data and collect fractionations.

References

Arai, Tetsuaki, Masato Hasegawa, Haruhiko Akiyama, Kenji Ikeda, Takashi Nonaka, Hiroshi Mori, David Mann, et al. 2006. “TDP-43 Is a Component of Ubiquitin-Positive Tau-Negative Inclusions in Frontotemporal Lobar Degeneration and Amyotrophic Lateral Sclerosis.” *Biochemical and Biophysical Research Communications* 351 (3): 602–11.

Axten, Jeffrey M., Jesús R. Medina, Yanhong Feng, Arthur Shu, Stuart P. Romeril, Seth W. Grant, William Hoi Hong Li, et al. 2012. “Discovery of 7-Methyl-5-(1-[3-(trifluoromethyl)phenyl]acetyl-2,3-Dihydro-1H-Indol-5-Yl)-7H-pyrrolo[2,3-D]pyrimidin-4-Amine (GSK2606414), a Potent and Selective First-in-Class Inhibitor of Protein Kinase R (PKR)-like Endoplasmic Reticulum Kinase (PERK).” *Journal of Medicinal Chemistry* 55 (16): 7193–7207.

Barmada, Sami J., Shulin Ju, Arpana Arjun, Anthony Batarse, Hilary C. Archbold, Daniel Peisach, Xingli Li, et al. 2015. “Amelioration of Toxicity in Neuronal Models of Amyotrophic Lateral Sclerosis by hUPF1.” *Proceedings of the National Academy of Sciences of the United States of America* 112 (25): 7821–26.

Calfon, Marcella, Huiqing Zeng, Fumihiko Urano, Jeffery H. Till, Stevan R. Hubbard, Heather P. Harding, Scott G. Clark, and David Ron. 2002. “IRE1 Couples Endoplasmic Reticulum Load to Secretory Capacity by Processing the XBP-1 mRNA.” *Nature* 415 (6867): 92–96.

Chiu, Shang-Yi, Fabrice Lejeune, Aparna C. Ranganathan, and Lynne E. Maquat. 2004. “The Pioneer Translation Initiation Complex Is Functionally Distinct from but Structurally Overlaps with the Steady-State Translation Initiation Complex.” *Genes & Development* 18 (7): 745–54.

Dever, T. E., L. Feng, R. C. Wek, A. M. Cigan, T. F. Donahue, and A. G. Hinnebusch. 1992. “Phosphorylation of Initiation Factor 2 Alpha by Protein Kinase GCN2 Mediates Gene-Specific Translational Control of GCN4 in Yeast.” *Cell* 68 (3): 585–96.

Ding, Wen-Xing, Hong-Min Ni, Wentao Gao, Yi-Feng Hou, Melissa A. Melan, Xiaoyun Chen, Donna B. Stolz, Zhi-Ming Shao, and Xiao-Ming Yin. 2007. “Differential Effects of Endoplasmic Reticulum Stress-Induced Autophagy on Cell Survival.” *The Journal of Biological Chemistry* 282 (7): 4702–10.

Gardner, Lawrence B. 2008. “Hypoxic Inhibition of Nonsense-Mediated RNA Decay Regulates Gene Expression and the Integrated Stress Response.” *Molecular and Cellular Biology* 28 (11): 3729–41.

———. 2010. “Nonsense-Mediated RNA Decay Regulation by Cellular Stress: Implications for Tumorigenesis.” *Molecular Cancer Research: MCR* 8 (3): 295–308.

Guo, Weirui, Yanbo Chen, Xiaohong Zhou, Amar Kar, Payal Ray, Xiaoping Chen, Elizabeth J. Rao, et al. 2011. “An ALS-Associated Mutation Affecting TDP-43 Enhances Protein Aggregation, Fibril Formation and Neurotoxicity.” *Nature Structural & Molecular Biology* 18 (7): 822–30.

Han, Jaeseok, Sung Hoon Back, Junguk Hur, Yu-Hsuan Lin, Robert Gildersleeve, Jixiu Shan, Celvie L. Yuan, et al. 2013. “ER-Stress-Induced Transcriptional Regulation Increases Protein Synthesis Leading to Cell Death.” *Nature Cell Biology* 15 (5): 481–90.

Harding, H. P., Y. Zhang, and D. Ron. 1999. “Protein Translation and Folding Are Coupled by an Endoplasmic-Reticulum-Resident Kinase.” *Nature* 397 (6716): 271–74.

Hetz, Claudio. 2012. “The Unfolded Protein Response: Controlling Cell Fate Decisions under ER Stress and beyond.” *Nature Reviews. Molecular Cell Biology* 13 (2): 89–102.

Hu, Wenqian, Christine Petzold, Jeff Coller, and Kristian E. Baker. 2010. “Nonsense-Mediated mRNA Decapping Occurs on Polyribosomes in Saccharomyces Cerevisiae.” *Nature Structural & Molecular Biology* 17 (2): 244–47.

Karam, Rachid, Chih-Hong Lou, Heike Kroeger, Lulu Huang, Jonathan H. Lin, and Miles F. Wilkinson. 2015. “The Unfolded Protein Response Is Shaped by the NMD Pathway.” *EMBO Reports* 16 (5): 599–609.

Lagier-Tourenne, Clotilde, Magdalini Polymenidou, Kasey R. Hutt, Anthony Q. Vu, Michael Baughn, Stephanie C. Huelga, Kevin M. Clutario, et al. 2012. “Divergent Roles of ALS-Linked Proteins FUS/TLS and TDP-43 Intersect in Processing Long Pre-mRNAs.” *Nature Neuroscience* 15 (11): 1488–97.

Lee, Hui-Ling Rose, and Joseph P. Dougherty. 2012. “Pharmaceutical Therapies to Recode Nonsense Mutations in Inherited Diseases.” *Pharmacology & Therapeutics* 136 (2): 227–66.

Linde, Liat, Stephanie Boelz, Malka Nissim-Rafinia, Yifat S. Oren, Michael Wilschanski, Yasmin Yaacov, Dov Virgilis, et al. 2007. “Nonsense-Mediated mRNA Decay Affects Nonsense Transcript Levels and Governs Response of Cystic Fibrosis Patients to Gentamicin.” *The Journal of Clinical Investigation* 117 (3): 683–92.

Ling, Jonathan P., Olga Pletnikova, Juan C. Troncoso, and Philip C. Wong. 2015. “TDP-43 Repression of Nonconserved Cryptic Exons Is Compromised in ALS-FTD.” *Science* 349 (6248): 650–55.

Ling, Shuo-Chien, Magdalini Polymenidou, and Don W. Cleveland. 2013. “Converging Mechanisms in ALS and FTD: Disrupted RNA and Protein Homeostasis.” *Neuron* 79 (3): 416–38.

Lou, Chih H., Ada Shao, Eleen Y. Shum, Josh L. Espinoza, Lulu Huang, Rachid Karam, and Miles F. Wilkinson. 2014. “Posttranscriptional Control of the Stem Cell and Neurogenic Programs by the Nonsense-Mediated RNA Decay Pathway.” *Cell Reports* 6 (4): 748–64.

Lykke-Andersen, Søren, and Torben Heick Jensen. 2015. “Nonsense-Mediated mRNA Decay: An Intricate Machinery That Shapes Transcriptomes.” *Nature Reviews. Molecular Cell Biology* 16 (11): 665–77.

Maquat, L. E., A. J. Kinniburgh, E. A. Rachmilewitz, and J. Ross. 1981. “Unstable Beta-Globin mRNA in mRNA-Deficient Beta O Thalassemia.” *Cell* 27 (3 Pt 2): 543–53.

Maquat, Lynne E., and Chenguang Gong. 2009. “Gene Expression Networks: Competing mRNA Decay Pathways in Mammalian Cells.” *Biochemical Society Transactions* 37 (Pt 6): 1287–92.

Mendell, Joshua T., Neda A. Sharifi, Jennifer L. Meyers, Francisco Martinez-Murillo, and Harry C. Dietz. 2004. “Nonsense Surveillance Regulates Expression of Diverse Classes of Mammalian Transcripts and Mutes Genomic Noise.” *Nature Genetics* 36 (10): 1073–78.

Neumann, Manuela, Deepak M. Sampathu, Linda K. Kwong, Adam C. Truax, Matthew C. Micsenyi, Thomas T. Chou, Jennifer Bruce, et al. 2006. “Ubiquitinated TDP-43 in Frontotemporal Lobar Degeneration and Amyotrophic Lateral Sclerosis.” *Science* 314 (5796): 130–33.

Nickless, Andrew, Erin Jackson, Jayne Marasa, Patrick Nugent, Robert W. Mercer, David Piwnica-Worms, and Zhongsheng You. 2014. “Intracellular Calcium Regulates Nonsense-Mediated mRNA Decay.” *Nature Medicine* 20 (8): 961–66.

Oren, Yifat S., Michelle L. McClure, Steven M. Rowe, Eric J. Sorscher, Assaf C. Bester, Miriam Manor, Eitan Kerem, et al. 2014. “The Unfolded Protein Response Affects Readthrough of Premature Termination Codons.” *EMBO Molecular Medicine* 6 (5): 685–701.

Oslowski, Christine M., and Fumihiko Urano. 2011. “Measuring ER Stress and the Unfolded Protein Response Using Mammalian Tissue Culture System.” *Methods in Enzymology* 490: 71–92.

Pain, V. M. 1994. “Translational Control during Amino Acid Starvation.” *Biochimie* 76 (8): 718–28.

Palacios, Isabel M. 2013. “Nonsense-Mediated mRNA Decay: From Mechanistic Insights to Impacts on Human Health.” *Briefings in Functional Genomics* 12 (1): 25–36.

Raimondeau, Etienne, Joshua C. Bufton, and Christiane Schaffitzel. 2018. “New Insights into the Interplay between the Translation Machinery and Nonsense-Mediated mRNA Decay Factors.” *Biochemical Society Transactions* 46 (3): 503–12.

Ramalho, Anabela S., Sebastian Beck, Michelle Meyer, Deborah Penque, Garry R. Cutting, and Margarida D. Amaral. 2002. “Five Percent of Normal Cystic Fibrosis Transmembrane Conductance Regulator mRNA Ameliorates the Severity of Pulmonary Disease in Cystic Fibrosis.” *American Journal of Respiratory Cell and Molecular Biology* 27 (5): 619–27.

Ron, David. 2002. “Translational Control in the Endoplasmic Reticulum Stress Response.” *The Journal of Clinical Investigation* 110 (10): 1383–88.

Rubio, Claudia, David Pincus, Alexei Korennykh, Sebastian Schuck, Hana El-Samad, and Peter Walter. 2011. “Homeostatic Adaptation to Endoplasmic Reticulum Stress Depends on Ire1 Kinase Activity.” *The Journal of Cell Biology* 193 (1): 171–84.

Sakaki, Kenjiro, Sawako Yoshina, Xiaohua Shen, Jaeseok Han, Melinda R. DeSantis, Mon Xiong, Shohei Mitani, and Randal J. Kaufman. 2012. “RNA Surveillance Is Required for Endoplasmic Reticulum Homeostasis.” *Proceedings of the National Academy of Sciences of the United States of America* 109 (21): 8079–84.

Samali, Afshin, Una Fitzgerald, Shane Deegan, and Sanjeev Gupta. 2010. “Methods for Monitoring Endoplasmic Reticulum Stress and the Unfolded Protein Response.” *International Journal of Cell Biology* 2010 (January): 830307.

Schadewijk, Annemarie van, Emily F. A. van’t Wout, Jan Stolk, and Pieter S. Hiemstra. 2012. “A Quantitative Method for Detection of Spliced X-Box Binding Protein-1 (XBP1) mRNA as a Measure of Endoplasmic Reticulum (ER) Stress.” *Cell Stress & Chaperones* 17 (2): 275–79.

Wang, Ding, Jiri Zavadil, Leenus Martin, Fabio Parisi, Eugene Friedman, David Levy, Heather Harding, David Ron, and Lawrence B. Gardner. 2011. “Inhibition of Nonsense-Mediated RNA Decay by the Tumor Microenvironment Promotes Tumorigenesis.” *Molecular and Cellular Biology* 31 (17): 3670–80.

Wek, R. C., H-Y Jiang, and T. G. Anthony. 2006. “Coping with Stress: eIF2 Kinases and Translational Control.” *Biochemical Society Transactions* 34 (1): 7–11.

Welch, Ellen M., Elisabeth R. Barton, Jin Zhuo, Yuki Tomizawa, Westley J. Friesen, Panayiota Trifillis, Sergey Paushkin, et al. 2007. “PTC124 Targets Genetic Disorders Caused by Nonsense Mutations.” *Nature* 447 (7140): 87–91.

Yepiskoposyan, Hasmik, Florian Aeschimann, Daniel Nilsson, Michal Okoniewski, and Oliver Mühlemann. 2011. “Autoregulation of the Nonsense-Mediated mRNA Decay Pathway in Human Cells.” *RNA* 17 (12): 2108–18.

Yoshida, Hiderou, Kyosuke Haze, Hideki Yanagi, Takashi Yura, and Kazutoshi Mori. 1998. “Identification of the Cis-Acting Endoplasmic Reticulum Stress Response Element Responsible for Transcriptional Induction of Mammalian Glucose-Regulated Proteins: INVOLVEMENT OF BASIC LEUCINE ZIPPER TRANSCRIPTION FACTORS.” *The Journal of Biological Chemistry* 273 (50): 33741–49.

Yoshida, H., T. Matsui, A. Yamamoto, T. Okada, and K. Mori. 2001. “XBP1 mRNA Is Induced by ATF6 and Spliced by IRE1 in Response to ER Stress to Produce a Highly Active Transcription Factor.” *Cell* 107 (7): 881–91.

Zhang, Peichuan, Barbara C. McGrath, Jamie Reinert, Deanne S. Olsen, Li Lei, Sangeeta Gill, Sheree A. Wek, et al. 2002. “The GCN2 eIF2alpha Kinase Is Required for Adaptation to Amino Acid Deprivation in Mice.” *Molecular and Cellular Biology* 22 (19): 6681–88.

Chapter 4: Knocking out *Upf2* reduces neural progenitor cell viability

Abstract

Nonsense-mediated RNA decay (NMD) is an essential post-transcriptional quality control mechanism degrading aberrant RNA transcripts. In addition to preventing the expression of “nonsense” RNA, NMD has been reported to target normal RNA transcripts to finetune gene expression. For example, the last chapter revealed cellular stresses inhibit NMD through the PERK signaling pathway. This chapter further explores NMD interaction with biological processes, especially neuronal development. A conditional *in vitro* NMD deficient neural progenitor cell (NPC) system was pioneered using adeno-associated virus serotype 9 (AAV9) carrying Cre recombinase. AAV9 successfully induced *Upf2* knockout and attenuated NMD, upregulating NMD genes such as *Gadd45b*, *Gadd45g*, *Parp14*, *Parp3*, *Atr*, and *Mre11a*. As a result, NPC viability was reduced significantly in *Upf2* knockout samples. It is evident that NMD could directly affect NPC viability. In an attempt to rescue such phenotype, two candidates, downstream *Gadd45b* and *Gadd45g*, were knocked out in the UPF2 null background using the CRISPR-Cas9 system. No NPC viability rescue was observed. These findings provide evidence and importance of NMD in NPC survival and early brain development.

Introduction

Nonsense mediated RNA decay (NMD) plays an essential role in post transcriptional regulation to finetune the transcriptome and maintain normal cellular function (Kurosaki, Popp, and Maquat 2019; Lykke-Andersen and Jensen 2015; Hug, Longman, and Cáceres 2016; Chang, Imam, and Wilkinson 2007; Kurosaki and Maquat 2016). It actively integrates into various cellular and biological processes such as alternative splicing, unfolded protein responses (UPR), amino acid deprivation, and cellular stresses. For instance, ER stress can inhibit NMD through PERK activation (Li et al. 2017; Karam et al. 2015). Hypoxia can also inhibits NMD through phosphorylation of eIF2α (Gardner 2008). Increasing evidence suggests through these biological network intersections, NMD is able to play crucial roles in mediating cell physiology, especially in neuronal development.

During early neuronal development, NMD works in conjunction with alternative splicing (AS-NMD) to modulate synapse formation. Study shows at early mouse embryonic stages, an important synaptic formation gene, *Psd-95* is actively degraded by the NMD process. Later in that development, exon 18 of *Psd-95* is alternatively spliced, prompting an escape of NMD fate and expression of PSD-95 to aid neuronal maturate (Zheng 2016; Zheng et al. 2012). Similar AS-NMD regulation has also been reported in one of *Psd-95*'s splicing regulators - nPtbp (Ptbp2, an NMD target). The alternation between Ptb and nPtb, encourages neuron maturation and differentiation (Boutz et al. 2007). Axon

guidance gene *Robo3.2* is another example of AS-NMD modulating axonogenesis through switching between translational isoform (*Robo3.1*) and the NMD isoform to maintain the delicate balance of gene expression at the right time for the right amount (Colak et al. 2013; Boutz et al. 2007).

In addition, miR-128 microRNA is shown to regulate UPF1 expression. Such microRNA repression of NMD leads to transcriptome wide differentially expressed neural genes, revealing a new mode of NMD regulation in neurons (Bruno et al. 2011). Additional microRNAs such as miRNAs miR-9, miR-124 and miR-125 have been identified to promote similar miRNA - NMD circuitry that regulates neural development by indirectly upregulating downstream NMD targets like *Smad7* (C. H. Lou et al. 2014; Wang et al. 2013).

Some NMD core factors are directly involved in the neurogenesis network. Take UFP1, study has shown UPF1 and an exon junction factor eIF4AII directly regulate *Arc* mRNA transcript in dendrites. The depletion of either factor increases *Arc* abundancy and leads to hyper expression of ARC, a protein required for long-term potentiation and synapse strength in mature neurons (Giorgi et al. 2007). Another role of UPF1 was reported in the reducing the cellular toxicity from *Tdp-43* and *Fus* induced amyotrophic lateral sclerosis (ALS) and frontotemporal dementia, by accelerating NMD degradation of harmful misspliced transcripts (Barmada et al. 2015; Ling et al. 2015). Additionally, research shows UPF3B can cause intellectual impairment strongly associated with autism spectrum disorder (ASD), attention deficit hyperactivity disorder

(ADHD) and schizophrenia (SCZ) (Huang et al. 2018; Jolly et al. 2013; Nguyen et al. 2012). This could because of the expression profile change when missense UPF3B start promotes neural stem cells proliferation at the expense of differentiation, severely hinder neurite formation and neuron maturation (Alrahbeni et al. 2015).

Though many studies are focused on the role of NMD in mature neurons and neural degenerative diseases, not much is understood at the early embryonic stage neural progenitor cells (NPC) (Han et al. 2018). NPCs are a type of multipotent precursor cells capable of self-renewing. They can later differentiate into most glial and neural cell types (Martínez-Cerdeño and Noctor 2018). An NMD - NPC model could be a powerful “all-in-one” tool to study NMD functions in neural development, differentiation, and related neurological conditions. However, no such NPC model is currently available. Therefore, this chapter aims to present a novel NPC conditional UPF2 knockout model that could be employed to benefit all NMD related researches in the early neural development field.

Results

Neural progenitor cell harvesting and culturing from Upf2$^{loxP/loxP}$; Emx1-cre mouse

Fresh neural progenitor cells directly from the mouse cortice were harvested and cultured *in vitro* to study *Upf2$^{loxP/loxP}$* knockout induced NMD inhibition in neuronal development. First, *Upf2$^{loxP/LoxP}$* male mice were bred with *Upf2$^{loxP/loxP}$* females to generate homozygous *Upf2$^{loxP/loxP}$* embryos (Zheng et al. 2012). At embryonic day 14.5 (E14.5), pregnant females were sacrificed and the embryonic mice brain cortex were harvested for culturing in NPC growth media. Neurospheres were formed and digested for culturing monolayer NPCs (Figure 14A). At the same time, embryonic mice tails were used to genotype *Upf2$^{loxP/loxP}$* transgenes (Figure 14B). Homozygous *Upf2$^{loxP/loxP}$* NPCs were cultured from T25 flasks as neurospheres to the third passage (P3) in monolayer before proceeding (Figure 14D). These results indicate successful *in vitro* culturing of NPCs carrying the loxP transgenes flanking Upf2 exon 2 and exon 3. When Cre is introduced to the *Upf2$^{loxP/loxP}$* NPCs, the NPC population will produce conditional *Upf2* knockout and ready to be used for NMD related studies.

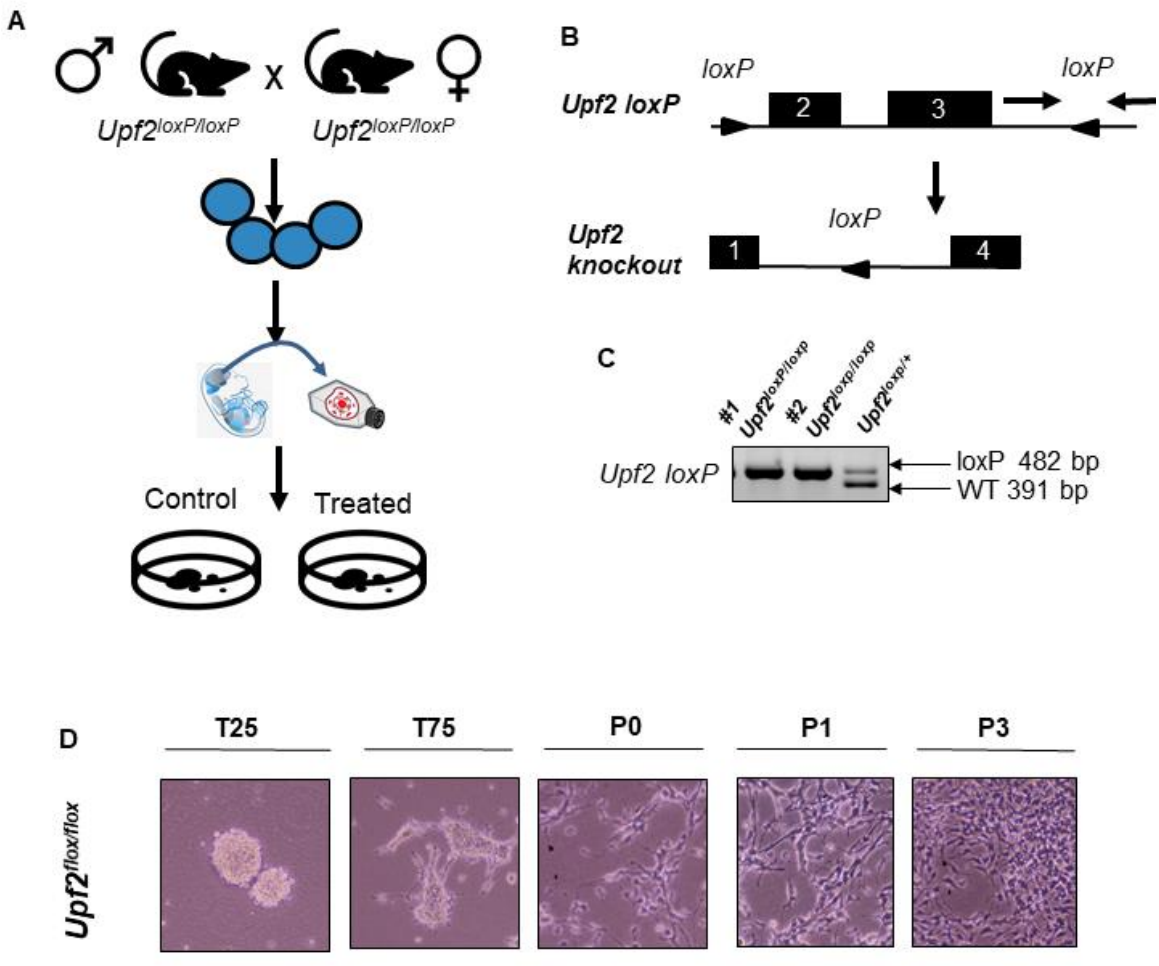

Figure 14. NPC culturing from mouse cortex. *(A)* Schematics demonstrating strategy harvesting and culturing *Upf2* knockout neural progenitor cells as a model to study NMD in NPC. *(B)* Design of genotyping primers used to confirm loxP sequence. One set of forward and reverse primers amplify the transgenic loxP gene. Successful knockout should completely remove exon 2 and exon 3 (lower panel). *(C)* Genotyping image of agarose EtBr gel from mouse tail DNA samples. *Upf2*$^{loxP/loxP}$ using the genotyping primer sets in B. #1 and #2 are littermates, while the third sample is a heterozygous mouse showing both loxP transgene and the wildtype Upf2 bands as control. (*D*) Representative NPC cultures *in vitro* derived directly from harvested mouse cortical neurons. Culturing time integrals from T25 flask, T75 flask, passage 0 monolayer (P0), passage 1 monolayer (P1), to passage 3 monolayer (P3). Normal *Upf2*$^{loxP/loxP}$ NPCs.

Generating Upf2 conditional knockout neural progenitor cell using AAV9

Due to the difficulties of transfection in the NPCs from previous experiences, viral particles carrying Cre recombinase was preferred to induce knockout (data not shown). Adeno associated virus serotype 9 (AAV9) carrying Cre has been shown to be effective in neurons and the central nervous system (Hudry and Vandenberghe 2019). It is used to drive CRE expression in this study under the CMV promoter (Figure 15A). To validate the AAV9 induced Cre knockout efficiency, a tri-primer set complimenting exon 1 as forward primer; exon 2 and exon 4 as reverse primers were designed to confirm knockouts (Figure 15B). Using RT-PCR splicing assay, the tri-primer set was also able to quantify the exact knockout ratio as shown in Figure 15C. Quantification using molarity showed that AAV9 was extremely potent in expressing Cre recombinase. 95% knockout was achieved within 72 hours of infection in the NPCs when using 500 x 10^3 MOI (Figure 15D). Additional RT-qPCR on endogenous NMD targets *Prdg*, *Gadd45b*, and *Gadd45g* were used to confirm the knockout (Figure 15D). *Prdg* was upregulated for 8 folds while *Gadd45b* and *Gadd45g* achieved 10- and 16-folds upregulation respectively. Altogether, AAV9 carrying Cre recombinase was potent enough to generate conditional *Upf2* null NPCs *in vitro.*

A

Serotype	Promo/ PolyA	TransGene	Reporter
AAV9	CMV/WPRE.SV40	CRE	eGFP
AAV9	CMV	NA	eGFP

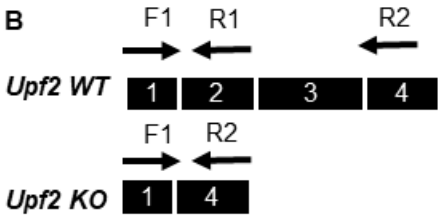

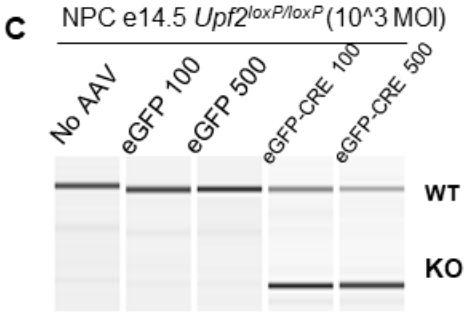

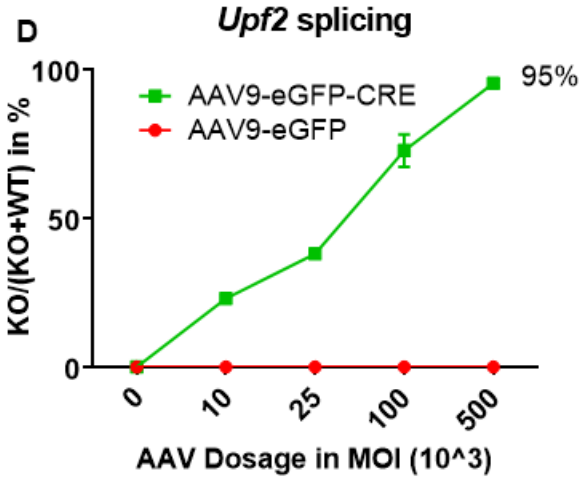

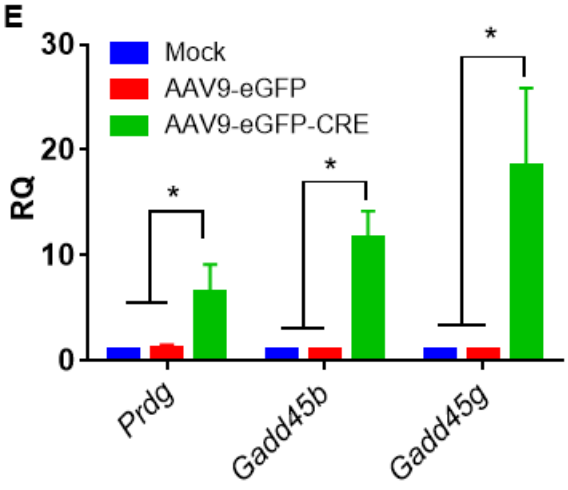

Figure 15. Generation of *Upf2* knockout neural progenitor cell model *in vitro* using AAV9. (A) Major adeno-associated viral construct features. (B) Design of the splicing tri-primer set used to quantify knockout ratio in an NPC population using RT-PCR. (C) Qiaxcel digital PCR splicing assay images of UPF2 treated with different dosages of AAV9 carrying eGFP and eGFP-CRE constructs to induce knockout. (D) Quantified splicing percentage of knockout detected by Qiaxcel Screen Gel in nmols. (E) RT-qPCR expression of potential NMD targets treated by Mock, AAV9-eGFP (500 x 10^3 MOI), and AAV9-eGFP-CRE (500 x 10^3 MOI). One-way ANOVA test was used to determine significant ratio changes between different samples, followed by a Tukey's multiple comparison test. N = 3. (*) $P < 0.05$. Error bars represent mean ± SEM.

Table 6. UPF2 splicing tri-primer sequence

Splicing Primers	Forward	Reverse	Tm	Size (inclusion)	Size (exclusion)
Upf2_Splicing	GAGTTGGTGC TGGGAAACC	TCCTTCTTGGCAG TGACCTT	60	208	
		CATATTGCTTGTG CCTGTCC	60	>1200	100

Table 7. NMD RT-qPCR prime

Gene Name	Forward	Reverse	Size (bps)
Gadd45g	TGCCTTGGAGAAGCTCAG TT	GTCACTCGGGAAGGGTGAT	83
Gadd45b	GCCCGAGACCTGCACTG CCT	CCATTGGTTATTGCCTCTGCTCT CTT	124
Pdrg1	CAAGGGCAGGATTGTCTG TT	CTCTTGCACAAAGCAACCAA	94

NPC viability is significantly reduced in Upf2 deficient population

Once *Upf2* knockout and NMD inhibition were confirmed, a clear phenotype was observed in NPCs lacking *Upf2* - decreased total cell viability. The cell viability was measured each 24 hours after the initial 72 hours of AAV9 transduction using live cell counts (Figure 16A). AAV9 carrying reporter eGFP sequences can be directly observed under fluorescent microscope and maintained potent eGFP signal even at 96 hours after the initial 72 hours infection (168 hours total), one week after first introducing the virus (Figure 16B). NPCs collected at each time point were counted and quantified to generate a growth curve. NPCs with Cre recombinase induced Upf2 knockout started to show significantly lower viable cells at 48 hours after replating and increased only marginally overtime (Figure 16C). On the other hand, mock NPCs without AAV9 treatment and NPCs infected with eGFP reporter only AAV9 showed normal growth achieving 500,000 to 600,000 cells after 96 hours (Figure 16C). These results showed *Upf2* is important in neuronal development and is an essential gene for NPC survival during embryonic developmental stage.

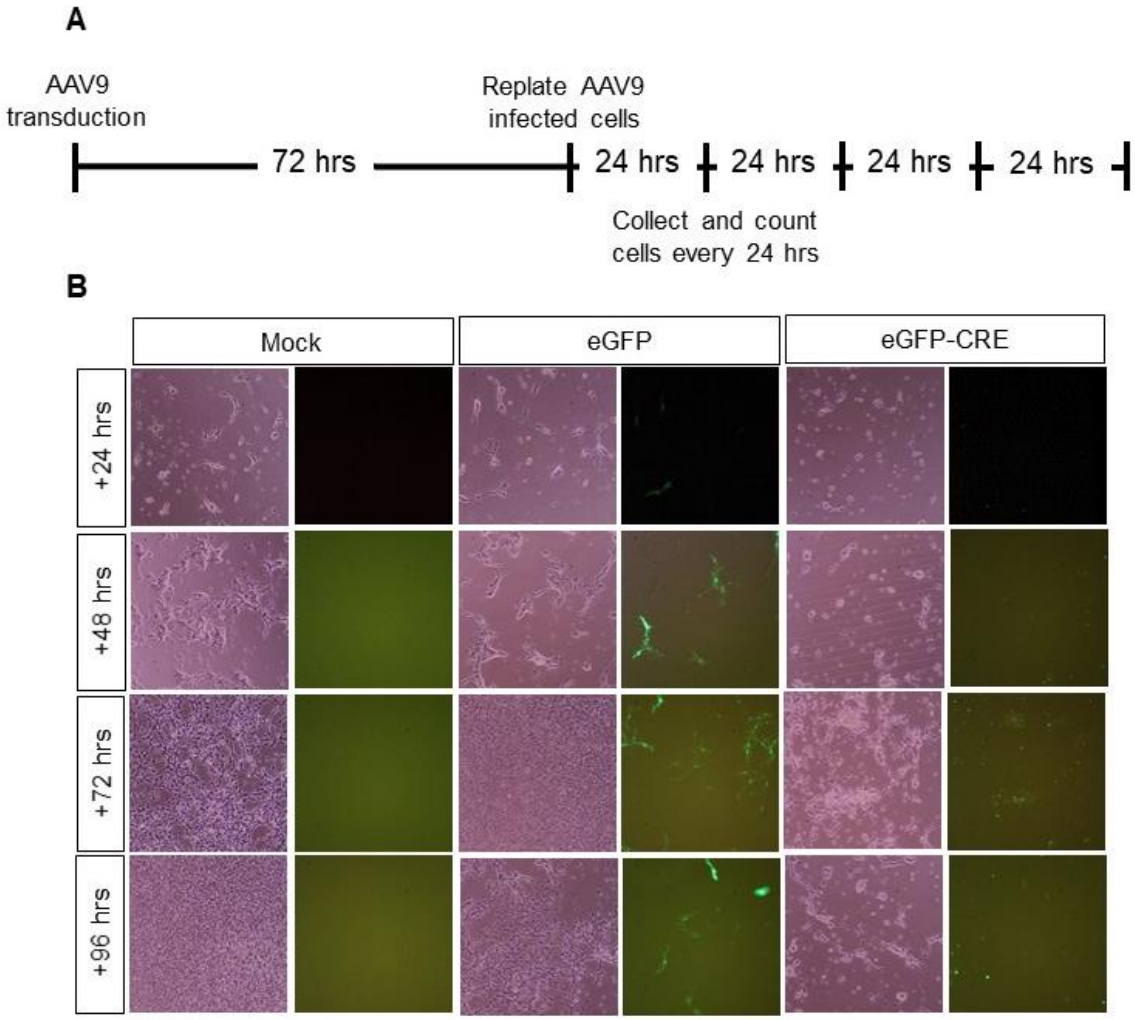
A
AAV9 transduction
72 hrs
Replate AAV9 infected cells
24 hrs
24 hrs
24 hrs
24 hrs
Collect and count cells every 24 hrs
B
Mock
eGFP
eGFP-CRE
+24 hrs
+48 hrs
+72 hrs
+96 hrs
C
Upf2loxP/loxP
eGFP-CRE
eGFP
Mock
Viable Cells (10^4)
80
60
40
20
0
*
*
24 hrs
48 hrs
72 hrs
96 hrs

Figure 16. *Upf2* knockout induced by AAV9 decrease NPC viability. (*A*) AAV9 treatment timeline and experiment strategy of NPC viability assay using CytoSmart cell counter. (*B*) Representative images of NPC condition in 24 wells after 72 hours (+24 hrs means 24 hours after, 96 hours initial infection) of initial AAV9 transduction in 6 wells plate. GFP brightness is indicative of positive infection. (*C*) Temporal NPC viability (live cell counts) using Corning CytoSMART Cell Counter 3.0. N = 3. A two-way ANOVA test followed by Dunnett's multiple comparison tests was used to determine significant expression changes between samples. (*) $P < 0.05$. Error bars represent mean ± SEM.

Generating monoclonal Gadd45b and Gadd45g knockouts in Upf2$^{loxP/lox}$ neural progenitor cells using CRISPR-Cas9 system

Many endogenous NMD targets have been reported to interfere with cell viability. A recent study showed *Gadd45* in drosophila is directly targeted by NMD and is responsible for optical cell survival (Nelson et al. 2016). However, the underlying mechanism for such survival rescue were not disclosed and such phenomenon was not described in higher vertebrates. In mammals, there are three homologues of the *Gadd45* gene: *Gadd45a*, *b* and *g* (Zhang, Yang, and Liu 2014). Out of the three, *Gadd45b* and *Gadd45g* are of interest because they are upregulated for 3 to 4 folds in previous *Upf2* knockout mice cortical RNAseq data and almost 10 folds in the NPC RT-qPCR (Figure 15D), making them potential candidates to rescue NPC viability. The logic is to first knockout these two genes in the *Upf2$^{loxP/lox}$* background NPCs. Then, introduce Cre recombinase using AAV9 to create *Upf2* deficiency and reevaluate the NPC viability in hope of restored NPC counts.

The strategy to obtain two lineages of pure monoclonal NPC cells of *Upf2$^{loxP/loxP}$; Gadd45b$^{-/-}$* and *Upf2$^{loPx/loxP}$; Gadd45g$^{-/-}$* is to combine CRISPR-Cas9 system and single cell sorting (Figure 17A). CRISPR stands for clustered regularly interspaced short palindromic repeat. It is a powerful gene editing method that can be easily used to manipulate target genome in most cell types (Hsu, Lander, and Zhang 2014). NPCs are transfected with two *sgRNA* - Cas9 fusion plasmids along with an eGFP reporter plasmid as sorting signals. NPCs

with GFP positive signals were sorted one by one into each well and cultured into single colonies. These GFP positive cells are more likely to also uptake the *sgRNAs* infused with Cas9. Finally, these candidate cell colonies were checked for *Gadd45b* or *Gadd45g* knockouts. For *Gadd45b*, plasmids carrying a pair of *sgRNA423* and *sgRNA1898* (exact nucleotide target locations) with infused Cas9 nuclease were used to cut most of exon2, exon 3, exon 4 of the gene (Figure 17B). For *Gadd45g*, *sgRNA32* and *sgRNA1005* were used to remove exon 1, exon 2, and most of the exon 3 (Figure 17C). Both NPC lines were confirmed by sequencing. Gadd45b (B) sequencing result indicated a small insertion sequence of “CGCAGGG” while the Gadd45g (C) sequencing results showed a heterogenous NPC genotype. That is one complete knock out allele and one with an extra “C” nucleotide from the nonhomologous end joining repairing process (NHEJ), causing a frameshift shown as double peak in the sequencing result. However, most of both genes were successfully excised, the nonfunction knockouts should be guaranteed.

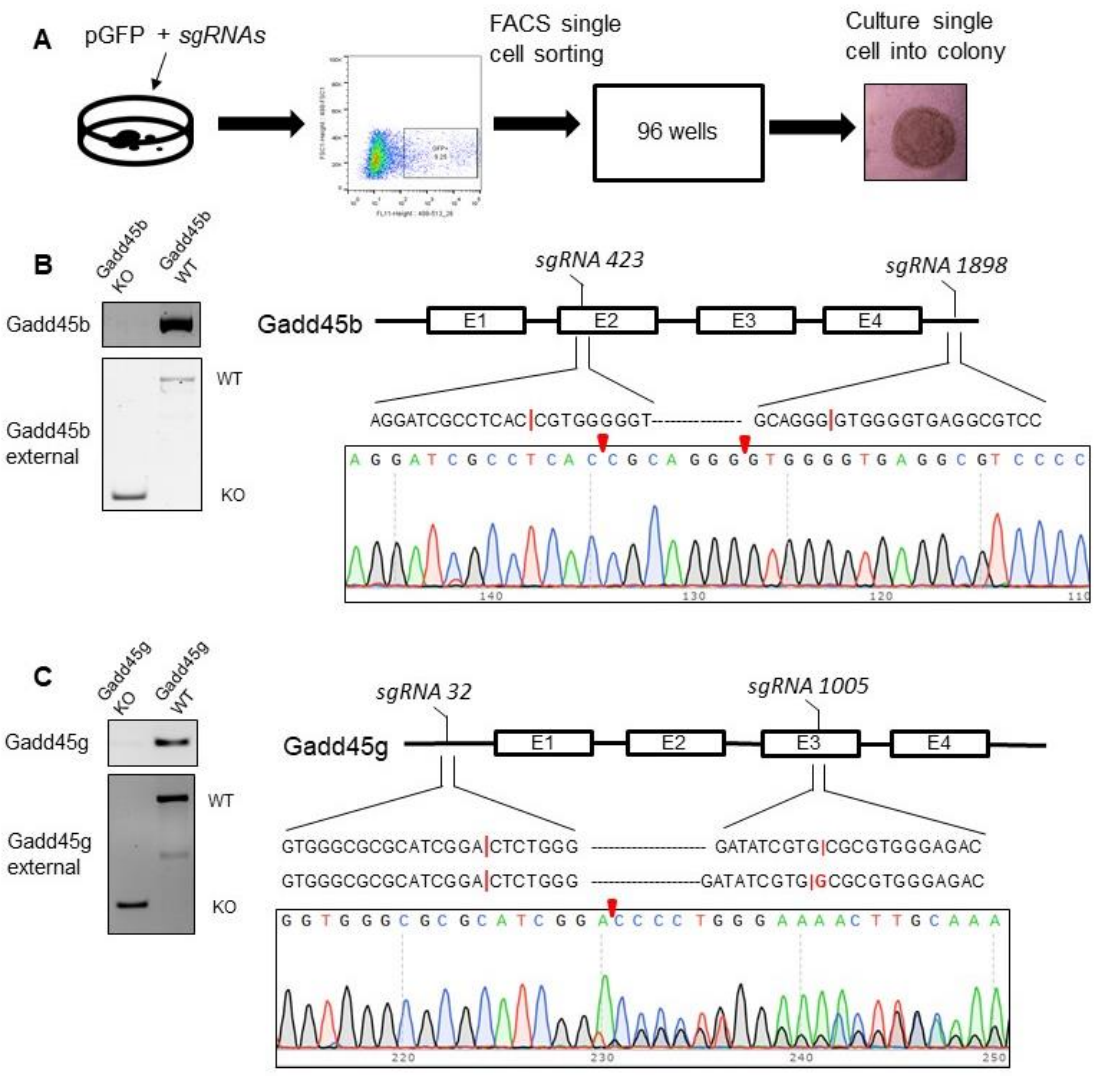

Figure 17. Generation of *Gadd45b* and *Gadd45g* CRISPR-Cas9 knockouts from single cell colonies. (A) Steps to generate CRISPR-Cas9 knockout NPC lines using FACS single cell sorting. Genotyping of SyBr Safe gel images and sequencing confirmation of Gadd45b (B) and Gadd45g (C) knockout from isolated NPC colony. Note Gadd45b (B) sequence results indicated a small insertion sequence of “CGCAGGG”. Gadd45g (C) sequencing results showed a heterogenous NPC genotype of one perfectly knocked out allele while the other allele obtained an insertion of “C”, causing a frameshift shown as double peak in the result.

Knocking out Gadd45b and Gadd45g in Upf2$^{loxP/loxP}$ neural progenitor cells background did not rescue cell viability

The confirmed *Upf2$^{loxP/loxP}$; Gadd45b$^{-/-}$* and *Upf2$^{loxP/loxP}$; Gadd45g$^{-/-}$* NPC lines were used for the same cell viability assay shown in Figure 16. By eliminating *Gadd45b* and *Gadd45g* in the *Upf2$^{loP/loxP}$* background, AAV9 carrying Cre recombinase would still inhibit NMD by Upf2 excision but no longer able to upregulate the *Gadd45* genes. Thus, possibly restoring the adverse effects from NMD inhibition and NPC viability. However, *Gadd45b* and *Gadd45g* knockouts in the *Upf2$^{loxP/loxP}$* NPC background were not able to restore cell viability. *Upf2$^{loxP/loxP}$; Gadd45b$^{-/-}$* NPCs expressing CRE were still significantly less than the mock and eGFP control (Figure 18A). *Upf2$^{loxP/loxP}$; Gadd45g$^{-/-}$* were also unable to increase cell viability after being exposed with Cre virus when compared with mock and GFP samples (Figure 18B). It was noted that the *Gadd45g* knockout line exhibited visibly slower proliferation rate than *Gadd45b* and *Upf2$^{loxP/loxP}$* lines based on total live cell numbers showed cell growth curves. Therefore, *Gadd45g* may be affect NPC growth independently. Additional NMD rescuing candidates should be considered.

CRISPR edited NPCs failed to rescue NMD induced cell viability reduction, the underlying mechanism remains unclear. One possible hypothesized mechanism is presented in Figure 18C where knocking out core NMD protein UPF2 leads to a plethora of differentially expressed genes. These “cryptic” genes are now expressed and contribute to cellular toxicity that leads to

reduced cell viability. This hypothesis awaits to be tested in future studies.

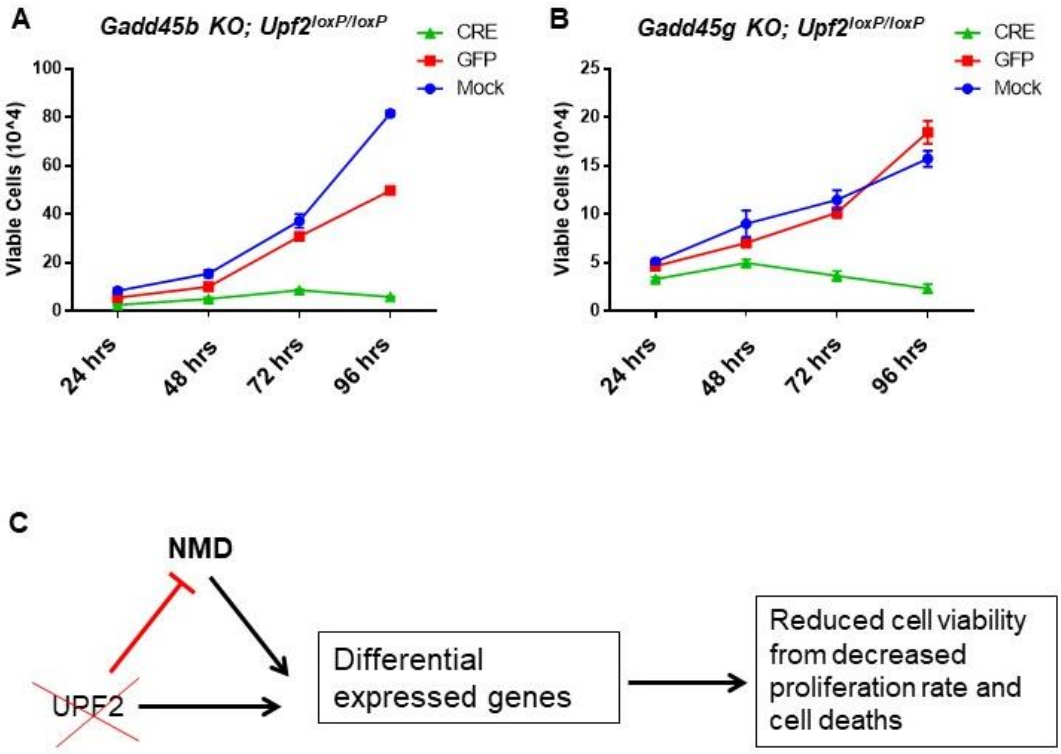

Figure 18. *Gadd45b* and *Gadd45g* CRISPR-Cas9 knockouts fail to rescue Upf2 induced cell viability issue. NPC viability assay of *Gadd45b (A)* and *Gadd45g (B)* CRISPR knockout in *Upf2* knockout NPC induced by AAV9. Viable / live cells were counted using CytoSmart cell counter at indicated time after initial 72 hours transduction. n = 3. Error bars represent mean ± SEM. (C) Hypothesized mechanism of cell viability reduction from *Upf2* knockout either through direct or NMD mediated downstream differentially expressed genes.

Discussion

In this study, a novel Upf2 conditional knockout NPC model was generated. Since NMD core factors UPF1 and SMG1 have been reported to be embryonic lethal (Medghalchi et al. 2001; McIlwain et al. 2010), *Upf2*$^{loxP/loxP}$ transgenic mouse was a good candidate to establish a conditional NMD deficient system (Zheng et al. 2012). First, NPCs were derived directly from cortical neurospheres and cultured successfully into monolayers (Figure 14). These NPCs were passaged up to sixteen times (P16) without showing any observable phenotypic changes (data not shown). Such self-renewal property provides a flexible time window for most *in vitro* mechanism studies. However, directly harvested *Upf2*$^{loxP/loxP}$; *Emx1-cre* NPCs were not complete *Upf2* knockout when cultured *in vitro*, possibly due to insufficient *Emx1* promoter strength (data not shown). A secondary Cre induction method was required.

To express Cre recombinase, AAV9 was used. NPCs are hard to transfect using lipofectamine or electroporation from past experiences. AAV9 overcomes the difficulty to infect transgenic NPCs with Cre recombinase with a CMV promoter. This combination was most potent in driving Cre expression in neurons (Pattali, Mou, and Li 2019; Kantor et al. 2014). Indeed, eGFP reporter signals show a transduction rate of nearly 100% (Figure 16B). The induced Cre can also achieve 95% knockout efficiency within 72 hours with NMD reporter genes significantly upregulated (Figure 15). These data confirmed the novel AAV9-NPC system can successfully attenuate NMD *in vitro* and used for future experiments.

After using AAV9 to induce UPF2 knockout and NMD deficiency, the infect NPC cells showed significant viability reduction (Figure 16C). Given the large scale and importance of NMD in biological processes, this was not surprising (C. H. Lou et al. 2014; Weischenfeldt et al. 2008; C.-H. Lou et al. 2016; Han et al. 2018). However, understanding the mechanism is of more importance in the neuronal development and therapeutic point of view. The two candidate genes, *Gadd45b* and *Gadd45g* failed to rescue NMD induced phenotype in NPC (Figure 19A and B), though the only *Gadd45* homolog in drosophila was able increase cell survival (Nelson et al. 2016). A divergence from mammal and drosophila NMD models. It is possible that *Gadd45b* and *Gadd45g* have redundant functions and a future double knockout model could provide more insight into the NMD cell survival mechanism.

Without successful rescue, the cell viability reduction via *Upf2* knockout remains vague. It is hypothesized that differentially expressed genes when NMD is inhibited can accumulate toxic transcripts that promote apoptosis and / or lowered proliferation rate (Figure 19C). To answer these questions, the widely used annexin-V FITC apoptosis assay can be used to quantify apoptotic rates between NMD and control groups (Vermes et al. 1995). FITC conjugated annexin-V binds to phosphatidylserine is a universal marker to detect apoptotic cells. Along with PI DNA staining, both early and late stages of cell apoptosis could be quantified (Riccardi and Nicoletti 2006). PI staining by itself can also be used in cell cycle analysis to determine NMD effects on proliferation (Cecchini,

Amiri, and Dick 2012).

Finally, an RNA sequencing library based on the conditional knockout NPC line could be useful in determining the next step. The large scale transcriptome data could reveal clusters of genes that are differentially expressed. It can narrow down the potential list of targets and even reveal novel candidates. Discovering the pathway could help researchers understand the role of UPF2 and NMD in neural progenitor cell renewal and brain development, in turn, providing therapeutic approaches for NMD related neurodegenerative diseases.

Materials and Methods *Animals*

Conditional *Upf2* knockout (that is, *Upf2*$^{loxP/loxP}$*; Emx1-cre*) mice were generated by first breeding *Upf2*$^{loxP/loxP}$ mice to *Emx1-cre* mice and subsequently breeding *Upf2*$^{loxP/+}$*; Emx1-cre* mice to *Upf2*$^{loxP/loxP}$ mice (Zheng et al. 2012). At E14.5 days, mice were dissected under a dissection microscope to obtain cortice. Isolated cortex tissues were then digested with TryPLE Express (Life Technology cat. no. 12604021) for 15 minutes at 37 C dry bath. Followed by spindown removal of TryPLE and resuspension in complete NPC culturing media (DMEM/F12, 1x glutamax, B 27, 0.2 µg/ml FGF and 0.2 µg/ml EGF) in a T25 culturing flask for further NPC growth. All animal procedures were approved by the Institutional Animal Care and Use Committee at UCR.

NPC cultures and viability assay

Freshly dissected cortex tissues were cultured in complete NPC media T25 for three days. Additional 0.2 µg/ml FGF and 0.2 µg/ml EGF were added on day three and cultured for two more days. Spindown, wash, and resuspend neurosphere to transfer to T75 after 5 days. Neurospheres were cultured in T75 for three to five more days before plating in monolayer six well plates coated with NPC coating media (1 µg/ml fibronectin and 50 µg/ml polyornithine in autoclaved H2O). Plates were covered with NPC coating media for two hours in 37 C incubator, discard media and let surface dry before seeding with NPC.

250,000 monolayer NPC were plated in six well plates and infected with AAV9-eGFP (ADDGENE, cat. no. 105530-AAV9) or AAV9-eGFP-CRE (ADDGENE, cat. no. 105545-AAV9) at 500,000 MOI in 1 ml of complete NPC mediate. Changed to 2 ml of fresh complete NPC media after the first 12 to 14 hours of infection. After 72 hours from initial infection, NPC were harvested with TryPLE and replated into 24 well plates at a density of 44,000 cells per well. NPCs were then counted using Corning CytoSMART 3.0 cell counter each 24 hours to generate a viability / survival curve.

RNA extraction, cDNA synthesis, splicing assay, and RT-qPCR

TRIzol (Life Technologies, cat. no. 15596-018) was directly added to the cells or mouse brain tissues to extract total RNA following the TRIzol reagent standard protocol. Isolated RNA was treated with 4 units of Turbo DNase (Ambion) at 37°C for 35 min to degrade all remaining genomic DNA. After the

DNase treatment, RNA was purified using phenol-chloroform (pH 4.5, VWR cat. no. 97064-744). RNA concentrations were measured using a Nanodrop 2000c (Thermo Fisher). One microgram of freshly isolated DNA-free RNA was converted to cDNA using 1 µL random hexamers (30 µM) and 200 units of Promega M-MLV reverse transcriptase (cat. no. M1705) following the Promega protocol in a 20 µL reaction. RT-qPCR experiments were conducted using a QuantStudio 6 Real-Time PCR instrument with 2× Power SYBR Green PCR master mix (Life Tech) following the Life Tech protocol. Each 10 µL reaction contained 0.3 µL cDNA, 5 µL 2× Power SYBR Green PCR master mix, 0.3 nM forward primer, and 0.3 nM reverse primer. The QuantStudio 6 RT-qPCR run program was as follows: 50°C for 2 min; 95°C for 15 sec and 60°C for 1 min, with the 95°C and 60°C steps repeated for 40 cycles; and a melting curve test from 60°C to 95°C at a 0.05°C/sec measuring rate. QuantStudio Real-Time PCR software was used for the analysis. All RT-qPCR reactions were conducted with three technical replicates along with a no template control (NTC, not amplified). Outliers were excluded when the coefficient of variation of Ct for the three technical replicates was larger than 0.3. Relative expression (fold changes) was calculated using the ΔΔCt method. For the splicing assays of the NMD exons, PCR was performed using New England Biolab Taq DNA polymerase (cat. no. M0267E). All statistical analysis was performed using GraphPad Prism 6.

Monoclonal gene editing with CRISPR sgRNA

300,00 NPCs were plated in coated six well plates coated with 2 ml of complete NPC media. Reverse transfect cells with 0.4 µg of each CRISPR-sgRNA plasmids flanking *Gadd45b* or *Gadd45g* and 0.2 µg eGFP plasmid (sorting signal). The total 1 µg of plasmids were mixed with 2.5 µl of transfection agent Lipofectamine 2000 (Life Technology) in 200 µl of Opti-MEM (Life Technology) for 20 minutes before adding into cells. Change to fresh complete NPC media after 6 hours and let transfect for another 42 hours (total of 48 hours) before single cell sorting.

Cells were washed one time with warm 1x PBS and digested for five minutes with TryPLE Express (Life Technology cat. no. 12604021). Resuspend cells in warm complete NPC media and spin down. Aspirate media and wash the cell pellet two times with cold 1x PBS. After the last wash, resuspend cells in cold 1 x PBS and keep on ice until sorting. Strain cells and sort using a MoFlo Astrios EQ (Beckman Coulter) according to the manufacturers' protocol. Before sorting, the instrument was calibrated to maximize cell survival during the process. Gate GFP positive cells and sort one single cell per well directly into coated 96 well plates with 500 µl of complete NPC media. Directly transfer populated plates back to the incubator after sorting. Continue observing colony growth and genotype to confirm knockout cell colonies. Culture confirmed colonies in 96 wells, 12 wells, 6 wells, and finally, 100 mm dish. Extra cells were frozen down and used for the experiments described in this chapter.

References

Alrahbeni, Tahani, Francesca Sartor, Jihan Anderson, Zosia Miedzybrodzka, Colin McCaig, and Berndt Müller. 2015. “Full UPF3B Function Is Critical for Neuronal Differentiation of Neural Stem Cells.” *Molecular Brain* 8 (May): 33.

Barmada, Sami J., Shulin Ju, Arpana Arjun, Anthony Batarse, Hilary C. Archbold, Daniel Peisach, Xingli Li, et al. 2015. “Amelioration of Toxicity in Neuronal Models of Amyotrophic Lateral Sclerosis by hUPF1.” *Proceedings of the National Academy of Sciences of the United States of America* 112 (25): 7821–26.

Boutz, Paul L., Peter Stoilov, Qin Li, Chia-Ho Lin, Geetanjali Chawla, Kristin Ostrow, Lily Shiue, Manuel Ares Jr, and Douglas L. Black. 2007. “A Post-Transcriptional Regulatory Switch in Polypyrimidine Tract-Binding Proteins Reprograms Alternative Splicing in Developing Neurons.” *Genes & Development* 21 (13): 1636–52.

Bruno, Ivone G., Rachid Karam, Lulu Huang, Anjana Bhardwaj, Chih H. Lou, Eleen Y. Shum, Hye-Won Song, et al. 2011. “Identification of a microRNA That Activates Gene Expression by Repressing Nonsense-Mediated RNA Decay.” *Molecular Cell* 42 (4): 500–510.

Cecchini, Matthew J., Mehdi Amiri, and Frederick A. Dick. 2012. “Analysis of Cell Cycle Position in Mammalian Cells.” *Journal of Visualized Experiments: JoVE*, no. 59 (January). https://doi.org/10.3791/3491.

Chang, Yao-Fu, J. Saadi Imam, and Miles F. Wilkinson. 2007. “The Nonsense-Mediated Decay RNA Surveillance Pathway.” *Annual Review of Biochemistry* 76: 51–74.

Colak, Dilek, Sheng-Jian Ji, Bo T. Porse, and Samie R. Jaffrey. 2013. “Regulation of Axon Guidance by Compartmentalized Nonsense-Mediated mRNA Decay.” *Cell* 153 (6): 1252–65.

Gardner, Lawrence B. 2008. “Hypoxic Inhibition of Nonsense-Mediated RNA Decay Regulates Gene Expression and the Integrated Stress Response.” *Molecular and Cellular Biology* 28 (11): 3729–41.

Giorgi, Corinna, Gene W. Yeo, Martha E. Stone, Donald B. Katz, Christopher Burge, Gina Turrigiano, and Melissa J. Moore. 2007. “The EJC Factor eIF4AIII Modulates Synaptic Strength and Neuronal Protein Expression.” *Cell* 130 (1): 179–91.

Han, Xin, Yanling Wei, Hua Wang, Feilong Wang, Zhenyu Ju, and Tangliang Li.

2018. “Nonsense-Mediated mRNA Decay: A ‘Nonsense’ Pathway Makes Sense in Stem Cell Biology.” *Nucleic Acids Research* 46 (3): 1038–51.

Hsu, Patrick D., Eric S. Lander, and Feng Zhang. 2014. “Development and Applications of CRISPR-Cas9 for Genome Engineering.” *Cell* 157 (6): 1262–78.

Huang, L., E. Y. Shum, S. H. Jones, C-H Lou, J. Dumdie, H. Kim, A. J. Roberts, et al. 2018. “A Upf3b-Mutant Mouse Model with Behavioral and Neurogenesis Defects.” *Molecular Psychiatry* 23 (8): 1773–86.

Hudry, Eloise, and Luk H. Vandenberghe. 2019. “Therapeutic AAV Gene Transfer to the Nervous System: A Clinical Reality.” *Neuron* 101 (5): 839–62.

Hug, Nele, Dasa Longman, and Javier F. Cáceres. 2016. “Mechanism and Regulation of the Nonsense-Mediated Decay Pathway.” *Nucleic Acids Research* 44 (4): 1483–95.

Jolly, Lachlan A., Claire C. Homan, Reuben Jacob, Simon Barry, and Jozef Gecz. 2013. “The UPF3B Gene, Implicated in Intellectual Disability, Autism, ADHD and Childhood Onset Schizophrenia Regulates Neural Progenitor Cell Behaviour and Neuronal Outgrowth.” *Human Molecular Genetics* 22 (23): 4673–87.

Kantor, Boris, Rachel M. Bailey, Keon Wimberly, Sahana N. Kalburgi, and Steven J. Gray. 2014. “Chapter Three - Methods for Gene Transfer to the Central Nervous System.” In *Advances in Genetics*, edited by Theodore Friedmann, Jay C. Dunlap, and Stephen F. Goodwin, 87:125–97. Academic Press.

Karam, Rachid, Chih-Hong Lou, Heike Kroeger, Lulu Huang, Jonathan H. Lin, and Miles F. Wilkinson. 2015. “The Unfolded Protein Response Is Shaped by the NMD Pathway.” *EMBO Reports* 16 (5): 599–609.

Kurosaki, Tatsuaki, and Lynne E. Maquat. 2016. “Nonsense-Mediated mRNA Decay in Humans at a Glance.” *Journal of Cell Science* 129 (3): 461–67.

Kurosaki, Tatsuaki, Maximilian W. Popp, and Lynne E. Maquat. 2019. “Quality and Quantity Control of Gene Expression by Nonsense-Mediated mRNA Decay.” *Nature Reviews. Molecular Cell Biology* 20 (7): 406–20.

Ling, Jonathan P., Olga Pletnikova, Juan C. Troncoso, and Philip C. Wong. 2015. “TDP-43 Repression of Nonconserved Cryptic Exons Is Compromised in ALS-FTD.” *Science* 349 (6248): 650–55.

Li, Zhelin, John K. Vuong, Min Zhang, Cheryl Stork, and Sika Zheng. 2017. “Inhibition of Nonsense-Mediated RNA Decay by ER Stress.” *RNA* 23 (3): 378–94.

Lou, Chih-Hong, Jennifer Dumdie, Alexandra Goetz, Eleen Y. Shum, David Brafman, Xiaoyan Liao, Sergio Mora-Castilla, et al. 2016. “Nonsense-Mediated RNA Decay Influences Human Embryonic Stem Cell Fate.” *Stem Cell Reports* 6 (6): 844–57.

Lou, Chih H., Ada Shao, Eleen Y. Shum, Josh L. Espinoza, Lulu Huang, Rachid Karam, and Miles F. Wilkinson. 2014. “Posttranscriptional Control of the Stem Cell and Neurogenic Programs by the Nonsense-Mediated RNA Decay Pathway.” *Cell Reports* 6 (4): 748–64.

Lykke-Andersen, Søren, and Torben Heick Jensen. 2015. “Nonsense-Mediated mRNA Decay: An Intricate Machinery That Shapes Transcriptomes.” *Nature Reviews. Molecular Cell Biology* 16 (11): 665–77.

Martínez-Cerdeño, Verónica, and Stephen C. Noctor. 2018. “Neural Progenitor Cell Terminology.” *Frontiers in Neuroanatomy* 12 (December): 104.

McIlwain, David R., Qun Pan, Patrick T. Reilly, Andrew J. Elia, Susan McCracken, Andrew C. Wakeham, Annick Itie-Youten, Benjamin J. Blencowe, and Tak W. Mak. 2010. “Smg1 Is Required for Embryogenesis and Regulates Diverse Genes via Alternative Splicing Coupled to Nonsense-Mediated mRNA Decay.” *Proceedings of the National Academy of Sciences of the United States of America* 107 (27): 12186–91.

Medghalchi, S. M., P. A. Frischmeyer, J. T. Mendell, A. G. Kelly, A. M. Lawler, and H. C. Dietz. 2001. “Rent1, a Trans-Effector of Nonsense-Mediated mRNA Decay, Is Essential for Mammalian Embryonic Viability.” *Human Molecular Genetics* 10 (2): 99–105.

Nelson, Jonathan O., Kristin A. Moore, Alex Chapin, Julie Hollien, and Mark M. Metzstein. 2016. “Degradation of Gadd45 mRNA by Nonsense-Mediated Decay Is Essential for Viability.” *eLife* 5 (March). https://doi.org/10.7554/eLife.12876.

Nguyen, L. S., L. Jolly, C. Shoubridge, W. K. Chan, L. Huang, F. Laumonnier, M. Raynaud, et al. 2012. “Transcriptome Profiling of UPF3B/NMD-Deficient Lymphoblastoid Cells from Patients with Various Forms of Intellectual Disability.” *Molecular Psychiatry* 17 (11): 1103–15.

Pattali, Rithu, Yongchao Mou, and Xue-Jun Li. 2019. “AAV9 Vector: A Novel Modality in Gene Therapy for Spinal Muscular Atrophy.” *Gene Therapy* 26

(7-8): 287–95.

Riccardi, Carlo, and Ildo Nicoletti. 2006. “Analysis of Apoptosis by Propidium Iodide Staining and Flow Cytometry.” *Nature Protocols* 1 (3): 1458–61.

Vermes, I., C. Haanen, H. Steffens-Nakken, and C. Reutelingsperger. 1995. “A Novel Assay for Apoptosis. Flow Cytometric Detection of Phosphatidylserine Expression on Early Apoptotic Cells Using Fluorescein Labelled Annexin V.” *Journal of Immunological Methods* 184 (1): 39–51.

Wang, Gang, Bowen Jiang, Chenliang Jia, Baofeng Chai, and Aihua Liang. 2013. “MicroRNA 125 Represses Nonsense-Mediated mRNA Decay by Regulating SMG1 Expression.” *Biochemical and Biophysical Research Communications* 435 (1): 16–20.

Weischenfeldt, Joachim, Inge Damgaard, David Bryder, Kim Theilgaard-Mönch, Lina A. Thoren, Finn Cilius Nielsen, Sten Eirik W. Jacobsen, Claus Nerlov, and Bo Torben Porse. 2008. “NMD Is Essential for Hematopoietic Stem and Progenitor Cells and for Eliminating by-Products of Programmed DNA Rearrangements.” *Genes & Development* 22 (10): 1381–96.

Zhang, Li, Zhaojuan Yang, and Yongzhong Liu. 2014. “GADD45 Proteins: Roles in Cellular Senescence and Tumor Development.” *Experimental Biology and Medicine* 239 (7): 773–78.

Zheng, Sika. 2016. “Alternative Splicing and Nonsense-Mediated mRNA Decay Enforce Neural Specific Gene Expression.” *International Journal of Developmental Neuroscience: The Official Journal of the International Society for Developmental Neuroscience*, March. https://doi.org/10.1016/j.ijdevneu.2016.03.003.

Zheng, Sika, Erin E. Gray, Geetanjali Chawla, Bo Torben Porse, Thomas J. O’Dell, and Douglas L. Black. 2012. “PSD-95 Is Post-Transcriptionally Repressed during Early Neural Development by PTBP1 and PTBP2.” *Nature Neuroscience* 15 (3): 381–88, S1.

Chapter 5: Conclusion and future directions

Conclusion

The dissertation work focuses on discovering the importance of nonsense mediated RNA decay (NMD) in cell biology and its interaction with cellular processes. A new and convenient AS-NMD reporter assay was developed to monitor NMD activities. This assay greatly reduced the cost and accurately measured NMD changes during drug treatments and stress responses. Its sensitivity and broad range not only identified NMD modulators, but also helped uncovered the NMD inhibition mechanism by ER stress through PERK activation (Figure 19). The NMD inhibition was completely rescued upon PERK inhibition and RNAi knockdowns, an alternative pathway from previously reported calcium mediated thapsigargin-NMD inhibition (Nickless et al. 2014). The findings further enriched the intricate network of NMD interactions with different stress responses.

In the context of cell biology during neuronal development, NMD is shown to directly affect neural progenitor cell (NPC) viability, likely, through differential expression of genes. The novel conditional *Upf2* knockout NPC using AAV9 provides a new platform to study NMD. These NMD deficient NPCs also showed significant reduction in viability. This observation has never been reported before, highlighting the importance of NMD regulation during NPC renewal which could explain related neurodegenerative diseases upon further investigations.

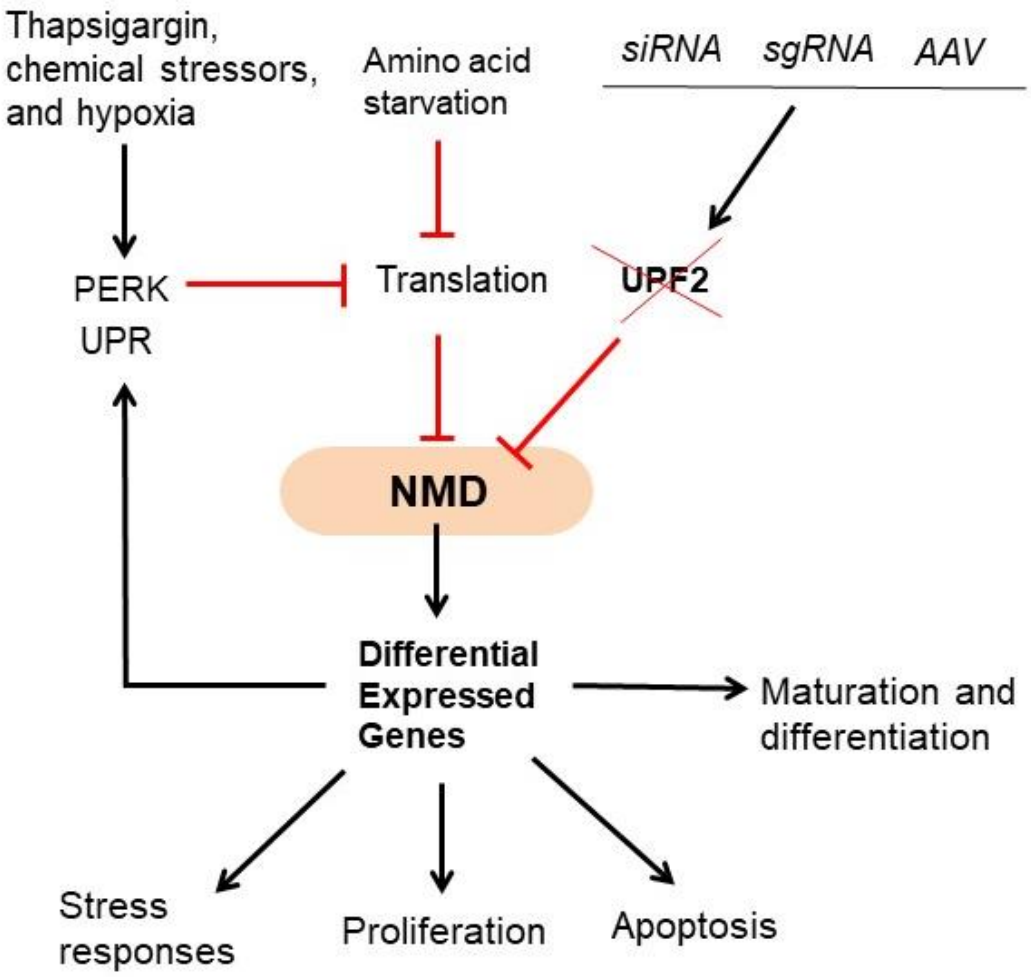

Figure 19. NMD inhibition and its downstream effects in molecular and cellular biology. Hypoxia and chemical stressors such as thapsigargin can cause ER stress and activate UPR and PERK pathways that attenuate translation and collapse polysomes. Amino acid starvation also leads to the decreased translation activity. When polysomes dissemble, the insufficient ribosomal screening of NMD targets results in differentially expressed genes. This phenomenon can trigger downstream stress responses, cell proliferation, apoptosis, and differentiation. At the same time, these stress response genes such as *Ire1α* are upregulated to help cope with cellular stress and completing the NMD feedback loop. Knocking down or knocking out core NMD factors like UPF2 inhibit NMD and similar downstream biological implications occurs.

Future Directions

To expand the AS-NMD assay, reporter genes can be measured in a more systematic way. For example, a large scale RT-qPCR using automation incorporating AS-NMD reporters could significantly increase screening efficiency . The customized NMD reporter can then screen chemical molecules, cell lines, tissues, and individual transcriptomes. It can also be improved to include additional reporters or direct NMD targets for more comprehensive and function-oriented analysis. Ultimately, the AS-NMD reporter assay can be used in NMD related disease diagnostics.

To follow up on the conditional *Upf2* deficiency NPC model, an important next step is to decipher the NMD related cell viability pathways. NMD effects in NPC renewal and differentiation remain unclear, generating a large sequencing library from the conditional knockout NPCs transcriptome can create a profile that narrows down the essential candidates. A more systematic screen is also needed after identifying potential candidates for rescue. The CRISPR monoclonal protocol presented in this dissertation can be scaled up to generate a genome wide CRISPR library using the GeCKO approach for positive screening (Kurata et al. 2018; Zhou et al. 2014; Doudna and Charpentier 2014; Joung et al. 2017). Nonetheless, the Upf2 conditional knockout NPC line can be used as a standalone NMD model cell line in the field.

Though this dissertation work is centered around cortical NPCs, AAV9 usage can be expanded to neurons at different developmental stages in a search

for NMD function in neuron longevity, proliferation, maturation and differentiation, synaptic formation, migration, and axon genesis. One example is to check whether NMD inhibition using AAV9 system could disrupt normal NPC metabolism (Weischenfeldt et al. 2008; Sartor et al. 2015). A tailored followup gene analysis could identify candidates affected by the NMD attenuation along the metabolic, cell cycle, and apoptotic pathways. Possibly, revealing new clinical targets for NMD related genetic diseases in the future (Popp and Maquat 2016; Kurosaki, Popp, and Maquat 2019).

References

Decalf, Jérémie, Matthew L. Albert, and James Ziai. 2019. “New Tools for Pathology: A User’s Review of a Highly Multiplexed Method for in Situ Analysis of Protein and RNA Expression in Tissue.” *The Journal of Pathology* 247 (5): 650–61.

Doudna, Jennifer A., and Emmanuelle Charpentier. 2014. “Genome Editing. The New Frontier of Genome Engineering with CRISPR-Cas9.” *Science* 346 (6213): 1258096.

Joung, Julia, Silvana Konermann, Jonathan S. Gootenberg, Omar O. Abudayyeh, Randall J. Platt, Mark D. Brigham, Neville E. Sanjana, and Feng Zhang. 2017. “Genome-Scale CRISPR-Cas9 Knockout and Transcriptional Activation Screening.” *Nature Protocols* 12 (4): 828–63.

Kurata, Morito, Kouhei Yamamoto, Branden S. Moriarity, Masanobu Kitagawa, and David A. Largaespada. 2018. “CRISPR/Cas9 Library Screening for Drug Target Discovery.” *Journal of Human Genetics* 63 (2): 179–86.

Kurosaki, Tatsuaki, Maximilian W. Popp, and Lynne E. Maquat. 2019. “Quality and Quantity Control of Gene Expression by Nonsense-Mediated mRNA Decay.” *Nature Reviews. Molecular Cell Biology* 20 (7): 406–20.

Nickless, Andrew, Erin Jackson, Jayne Marasa, Patrick Nugent, Robert W. Mercer, David Piwnica-Worms, and Zhongsheng You. 2014. “Intracellular Calcium Regulates Nonsense-Mediated mRNA Decay.” *Nature Medicine* 20 (8): 961–66.

Popp, Maximilian W., and Lynne E. Maquat. 2016. “Leveraging Rules of Nonsense-Mediated mRNA Decay for Genome Engineering and Personalized Medicine.” *Cell* 165 (6): 1319–22.

Sartor, Francesca, Jihan Anderson, Colin McCaig, Zosia Miedzybrodzka, and Berndt Müller. 2015. “Mutation of Genes Controlling mRNA Metabolism and Protein Synthesis Predisposes to Neurodevelopmental Disorders.” *Biochemical Society Transactions* 43 (6): 1259–65.

Weischenfeldt, Joachim, Inge Damgaard, David Bryder, Kim Theilgaard-Mönch, Lina A. Thoren, Finn Cilius Nielsen, Sten Eirik W. Jacobsen, Claus Nerlov, and Bo Torben Porse. 2008. “NMD Is Essential for Hematopoietic Stem and Progenitor Cells and for Eliminating by-Products of Programmed DNA Rearrangements.” *Genes & Development* 22 (10): 1381–96.

Zhou, Yuexin, Shiyou Zhu, Changzu Cai, Pengfei Yuan, Chunmei Li, Yanyi Huang, and Wensheng Wei. 2014. “High-Throughput Screening of a CRISPR/Cas9 Library for Functional Genomics in Human Cells.” *Nature* 509 (7501): 487–91.